Humboldt-Universität zu Berlin

Dissertation

Safety analysis of TCR gene-modified T cells

Zur Erlangung des akademischen Grades

doctor rerum naturalium (Dr. rer. nat.)

im Fach Biologie

eingereicht an der

Mathematisch-Naturwissenschftlichen Fakultät I

Diplom-Biologin Simone Reuß

Dekan: Prof. Dr. Andreas Herrman

Gutachter/in: 1. Prof. Dr. Wolfgang Uckert

2. Prof. Dr. Antonio Pezzutto

3. Prof. Dr. Dorothee von Laer

Datum der Einreichung: 27.10.2011

Datum der Promotion: 21.02.2012

Content

Summary

T cell receptor (TCR) gene therapy is a new therapy for cancer which showed first clinical success but at the same time risk factors evolved. After TCR gene transfer the endogenous TCR is simultaneously expressed with the transgenic TCR. This can have several consequences. First, the expression and functionality of the transferred TCR might be diminished due to competition with the endogenous TCR for cell surface expression. Second, the TCR chains can mispair with each other which would lead to TCRs with unknown specificities and to a reduced expression and functionality of the transferred TCR. Both aspects were analyzed in the first part of this thesis. To do that, dual TCR T cells were generated with the particularity that one TCR was inducible in its expression by a doxycycline (Dox)-regulated vector. First, the TCR expression was characterized in single TCR T cell clones either harboring the lymphochoriomeningitis virus-specific P14 TCR or the ovalbumin-specific OT-I TCR. The TCR expression was shown to be dependent on the Dox concentration. In dual TCR T cell clones, the endogenous TCR (either P14 or OT-I TCR) was constitutively expressed. After induction of second TCR expression, the endogenous TCR was still detectable on the cell surface. The induced TCR gained functionality whereas the endogenous TCR lost it. One reason was the lower expression level of the endogenous TCR. Another reason was the mispairing of TCR chains which was detected by fluorescence resonance energy transfer (FRET) technique. The endogenous P14 TCR reduced its pairing when the OT-I expression was induced which was not the case for the endogenous OT-I TCR, but mispaired TCR dimers were detected in both cell clones. Recently, it was shown that a second cysteine bridge in the constant region of the TCR might lead to preferable pairing. Therefore, a second cysteine bridge was introduced in the P14 TCR, but no clear benefit could be detected in two cell clones in regard of mispairing of TCR chains and functionality of the modified TCR. To assure that the observation was not limited to the cell clones, primary OT-I T cells and wild-type T cells were analyzed for cysteine-modified TCR expression. In wild-type cells, a tendency but not a significantly difference in mispairing could be observed between TCRs with a cysteine bridge or without.

The second analyzed possible side effect of TCR gene therapy is the insertional mutagenesis by the retroviral vector. The vector integration can modify the expression of surrounding genes. So far, gene-modified T cells did not show malignant outgrowth in clinical trials. The safety of differentiated T cells for TCR gene therapy was analyzed in an animal model. T cell transfer was combined with a repetitive stimulation to provide the opportunity for mutations to occur and manifest during cell division. OT-I TCR transgenic T cells were transduced with the P14 TCR and were transferred into lymphodepleted mice. Recipient mice were pretreated either with 200 mg/kg cyclophosphamide in the first experiment or with 100 mg/kg in the second one. The higher dose cyclophosphamide led to

toxicity in nine out of 20 animals which could be reduced with the lower dose to three out of 30 mice. Transferred T cells were regularly stimulated either with P14 or OT-I TCR-specific peptide in the first experiment or with a P14 TCR antigen-positive tumor cell line in both experiments. Peptide stimulation provided a stronger stimulus, but at the same time kept the transferred T cells on a lower level compared to tumor cell stimulation or without a stimulus. Over time, transferred T cells increased dramatically in the CD8 T cell compartment of recipient mice, but did not lead to T cell lymphomas. The proliferative capacity and the function of transferred T cells were confirmed at the end of the experiments after a year or later. The polyclonality of vector integrations could be confirmed in peripheral blood of recipient mice of the first experiment by linear amplification-mediated polymerase-chain reaction (LAM-PCR). As control, one group received green fluorescence protein (GFP)-transduced OT-I T cells and a high dose of lymphodepletion. Beside the cycloposphamide-related toxicity in three mice no malignancies were observed in the surviving nine mice. Also in this experiment, the transferred T cell enriched over time without stimulation. In conclusion, TCR gene-modified T cell transfer did not lead to outgrowth of mutated T cell clones even not with a repetitive stimulation, but the preconditioning can cause severe side effects.

Keywords: T cell receptor (TCR), Gene therapy, Regulated TCR expression, TCR mispairing, Insertional mutagenesis

Zusammenfassung

T-Zellrezeptor (TZR)-Gentherapie zeigte erste Erfolge in klinischen Studien, jedoch wurden gleichzeitig Risikofaktoren deutlich. Nach TZR-Gentransfer wird der endogene TZR ebenfalls exprimiert. Das kann verschiedene Konsequenzen haben. Erstens kann die Expression und Funktionalität des transferierten TZRs durch die Konkurrenz mit dem endogenen TZR um die Oberflächenexpression beeinträchtigt sein. Zweitens können die TZR-Ketten miteinander falsch paaren, was zu TZRs mit einer unbekannten Spezifität und zu einer verminderten Oberflächenexpression sowie Funktionalität des transgenen TZRs führen würde. Beide Aspekte wurden in dem ersten Teil der Arbeit untersucht. Dafür wurden T-Zellen mit zwei TZRs generiert mit der Besonderheit, dass die Expression des einen TZRs durch einen Doxicyclin (Dox)-regulierten Vektor induzierbar war. Zuerst wurde die Induzierbarkeit der einzelnen TZR-Expression des lmyphozytären Choriomeningitis-Virus-spezifischen P14 TZRs oder des Ovalbumin-spezifischen OT-I TZRs untersucht. Die TZR-Expression war abhängig von der Dox-Konzentration. In T-Zellkonen mit zwei TZRs wurde der endogene TZR (entweder P14 oder OT-I TZR) konstitutiv exprimiert. Nach Induktion der TZR-Expression blieb der endogene TZR auf der Oberfläche. Während der induzierte TZR Funktionalität zeigte, verlor der endogene diese. Ein Grund war das reduzierte Expressionslevel auf der T-Zelloberfläche. Ein anderer Grund war das falsche Paaren der TZR-Ketten, das mit Hilfe der Fluoreszenz-Resonanz-Energietransfer- (FRET-) Technik in beiden T-Zellkonen detektierbar war. Zudem verringerte der endogene P14 TZR, jedoch nicht der endogene OT-I TZR, seine Paarungseffizienz nach Induktion der Expression des zweiten TZRs. Kürzlich wurde gezeigt, dass eine zweite Cystein-Brücke in der konstanten Region des TZRs zu einer besseren TZR-Kettenpaarung führt. Deshalb wurde eine Cystein-Brücke in den P14 TZR eingebaut, jedoch führte dies nicht zu einem Vorteil in zwei analysierten Zellklonen bezüglich der Falschpaarung und der Funktionalität. Um sicher zu gehen, dass die Beobachtung nicht auf die Zellklone beschränkt war, wurden auch primäre OT-I T-Zellen sowie Wildtyp-T-Zellen analysiert. In den Wildtyp-T-Zellen konnte eine Tendenz aber keine signifikanter Unterschied zwischen TZRs mit oder ohne Cystein-Brücke jedoch nach weiterer Codon-Optimierung beobachtet werden.

Der zweite untersuchte Risikofaktor der TZR-Gentherapie ist die Insertionsmutagenese durch den retroviralen Vektor. Die Vektorintegration kann die Expression der umliegenden Gene beeinflussen. Gen-modifizierten T-Zellen zeigten bisher kein malignes Wachstum in klinischen Studien. Die sichere Verwendbarkeit von differenzierten T-Zellen für die TZR-Gentherapie wurde in einem Tiermodel, in dem T-Zelltransfer mit wiederholter Stimulierung der T-Zellen kombiniert wurde, analysiert. Die Stimulierung sollte die Mutationsrate durch Zellteilung erhöhen. Transgene OT-I T-Zellen wurden mit

dem P14 TZR transduziert und in lymphodepletierte Mäuse transferiert. Die Empfängermäuse wurden entweder mit 200 mg/kg in dem ersten oder mit 100 mg/kg Cyclophosphamid in dem zweiten Experiment behandelt. Die hohe Dosis führte zur Toxizität in neun von 20 Tieren, die mit der niedrigeren Dosis reduziert werden konnte (drei von 30 Tieren). Transferierte T-Zellen wurden regelmäßig mit P14- oder OT-I TZR-spezifischen Peptiden in dem ersten oder mit einer P14 TZR-Antigen-positiven Tumorzelllinie in beiden Experimenten stimuliert. Die Peptidstimulierung gab einen stärkeren Stimulus als die Tumorzellstimulierung, jedoch blieben die transferierten T-Zellen auf einem geringeren Level als mit der Tumorzellstimulierung oder ohne eine Stimulierung. Im Laufe der Zeit reicherten sich die transferierten T-Zellen in dem CD8-T-Zellkompartiment der Tiere dramatisch an, aber entwickelten sich nicht zu T-Zelllymphomen. Die Proliferationskapazität und die Funktionalität der transferierten T-Zellen wurden nach einem Jahr oder später bestätigt. Mit Hilfe der linear-amplifizierten Polymerasekettenreaktion konnte die Polyklonalität der Vektorintegrationen in peripherem Blut von Tieren des ersten Experimentes detektiert werden. Als Kontrolle wurden OT-I T-Zellen, transduziert mit dem grün-fluoreszierenden Protein (GFP), in Mäuse mit starker Lymphodepletion transferiert. Neben der Cyclophosphamid-zugeschriebenen Toxizität in drei Mäusen wurde in den überlebenden neun Mäusen keine Malignität beobachtet. Auch hier reicherten sich die transferierten T-Zellen ohne Stimulierung an. Es wurde gezeigt, dass TZR-gen-modifizierte T-Zellen auch nicht durch wiederholte Stimulierung malignes Wachstum aufweisen, jedoch kann die Lymphodepletion zu schweren Nebenwirkungen führen.

Schlagwörter: T-Zellrezeptor (TZR), Gentherapie, Regulierte TZR-Expression, TZR-Kettenpaarung, Insertionsmutagenese

1. INTRODUCTION

1.1 T CELL BIOLOGY

T lymphocytes beside B lymphocytes are responsible for the adaptive immunity. T cells recognize infected cells or cells which have taken up pathogens by the presentation of fragmented foreign protein via peptides loaded by major histocompatibility complexes (MHC) on the cell surface of the antigen-presenting cells (APCs). MHC class I molecules are specialized to present peptides originating from the cytosol like viral peptides to CD8 T lymphocytes, so called cytotoxic T cells (CTLs) [1,2]. This subtype of T cells is specialized to kill virus-infected cells and tumor cells by lysis and cytokine secretion. MHC class II molecules present peptides of proteins from intracellular vesicles to CD4 T cells which are referred to mostly as helper T cells [3,4].

1.1.1 FUNCTION OF T CELLS- FOCUS ON CD8 T CELLS

Naive T cells migrate through the peripheral blood and lymphoid organs. In the lymph nodes they can encounter APCs like mature dendritic cells (DCs), macrophages or B cells. Upon binding of the T cell receptor (TCR) and co-receptor CD4 or CD8 to the peptide-MHC, a signal is delivered into the cells. For the acquirement of full effector functions and expansion of mature CD4 [5] and CD8 [6] T cells a prolonged contact to 3-10 peptide-MHC of APCs and a synapse formation is needed [7].

Beside this first signal a second one has to be provided by a co-stimulatory molecule. The strongest co-stimulatory effect is given by B7 molecules (B7.1 and B7.2) on the APC which bind to the CD28 molecule on the T cell. Only with the co-stimulatory signal the T cell is activated without becoming anergic. The activated cell enters the cell cycle and produces interleukin-2 (IL-2) and the high-affinity version of the IL-2 receptor which boosts the intense IL-2-driven proliferation. Once activated, the T cell does not need a co-stimulatory signal when encountering the antigen a second time. Upon stimulation a T cell undergoes multiple rounds of cell division and can multiply by 50000 in a week [8]. During the expansion time T cells acquire effector functions like cytolytic properties and secretion of cytokines. The activated T cell can migrate into infected tissue due to chemotaxis and changed adhesion molecule surface expression on the T cell and on tissue cells. The contact to the target cell induces a clustering of TCRs, co-receptors and adhesion molecules which is called supramolecular adhesion complex (SMAC) [9,10,11]. The SMAC induces a change in the cytoskeleton of the T cells which leads to the release of effector molecules at the contact site. The CD8 T cells can be bound to several target cells but kills each cell at once after organization of the SMAC. Effector molecules for CD8 T cells are cytotoxic molecules like perforin, granzymes, granulysin and FAS ligand

as well as cytokines like interferon (IFN)-γ, tumor necrosis factor (TNF) -α and -β. These molecules are produced when a naive T cells sees its antigen the first time and are stored thereafter in lytic granules. The effector T cell produces more cytotoxic molecules and cytokines when it encounters the antigen again [12]. The successful stimulation of antigen-specific T cells is dependent on co-signals provided by the inflammatory environment caused by the infection. The TCR avidity determines the composition of the resulting effector cell population with high avidity T cells presenting the highest numbers. IL-12, type I IFN and IL-2 play an important role for the effector and memory cell development. A single antigen encounter is sufficient to drive the differentiation into effector and memory T cells but the extent of T cell expansion is dependent on the inflammatory signals. The recruitment of CD8 T cells already occurs after 6 - 24 hours (h) after antigen exposure [8].

After the expansion and effector phase, most T cells die and few (5 - 10 %) remain and develop into memory T cells which provide a life-long protection against the pathogen or related ones. How the differentiation exactly takes place is still subject of debate. During the effector phase it is suggested that short-lived effector cells can be differentiated from precursor memory effector cells by expression of natural killer cell receptors like KLRG1 and IL-7α receptor, respectively [8]. Fully differentiated memory T cells can be further differentiated into central and effector memory T cells. Central memory T cells are commonly located in lymphoid organs and show strong proliferation upon re-exposure to the antigen. Effector memory T cells are mainly located in the peripheral tissue and respond immediately with cytokine release upon antigenic restimulation [13]. As shown by Stemberg *et al.* a single T cell can develop into central and effector memory T cells [14]. The memory T cell compartment directed against one pathogen is not limited in size but can grow with subsequent infections although with some loss of previous immunity provided by effector memory T cells [15].

1.1.2 Structure of the T cell receptor complex

T cells harbor around 40000 TCR molecules on their surface [16]. In the majority of T cells the TCR molecules consist of two polypeptides, TCRα and TCRβ chain, which form a heterodimer (Figure 1) [17]. Few T cells harbor a TCR consisting of a TCRγ and TCRδ chain. In structure the extracellular domains of a TCR resembles a Fab fragment of an antibody with a variable immunoglobulin (Ig)-like region (vα and vβ) at the N-terminus and a constant Ig-like domain (cα and cβ) region at the C-terminus. The variable regions are further divided into complementary determining regions (CDR) 1 to CDR3. CDR1 and 2 are responsible for the binding to the MHC molecule and CDR3 is responsible for the peptide-binding. The TCRα and β chains are linked by a disulfide bond in the constant region. The constant region is followed by a hydrophobic transmembrane region and a short cytoplasmic part. Carbohydrates are attached to each variable and constant region which provide hydrogen bonds with the other chain.

The TCR complex comes to the cell surface together with the CD3 complex which consists of CD3γ, CD3δ and two CD3ε chains. A homodimer of the CD3ζ chain is associated intracellular [18]. The CD3γ, δ and ε proteins have an Ig-like domain in the extracellular part and a single immunoreceptor tyrosine-based activation motif called ITAM in the intracellular part. The ITAM can be phosphorylated twice by receptor-associated tyrosine kinases of the Src family and can be bound by other tyrosine kinases upon phosphorylation. The CD3ζ protein has only a very short extracellular domain and harbors three ITAMs in the intracellular part which are important for TCR signaling.

The co-receptors CD4 and CD8 stabilize the recognition by binding to the corresponding MHC. The sensitivity of CD4 and CD8 T cells is increased by 100-fold by co-receptor-binding to the MHC since both co-receptors interact with the tyrosine kinase Lck which enhances the TCR signaling. Whereas the CD4 molecule is a monomer comprising of four domains (D1-D4), CD8 is composed of a heterodimer of an α and a β chain. Beside the heterodimers also homodimers of the CD8α chains are found whose function remain under debate [19].

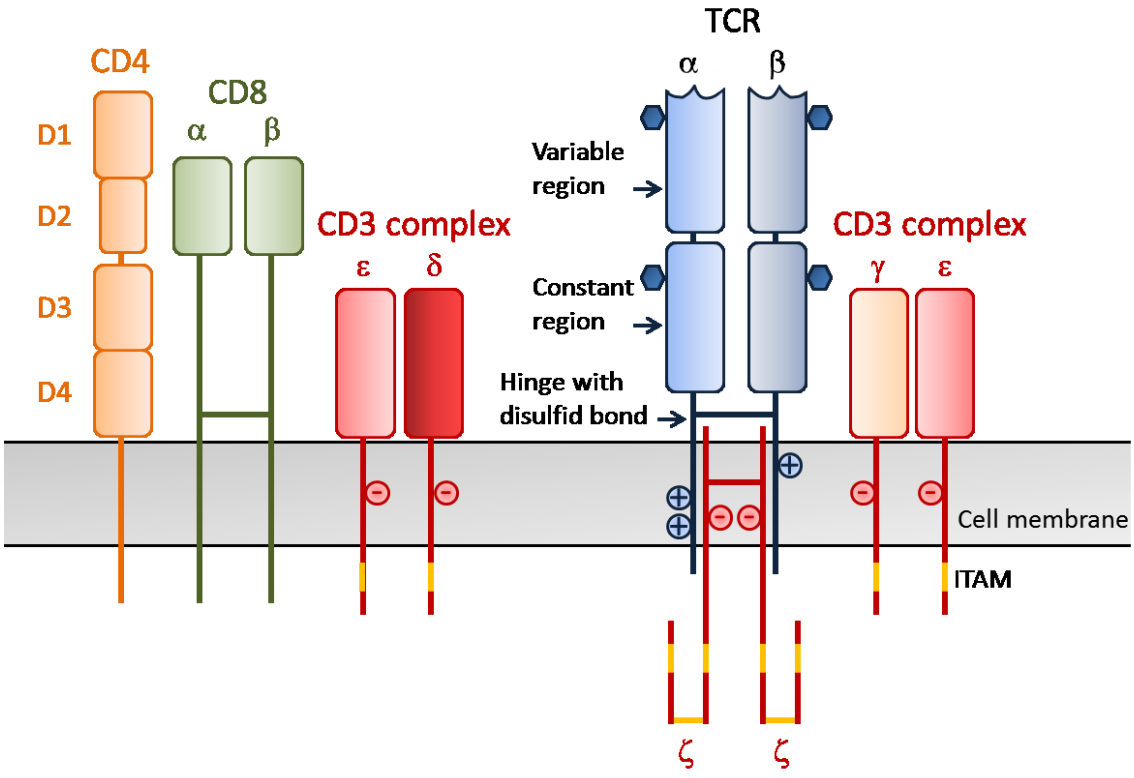

Figure 1 Schematic picture of the T cell receptor complex

TCRα and β chains are depicted in blue, CD3 components in red, the co-receptors CD8 in green and CD4 in orange. Both TCR chains are composed of a variable region, a constant region, a hinge with a disulfide bond, a transmembrane region and a cytoplasmic tail. Blue diamonds represent carbohydrates bound to TCR chains.

The CD3 complex is composed of two ε, one δ, one γ and two ζ chains. The intracellular CD3ζ chains are associated with the transmembrane and cytoplasmic domains of the TCR. The CD4 co-receptor is a monomer consisting of domains 1-4 (D1-D4). The co-receptor CD8 is composed of an α and a β chain which comprise both an extracellular domain, transmembrane region and a cytoplasmic tail. Horizontal lines show disulfide bonds in the CD8 receptor, in the TCR and between CD3ζ chains. Circles with minus and plus signs show charges of amino acid residues in the polypeptides. ITAMs are shown in yellow. (Adapted from [20]).

1.1.3 T CELL DEVELOPMENT

The diversity of TCR molecules arises from somatic gene rearrangement which is carried out by recombination proteins encoded by recombination-activating genes 1 and 2 (RAG-1 and RAG-2) in the thymus [21]. TCR gene rearrangement and gene organization resembles that of immunoglobulins. The TCRα locus consists of V and J gene segments whereas the locus of TCRβ contains additionally D segments. The rearrangement of the TCRα and β locus leads to a diversity of 10^4 TCRs. The possible TCR output is further increased up to theoretical 10^{15} TCR combinations by adding N-nucleotides and P-nucleotides in the junctional CDR3 regions of TCRα and TCRβ. Practical a diversity of 10^6 - 10^8 is estimated [22].

Precursor T lymphocytes are generated in the bone marrow and migrate into the thymus where they further develop (Figure 2). The thymus is organized into two zones: the inner medulla and the outer cortex. In both zones specialized epithelial cells, bone-marrow-derived macrophages and dendritic cells (DCs) are present. Double-negative (DN) thymocytes which do not express a TCR or a co-receptor migrate by chemokine signals from the cortico-medullary junction to the outer cortex region, the subcapsular zone (SCZ). They start to recombine the TCRβ locus with the combination of Dβ with Jβ gene segments and afterwards that of Vβ and DJβ gene segments. Only successful rearranged TCRβ chain will lead to further T cell development. The TCRβ chain protein is synthesized and delivered to the cell surface with an invariant pre-TCRα chain and the CD3 complex. TCR signals lead to up-regulation of both co-receptors CD4 and CD8 (double-positive (DP) thymocytes). After an intense cell expansion, the recombination of the TCRα chain locus is started with the combination of Vα and Jα gene segments. With the fully rearranged and expressed TCR the DP T cells interact with peptide-MHC of epithelial cells, first in the cortex later in the medulla. Upon encounter with a peptide-MHC of a cortical epithelial cell (TEC) the DP thymocytes are positively selected for proper self-MHC molecule binding. A second encounter with a positively selecting TEC is needed for the DP thymocytes to further maturate [23,24]. If correctly activated, they maturate to single-positive (SP) cells by down-regulation of one of the co-receptors dependent on the type of peptide-MHC

encounter they have made. Upon inappropriate binding with high affinity to self-MHC the TCR signal leads to apoptosis [25,26].

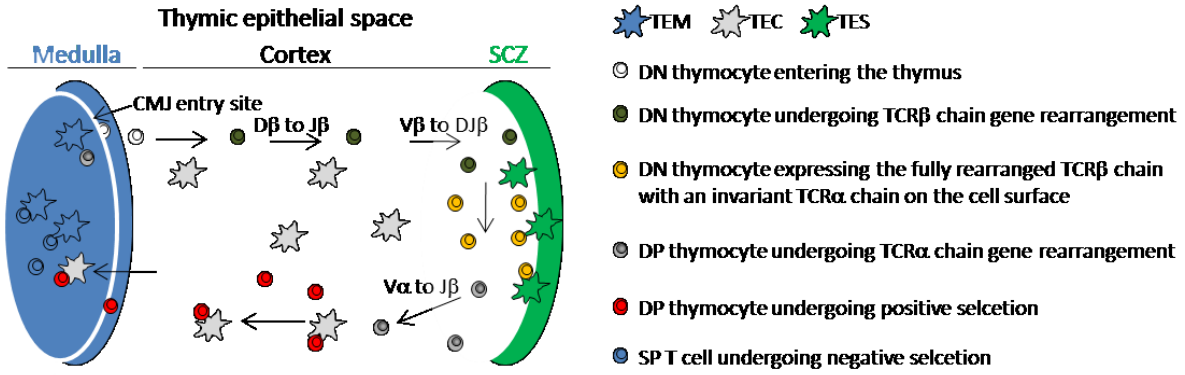

Figure 2 T cells mature in the thymus

Different stages of thymocytes development are shown. The thymus consists of different specialized zones: the medulla and the cortex. The T cell progenitors enter the thymus through cortico-medullary junction (CMJ). In the cortex and the subcapsular zone (SCZ) they encounter thymic epithelial cortical (TEC), subcapsular (TES) cell, macrophages and DCs (not all cell types are shown). In the medulla specialized thymic medullary epithelilal (TEM) cells are found. DN, DP, SP: double-negative, -positive, single-positive thymocyte. Picture adapted and simplified from [27].

DP thymocytes which do not encounter APCs and do not receive positively selecting signals also die in the cortex. During the maturation process of positively selected thymocytes the up-regulation of the chemokine molecule CCR7 directs them into the medulla [28,29]. The autoimmune regulator AIRE is expressed in medullary epithelial cells which leads to expression of tissue proteins [30]. Tissue antigens can be presented and tolerance is achieved against these antigens. Also few DCs from the skin and blood come to the border of the cortex and medulla in the thymus to present peptides [31]. By the described cells, most auto-reactive T cells are deleted. During the positive selection in the cortex and the negative selection in the medulla 95 % of the thymocytes die [32,33]. In the periphery, naive T cells are kept alive due to low-affinity interaction with self-peptides presented by self-MHCs [34].

1.2 ADOPTIVE T CELL THERAPY

Early observations of Ehrlich gave hints that the immune system can provide protection from cancer [35]. After inbred mouse strains were available, tumor transplantation experiments were done and showed T cell-mediated tumor rejection. The idea of adoptive T cell therapy is based on experiments showing that the immunity towards a tumor could be transferred by using the splenocytes of tumor-

immunized mice [36,37]. Therefore, Burnet and Thomas postulated the theory of immunosurveillance saying that the T lymphocytes protect the host from developing tumors [38,39], although with spontaneous autochthonous tumors the functional immunity mediated by T cells was doubted [40]. Afterwards, it was postulated that T cells cannot respond to spontaneously arising tumors but only to virus-induced once [41]. Lately, it was shown that mice transgenic for an inducible viral oncogene were not protected from the autochthonous developing tumors and that the T cells even get paralyzed in these mice, although this viral antigen could lead to tumor rejection in transplantation models [42,43]. The "cancer immunoediting" hypothesis by Schreiber *et al.* postulates that tumor cells are first eliminated by the immune system, but tumor cells which survive are “edited” in an equilibrium phase. The evolving variants might than escape the immune system [44,45].

1.2.1 TUMOR ANTIGENS

Responsible for the T cell response are the tumor antigens presented by MHC molecules on the tumor cell surface [20]. One can divide these antigens into two groups: tumor-specific antigens like mutated oncogenes, tumor suppressor genes or viral antigens and tumor-associated antigens (TAAs) like differentiation and tumor/testis antigens. Tumor-specific antigens are derived from mutated proteins due to point mutations or gene rearrangements which are involved in the cell transformation process and are only expressed by the tumor cells. The tumor suppressor p53 [46] or the oncogene ras [47] are the most prominent antigens. Viral antigens can lead to cell transformation, like proteins E6 and E7 of the human papilloma virus (HPV) in cervical cancer [48], latent proteins of the Epstein-Barr virus (EBV) in Burkitt’s lymphoma, post-transplant B cell lymphomas, Hodkin lymphomas and nasopharyngeal carcinomas [49,50] or proteins of the human T cell lymphotropic virus-1 (HTLV-1) in adult T cell leukemia and lymphomas [51]. TAAs are found in many tumor cell types but are also expressed on normal tissue. Differentiation antigens are only expressed in specific tissues where certain processes take place like the melanin production in the skin, but are therefore shared between tumors and healthy cells. Tyrosinase [52,53], Mart-1/Melan-A [54] and gp100 [55,56] serve as tumor-antigens in melanomas. Also in epithelial tissues, differentiation antigens are found like the prostate-specific antigen (PSA) in prostate tumors [57,58] or the mammaglobulin-A in breast cancer [59]. Over-expressed proteins are another group of TAAs found in tumor cells like the receptor Her2/neu in breast and ovarian cancer [60]. Antigens derived from proteins which were not correctly posttranslational modified can also serve as tumor antigens like the unglycosylated mucin, Muc-1, which is expressed in breast and pancreas cancer [61]. Testis antigens are normally only expressed in germ line cells of males but these do not express MHC molecules, therefore peptides are not presented on the cell surface [62]. Some tumors like glioma,

melanoma and breast cancer aberrantly express tumor/testis antigens to which the melanoma-associated antigens (MAGE-I and -II) [63], NY-ESO-1 [64] and SSX-2 [65] belong.

1.2.2 DONOR LYMPHOCYTE INFUSION

Donor lymphocyte infusions (DLI) are given after bone marrow transplantations to provide patients an anti-viral immunity or protection against recurrent leukemia. T cells confer a graft-versus-leukemia effect (GVL) which is directed against MHC class I and II in HLA-mismatched transplants settings or against minor histocompatibility antigens and also mutated antigens in matched transplant settings. On the same time, transferred cells might also target healthy tissue which can lead to severe graft-versus-host disease (GVHD) [66]. Beside this possible strong side effect, DLI is successful in the treatment of chronic myeloid leukemia (CML), but less successful in the treatment of acute myeloid leukemia or acute lymphoblastic leukemia (ALL) [67,68]. After allogeneic T cell depleted bone marrow or organ transplantation patients are prone to post-transplant lymphoproliferative disease (PTLD) which is driven by reactivation of latent viral infections with EBV and cytomegalovirus (CMV) or lytic adenovirus infection since endogenous virus-specific T cells had been depleted by chemotherapy before transplantation. As successful therapy polyclonal virus-specific CTLs were generated by *ex-vivo* stimulation with autologous EBV-transformed lymphoblastoid cell lines (LCLs) or CMV-transformed fibroblasts. Firstly shown by Riddell *et al.* in 1992, CMV-specific donor lymphocytes committed CMV-specific immune responses after bone marrow transplantations [69,70]. Heslop *et al.* transferred prophylactic EBV-specific T cells into immunocompromised patient and could restore EBV-immunity or even treat EBV-positive lymphomas [71,72,73]. Also, EBV-positive Hodgkin's disease [74] and nasopharyngeal carcinoma [75,76] were treatable. Newly, it's possible to generate CTLs bispecific for EBV and adenovirus which prevented PTLD and could clear adenoviral infection [77]. Until 2010, 114 patients have received EBV-specific CTLs. All 101 patients who received the lymphocytes as prophylaxis did not develop EBV-related lymphoproliferative disease, and 11 out of 13 with EBV-PTLD went into sustained complete remission [78].

The generation of CTLs specific for melanoma antigens could be easily derived from tumor-infiltrating lymphocytes (TILs) from patients with metastatic melanoma [79]. Melanoma-specific T cells were transferred in a number of clinical trials, firstly in 1988, where objective response rates were between 31 - 35 %. In later trials with increasing levels of lymphodepletion the objective response rate was 49 - 72 % [80]. But transferred T cells also targeted healthy tissue expressing the tumor-associated antigen which led to vitiligo [81].

Although T cell transfer seems to be feasible for the treatment of PTLD and melanoma, specific T cells cannot always be generated. Also, the avidity of the obtained T cells might not be optimal since high-avidity T cells are deleted in the process of negative selection. The generation of specific T cells takes a long time for the identification and expansion. This might not be practical for treatment of every patient. Early clinical trials showed short persistence of transferred T cells [82] which could be improved by increased lymphodepletion and IL-2 administration [80].

1.2.3 TCR GENE THERAPY

Alternative to the *ex-vivo* expansion of tumor-reactive T cells is the transfer of tumor antigen-specific TCR genes into T cells (Figure 3). This approach is more time-efficient and can be applied to HLA-matched patients. First TCR gene transfer in mouse splenocytes was done in 1986 by Dembic *et al.* [83] and in human T cells in 1999 [84]. The reactivity of the original T cell clone could be transferred to murine or human T cells by the TCR gene transfer. T cells showed cytolytic lysis and cytokine release upon coculture with cancer cell lines or peptide-loaded target cells. TCR-transduced T cells were investigated in animal models and also used in clinical trials. The first clinical trial was conducted by Morgan *et al.* in which two out of 17 patient showed tumor regression [85]. In this trial, a TCR recognizing the tumor-associated Mart-1 antigen was used to transduce autologous PBLs from HLA-A*0201-positive patients with metastatic melanomas. TCR transduction efficiencies ranged from 17 - 67 % (mean 42 %) as measured by TCRvβ staining. In patients who received T cells after a rapid-expansion protocol transferred cells were detectable during the monitored 90 day-period. 13 examined patients showed increased Mart-1 tetramer staining after adoptive T cell transfer. In the two patients with full clinical regression TCR-transduced T cells increased by factor 1400 and 30 in the peripheral blood and were kept at high levels one year after transfer with 20 - 70 % of gene-marked cells. In this trial, the clinical benefit was correlated with increased persistence of TCR-transduced T cells. Another trial was started using TCRs of higher affinity, again a TCR recognizing Mart-1 and a second recognizing the melanoma antigen gp100. The last mentioned TCR was isolated from a HLA-A2-transgenic mouse immunized with the peptide. Objective cancer regression was seen in 30 % of the patients treated with Mart-1 TCR-transduced autologous PBLs and 19 % in patients treated with gp100 TCR-transduced T cells. Unfortunately, it was observed that normal tissues like skin, eyes and ears expressing the antigens were also targeted. Some of these patients had to be treated with steroids [86]. In a recent clinical trial, a NY-ESO-1-specific TCR was employed for autologous T cell transduction. The cancer/testis antigen NY-ESO-1 is expressed in 80 % of synovial cell sarcomas and in 25 % of melanomas. Six patients with NY-ESO-1-positive synovial cell sarcomas and eleven with NY-ESO-1-positive melanomas were treated. Objective responses were observed in four patients with synovial cell sarcomas and in five with melanomas. Two of the melanoma patients

went into complete remission and one patient with synovial cell sarcoma showed partial response for 18 months [87]. In another study using a murine-derived TCR directed against the human carcinoembryonic antigen (CEA), three patients with metastatic colorectal cancer were treated. Serum CEA levels decreased in all patients by 74 – 99 % and one patient showed an objective regression of metastasis in lung and liver. Besides that, also a transient inflammatory colitis was observed in all patients showing the limitations of CEA as a target antigen [88]. One trial had just started with renal cell carcinoma patients which received autologous PBLs transduced with a modified renal cell carcinoma-specific TCR. The modification was done in the CDR3α region and led to improvement of tumor cell recognition [89]. The outcome of the trial is still pending.

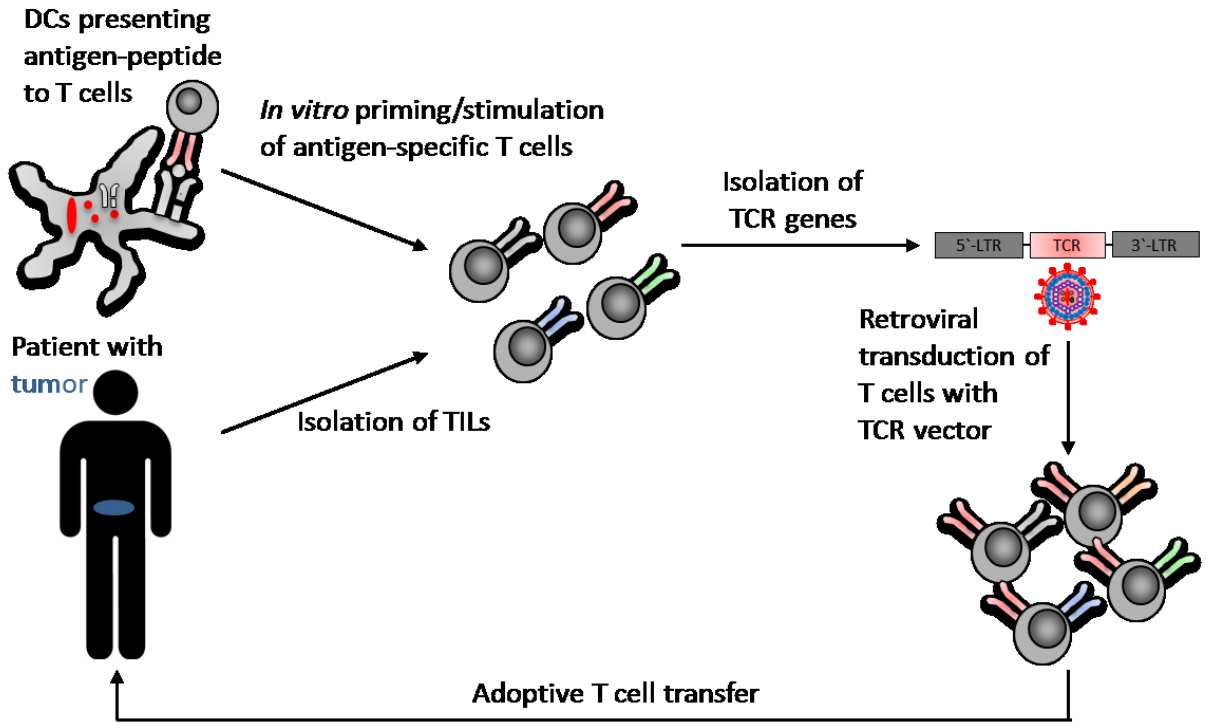

Figure 3 Principle of TCR gene therapy

TCRs are either isolated from TILs or from peripheral T cell clones stimulated with DCs pulsed with antigenic peptides or DCs expressing antigenic protein. The TCR genes are cloned into a retroviral vector. By viral transduction autologous or HLA-matched T cells receive the new antigen specificity. The TCR gene-modified T cells are given to the patient.

1.2.4 Improvement of TCR gene therapy

Although first success of TCR gene therapy was made, there are many steps to optimize this approach. Very important is the chosen TCR and its cognate antigen. Different points can be addressed to improve TCR gene therapy [90]:

- The TCR should be of high affinity which would detect low amounts of antigen on tumor cells. Also, high-affine TCRs are independent of the co-receptor and would function in CD8- as well as CD4-positive T cells which would have a synergistic effect on the anti-tumor activity.
- Since the transgenic TCR has to compete with the endogenous TCR for CD3 components, cell surface trafficking proteins needed for cell surface expression and also for signaling molecules, a strong expression is a prerequisite. The expression can be improved by the vector system or remodeling of the TCR amino acids or TCR structure.
- Normally, beside the transgenic TCR also the endogenous TCR is expressed which could form mispaired TCR heterodimers with a new unknown specificity ("off-target toxicity"). The prober pairing of TCR chains can be improved by TCR chain modifications.
- The environment in the host can be prepared with lymphodepletion or cytokine injections. This would enhance T cell function and persistence and would also have an influence on the tumor.
- The target antigen is an important issue for TCR gene therapy. It should desirable only be expressed on tumor cells but shared between patients. The antigen amount on the tumor cells should be high enough for recognition by T cells and should be cross-presented by the surrounding tumor stroma. Since such antigens are rare, TAAs have to be evaluated closely, especially in respect to on-target toxicity towards healthy cells expressing the antigen.

Enhancement of TCR expression

The TCR expression on the cell surface of transduced T cells is an important factor for the redirected specificity. The cell surface expression is determined by the TCR itself, CD3-complex recycling in the transduced cell and the expression system used for the gene transfer. Optimizations of the TCR and the expression system have been intensively examined. Stable transgene expression is obtained by usage of lenti- or γ-retroviral vectors. The promoter activity of the retroviral long terminal repeat (LTR) or other promoters can be used for the transcription of the gene. The analysis of a Moloney murine leukemia virus (Mo-MLV)-retroviral vector showed that transgene expression driven by the LTR, phosphoglycerate kinase (Pgk) or β-actin promoter was best in proliferating T cells but decreased in resting cells. Only the combination of LTR-driven transgene transcription with a β-interferon (IFN) scaffold attachment region led to enhanced expression in resting T cells [91]. A vector with LTRs derived from the myeloproliferative sarcoma virus (MPSV) showed a 75-fold higher expression than the Mo-MLV-based vector. Inclusion of a posttranscriptional regulatory element (PRE) from the woodchuck hepatitis virus in the MPSV-based vector (MP71) even increased the expression level in human T cells [92] by stabilization of the mRNA [93]. For lentiviral vectors several

promoters were tested for transgene expression as well. Here, the murine stem cell viral (MSCV) promoter performed best in activated PBLs as well as in minimal stimulated PBLs [94].

Since the TCR complex comprises two TCR chains, the expression system has to provide transcription of two genes. The transcription of the second gene can be driven by an internal promoter which is not as efficient as an internal ribosomal entry site (IRES) or a 2A element [95]. The IRES site confers coordinated gene expression but the gene downstream of the IRES site has a lower expression level [96]. The IRES site can lead to TCR expression [97,98], but in a lentiviral vector it was not sufficient [94]. The usage of a 2A element is superior for TCR gene expression [99]. It is used in viruses for the translation of a second protein from a long composite polypeptide by a ribosomal skipping mechanism and confers good expression of a second gene in retroviral vectors [100,101,102]. With the size of 60 nucleotides the 2A linker is much smaller than an IRES site (568 nucleotides) and is supposed to provide equal molar ratios of both proteins. The disadvantage of a 2A element is that it stays attached to the 5'-gene which could interfere with protein function or could be immunogenic but this effect was not observed so far in mice [103] (this dissertation). When used for TCR expression multiple studies with γ-retroviral [99] or lentiviral vectors showed superior expression and functionality compared to the usage of an IRES site [94]. Only one study demonstrated better performance of transduced T cells with an IRES-linked TCR *in vivo* [95].

Enhanced TCR expression can also be obtained by remodeling the TCR structure and sequence. The usage of optimal codons in the gene sequence can improve transgene expression. Since the genetic code is redundant, one can choose codons with the most frequently available tRNAs [104]. The usage of codon-optimization and the elimination of mRNA instability motifs and cryptic splice sites showed increased TCR transgene expression in PBLs [105].

As Sommermeyer *et al.* [106] showed certain TCRs can replace endogenous TCRs on the cell surface which would be the best situation for TCR gene therapy. He also showed that two strong TCRs can be coexpressed with reduced functionality of the endogenous TCR. The expression level is an important issue which might also be influenced by the formation of mispaired TCRs. This leads to a reduction of properly paired TCRs and to competition for the CD3 complex. When a murine TCR was expressed on human cells it replaced the human TCR [106]. This effect was further studied by Cohen *et al.* [107] who replaced the constant human region of the TCR with the murine one and observed enhanced expression of two TCRs in human PBLs. The so-called murinized TCRs showed high level of surface expression and increased functionality. Nevertheless, mixed dimers could be formed with TCRs harboring a human constant region [108]. The other important point is that the murine constant region is foreign for human patients and could induce an immune response. Such an immune response against a foreign protein was seen in a clinical trial where gene-modified T cells were

rejected by human immunodeficiency virus (HIV) patients [109]. To avoid such an rejection Cohen *et al*. [110] and Sommermeyer [111] could reduce the amount of murine residues to a minimum needed for the enhanced expression.

The enhancement of TCR functional avidity was also achieved by the removal of certain N-glycosylation sites in the constant regions of different human and murine TCRs which led to an increased functional avidity and a better tumor cell recognition compared to the wild-type cells [112]. Although the deglycosylated TCRs seem to be superior to wild-type TCRs, still mispairing with endogenous TCRs is not excluded.

For the reduction of mispairing another option is the addition of a second disulfide bridge in the constant region by mutating a distinct residue to a cysteine [113]. This second disulfide bridge was used to stabilize soluble TCRs for crystallization [114]. It increased properly paired TCR chains, enhanced TCR cell surface expression and increased functionality [113]. Here, only one amino acid is changed in both chains which reduces the possibility of an immune response upon adoptive transfer.

Voss *et al.* [108] found another possibility to mutate the TCR constant region for improvement of preferential pairing of TCR chains. By analyzing the crystal structure of a TCR they could determine a pair of amino acids in the constant regions which interact in a “knob-into-hole” configuration with each other. By mutating these residues the configuration was changed into a “hole-into-knob”. This change led to selective pairing of the transduced TCR chains and conserved its function.

The TCR molecule needs the CD3 complex to be transferred to the cell surface. For signal transduction the CD3ζ chain is responsible. Therefore, chimeric T cell receptors were constructed where the part of the constant region downstream of the extracellular cysteine residue which forms the disulfide bond was replaced by the CD3ζ chain [115,116]. These chimeric TCRs did not mispair with endogenous TCR chains, were expressed independently of available CD3 components and showed functionality. In another approach, the additional transfer of CD3 components together with the transgenic TCR conferred as well higher functionality. But the amount of transgenes is not practical and mispairing is not avoided in this approach [117].

Recently, a new TCR format was developed in which the constant regions were deleted and only the variable regions of the TCR are expressed together with the linked Lck tyrosine kinase and CD28 domain in a stabilized format. This newly modified TCR format showed functionality independent of the CD3 complex and the CD4 or CD8 co-receptor and did not lead to mispairing [118].

Preconditioning

Preconditioning modifies the host environment in favor of transferred cells. Removal of cytokine sinks by deleting host cells and providing space in the lymphoid compartment or the administration of cytokines can have a positive effect on the persistence and functionality of transferred cells. Patients with metastatic melanoma were pretreated with chemotherapy using fludarabine and cyclophosphamide and then received *in vitro* generated TILs combined with IL-2 administration after adoptive T cell transfer. Here, an increased response rate of 50 / 47 % was observed [80,119]. As shown in an animal model, total body irradiation led to enhanced anti-tumor efficacy of transferred T cells. This effect was not only due to deletion of regulatory T cells but also due to increased availability of IL-7 and IL-15 [120]. Also, the administration of IL-2 can already increase the persistence and the anti-tumor effect of transferred cells as shown with melanoma-specific CD8 T cell clones in patients of a phase-I clinical trial [121]. Administration of IL-15 is another option which supports the generation of memory T cells. In a nonhuman primate model, it was seen that IL-15 enriches memory CD8 T cells, CD4 T cells and NK cells. In contrast to IL-2 administration, IL-15 does not induce the proliferation of regulatory T cells and only shows transient toxicity [122]. IL-15 improved anti-tumor efficiency by transferred tumor-/ self-specific T cells as shown in an animal model [13].

1.3 SAFETY CONCERNS OF TCR GENE THERAPY

1.3.1 MISPAIRING OF TCR CHAINS

Mispairing of TCR chains harbors a risk for TCR gene therapy. When polyclonal T cells are used for TCR transduction it is not possible to predict mispaired TCRs versions. As shown in an animal model, the transfer of TCR-transduced polyclonal wild-type T cells into sublethal irradiated recipient mice and administration of high-dose IL-2 led to lethal autoimmunity after two weeks. This severe side effect was not seen with the transfer of untransduced T cells, GFP-transduced T cells or TCR transgenic T cells. The off-target toxicity could be confirmed to be induced by mixed TCR dimers since autoimmunity was also observed when T cells were transduced with only TCRvα or TCRvβ chains [123]. The use of T cell clones to minimize possible TCR mispaired versions still can harbor this risk of neoreactivity. The TCR-transduction of various virus-specific T cell clones showed new reactivities when tested against several LCLs. The newly gained allo-and also auto-reactivities where due to TCR mispairing as shown by transfer of TCRvα or TCRvβ chains and were MHC I or MHC II-restricted [124].

1.3.2 RECOGNITION OF SELF-ANTIGENS

It was already seen that upon transfer of melanoma-specific T cells healthy tissue expressing the TAA can be targeted, which is called on-target toxicity [81]. The same observation was made in one TCR gene therapy trial using redirected autologous T cells with high-avidity TCRs specific for melanoma antigens (MART-1 and gp100) [86]. The targeting led to destruction of melanocytes in the skin, eye and ear. Such events were not seen in the clinical trial before, targeting the same melanoma antigen but with a TCR of lower avidity [85]. 29 of 36 patients showed a widespread erythematous skin rash which was infiltrated by T cells. On day 5, destruction of epidermal melanocytes was already observed. As endogenous T cells were depleted at that time by preconditioning, the transferred T cells were the source of autoimmunity. Also, cell infiltrates in the eye were observed in several patients who had to be treated with steroids. In the infiltrates Mart-1 tetramer-positive T cells were found. Hearing loss occurred in some patients. All side effects resolved by time which could be due to the loss of transferred T cells or their suppression after treatment with steroids.
The self-antigen Survivin is expressed on a variety of tumor cells and seemed to provide a good TAA for TCR gene therapy. But Survivin-specific TCRs showed to be not useful for TCR gene therapy. After TCR transduction of PBLs, they commited MHC-restricted fratricide of T cells in the culture since the Survivin-expression was up-regulated in activated T cells [125]. This study showed again the limitations of TAAs for TCR gene therapy.

The recognition of self-antigen can not only be conferred by the transgenic TCR but also by the endogenous TCR. T cells harbor a certain avidity to self-antigens which assures their survival in the periphery by encountering self-peptide-MHC complexes [34]. Through ligation of the transgenic TCR to the tumor antigen the activated T cell could now target self-antigen via its endogenous TCR. That T cells can commit both functionalities was shown in transgenic mice harboring T cells with two TCRs [126]. T cells could confer anti-tumor response without causing autoimmunity when the tumor antigen was highly expressed, whereas the self-antigen was only present in low amounts. But self-tissue was targeted when the self-antigen was present in high amounts and the transferred T cells were either activated through the tumor antigen-specific TCR or the self-antigen-specific TCR [127]. In a similar model, it was also shown that TCR-transduced T cells recognizing a self-antigen only induced a response when activated by vaccination with this antigen [128].

1.3.3 INSERTIONAL MUTAGENESIS

Retroviral vectors are used for a stable transgene expression which is the result of provirus vector DNA integration into the host cell genome. A long time it was believed that the integration occurs randomly in the host genome. Mapping of the integration sites of MLV in the human genome showed that the virus integrates near transcription start sites of active genes [129] and was mostly

located in the first intron [130]. The affected genes are mainly involved in signaling, transcription or have kinase activity [130]. The lentiviral HIV integrates into actively transcribed genes, but not near the transcription start [129,131]. The virus vector can also have an influence on surrounding genes. Its promoter and enhancer regions in the LTRs can drive or enhance downstream or upstream adjacent genes. Also gene enhancers can be influenced by the provirus. In self-inactivating (SIN)-vectors the promoter and enhancer region are minimized to one LTR and have therefore a lower risk of insertional mutagenesis.

That vector integration can indeed lead to a malignant cell transformation in combination with other acquired mutations was observed in two clinical trials in France and in England. Patients with the X-linked severe combined immunodeficiency disease (SCID-X1) don't develop T cells, NK cells and have dysfunctional B cells due to a mutation in the gamma chain (γc) of the common cytokine receptors for IL-2, IL-4, IL-7, IL-9, IL-15, and IL-21 which support the development and function of the immune system. In these trials, patients were treated with autologous hematopoietic stem cells (HSCs) corrected with the γc encoding gene IL2RG by retroviral transfer [132,133,134]. Nine out of ten patients of the French trial could reconstitute their immune system upon treatment. After around 30 months, the two youngest patients developed malignant proliferation of T cells and had to be treated with chemotherapy. Analysis of vector integration sites in the blood of these patients revealed malignant T cell clones with integrations near the cellular proto-oncogene LMO2. The expression of the proto-oncogene was dysregulated and probably the cause of malignancy [135]. Two other patients developed T cell acute lymphoblastic leukemia (T-ALL) 33 and 68 months after transfer [136]. The vector mapping in the third patient showed upstream integration of the oncogene CCND2 and in the other patient integration in the second intron of LMO2 and near BML1. These genes were over-expressed to an abnormal level. The lymphoproliferation in three patients were of an immature phenotype and in one patient of a mature phenotype. The transgene IL2RG expression was of physiological level in all patients. Also, other chromosomal translocations, mutations of proto-oncogenes and deletions of suppressor genes were observed in the patients' blasts cells [136]. In the English trial, ten patients were successfully treated with gene-modified autologous HSCs [132,137]. One patient developed T-ALL after 24 months and was treated with chemotherapy. Analysis of the leukemic cells revealed vector integration near the LMO2 proto-oncogene. LMO2 was over-expressed in malignant cells. Additional DNA aberrations were found: a gain-of-function mutation in NOTCH1, a deletion of the tumor suppressor gene cyclin-dependent kinase 2A (CDKN2A), and a translocation of the TCRβ region to the STIL-TAL1 locus [138].

Another disease which was treated by gene therapy is the chronic granulomatous disease (CGD). This rarely inherited disease is caused by a dysfunctional nicotinamide dinucleotide phosphate (NADPH)

oxidase complex which is composed of five subunits. Most cases have mutations in the X-linked gp91^{phox} gene encoding for a membrane-spanning subunit. Defects in the NADPH oxidase lead to the impairment of antimicrobial activitiy of neutrophils and patients suffer from life-threatening bacterial and fungal infections. Until 2010, a total of 12 patients were treated by gene therapy in different trials in combination with myelosuppressive pretreatment [139]. Only three patients showed long-term engraftment with high-levels of gene-modified cells which was promoted by an insertional activation of *MDS1/EVI1, PRDM16, SETBP1* and resulted in clonal myeloproliferation [140,141]. The over-expression of EVI1 was shown to lead to genomic instability resulting in monosomy 7 by the impairment of centrosome duplication in two patients [142].

The adenosine deaminase-deficient SCID (ADA-SCID) is also treatable by gene therapy. Due to the absence of this enzyme, toxic purine metabolites accumulate which lead to impaired lymphocyte development, lymphocyte function and immunological unrelated abnormalities. In combination with a nonmyeloablative treatment gene-modified HSCs reconstituted T cell development and immune function. The administration of polyethylene glycol-modified bovine ADA (PEG-ADA) could be discontinued in most of the patients. The selective advantage of gene-modified cells *in vivo* led to success in these trials [143,144,145,146,147]. The analysis of vector integration in HSCs before and up to four years after transfer in five patients did not show a clonal selection although integrations could be mapped in the proximity of proto-oncogenes like LMO2 and genes involved in growth and self-renewal, but repopulating cells led to a highly polyclonal T cell population [148].

Recently, a gene therapy trial was started to treat patients with the Wiskott-Aldrich syndrome (WAS) which is an X-linked recessive immunodeficiency caused by a mutation in the WAS protein (WASP) [149]. The WASP is responsible for the actin polymerization in hematopoietic cells with involvement in signaling, cell locomotion and formation of the immunological synapse. The defect leads to functional disturbance of T, B, NK cells and their restrained migration resulting in infections, autoimmunity and thrombocytopenia. Retrovirally gene-modified autologous HSCs were transfused into patients after partial myeloablation. The cells engrafted successfully and a sustained gene marking in the myeloid and lymphoid compartment as well as in platelets could be observed followed by long-term clinical improvement of the patients. Analysis of vector integration showed polyclonality of gene-marked cells with integrations in genes involved in cell growth and immune responses in two patients [149]. So far, nine out of ten patients could be successfully treated, but the first adverse event occurred in one patient who developed leukemia probably due to insertional mutagenesis [150].

So far, there is only one clinical study published which used a lentiviral vector for gene-correction of HSCs. The X-linked adrenoleukodystrophy (ALD) could be treated with autologous HSCs transduced

with a lentiviral vector encoding the ABCD1 gene which product is the ALD protein [151]. The deficiency leads to a severe demyelination in the brain. In this trial, two patients were treated and demyelination stopped after 14 and 16 months. Polyclonal engraftment was accomplished with 9 and 14 % gene-marking in the lymphoid compartment as analyzed after 24 and 30 months.

The described adverse events in patients only occurred in gene therapy trials using retrovirally gene-modified HSCs. The integration pattern of retroviral vectors clearly influenced the severe side effects which were promoted by the *in vivo* selection advantage of gene-corrected HSCs. So far, the usage of gene-modified T cells appears to be safe in patients. Leukemic patients treated with allogeneic stem cell transplantation received donor lymphocytes transduced with the suicide gene herpes simplex thymidine kinase (HSV-Tk) [152]. The safety mechanism is adopted in this treatment to eventually abandon GVHD. Analysis of the transferred T cells showed no clonal outgrowth up to 9 years after treatment [153]. Transduced T cells showed stable transgene expression, normal phenotype and function. Quantitative analysis revealed that one fifth of the genes nearby the integration site were affected in expression without influencing the phenotype. A more detailed analysis of transduced T cells in two patients was done and showed no clonal dominance but polyclonality of the transferred T cell population [154].

In gene-marking studies where T cells were transduced with the truncated NGF receptor (ΔLNGFR) and transferred into animals as well as into humans no T cell-related malignancies were observed [155]. Even the transduction with the T cell oncogenes LMO2, TCL1 or ΔTrkA did not lead to malignant transformation of T cells when transferred into lymphopenic RAG-1-deficient mice whereas HSCs were transformed by these oncogenes [156]. But recently, transformation of T cells was observed *in vitro* when the proto-oncogene LMO2 was retrovirally transferred. The evolving T cell clone could overgrow competitor T cells *in vitro* but did not show outgrowth *in vivo*. Integration site analysis revealed proximity of the vector to the *IL2RA* and *IL15RA* genes which were over-expressed. In this study, it was shown that LMO2 can act synergistically with IL-2 in the transformation process of T cells [157].

1.4 TETRACYCLINE-REGULATED GENE EXPRESSION

1.4.1 PRINCIPLE OF TETRACYCLINE-REGULATED EXPRESSION SYSTEMS

In 1992, a regulated expression system was described by Gossen and Bujard [158]. The tetracycline (tet)-regulated expression is turned on if tetracycline (Tc) or the derivative doxycycline (Dox) is removed from the system which is called Tet-Off (Figure 4). In 1995, Gossen published an expression system which was inducible by supply of Dox called Tet-On [159]. Both expression systems can be regulated by the amount of Tc or Dox and the expression level is comparable to strong constitutive promoters [160]. Most of the elements of the Tet-Off and Tet-On sytems are derived from *Escherichia coli* (*E. coli*). In these bacteria the Tet repressor protein (TetR) inhibits transcription of the genes in the Tn*10* transposon by binding to the tet operator sequence (*tetO*) if Tc is not present. The TetR was modified by fusion of its first 207 amino acids with the C-terminal 127 amino acids of the Herpes simplex virus type 1 VP16 activation domain which was identified by Triezenberg *et al.* [161]. This converts the former TetR into a Tc-controlled transactivator (tTA) which activates gene expression in absence of Tc or Dox. In the Tet-On system, the tTA is mutated in four amino acids and called "reverse" Tet repressor (rTetR) which can only activate gene expression in the presence of Dox [159]. The Tc-response element (TRE) is composed of seven direct repeats of the *tetO* followed by a minimal CMV promoter which carries deletions in the enhancer regions. The gene is driven by activation of TRE-CMV promoter region.

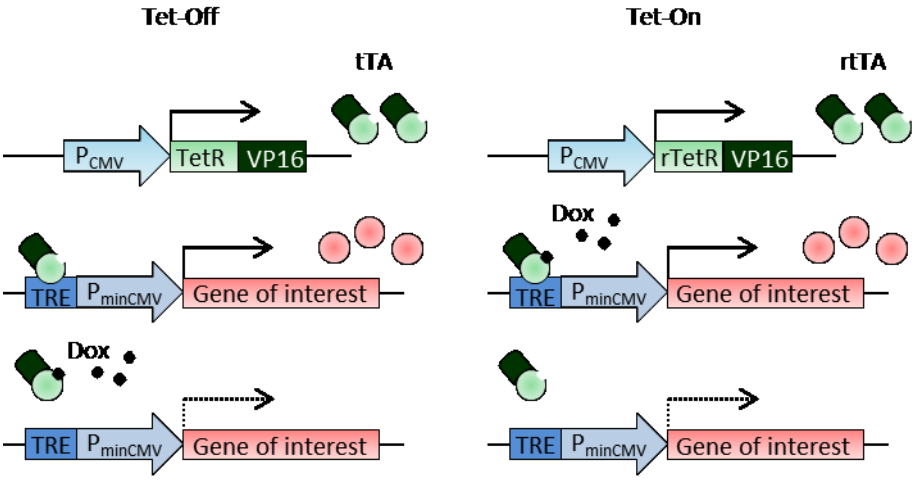

Figure 4 Schematic picture of the Tet-on and Tet-off system

The transactivator (tTA) (in green) is composed of a tet-repressor sequence (TetR) from *E. coli* and an activation domain VP16 from the Herpes simplex virus type 1. Its expression is constitutively driven by a CMV promoter (P_{CMV} in light blue). In the Tet-Off system it can bind to the Tet-responsive element (TRE) (in blue) which is fused to a minimal CMV promoter (P_{minCMV}). Transgene expression takes place (in pink). If Dox is added to the system

Dox-bound tTA cannot induce the expression anymore. In the Tet-on system the mutated rtTA can only induce expression when Dox is bound.

One difference between Tet-Off and Tet-On systems is that the Tet-On system is only responsive to Dox but not to Tc. Dox is compared to Tc more active, concentration from 0.01-1 µg/ml are enough compared to 1-2 µg/ml of Tc. These concentrations are below the cytotoxic level for cell culture and transgenic animals. The half-life of Dox is 24 h compared to only 12 h of Tc. Dox is therefore the preferable antibiotic.

In comparison to other eukaryotic regulatory elements, the Tet-system is specific in its gene regulation, provides higher and faster induction, only shows low background expression and can have higher expression levels than achieved with a constitutive promoter. Applications for the regulated systems have been established in mammalian, plant, amphibian, insect, and avian cell cultures and also in whole organisms like yeast, parasites, flies, amphibians and mammals like mice, rats, and nonhuman primates. In transgenic mice, the tTA or rtTA is engineered to be tissue-specific expressed and can be crossed to mice which express the tet-regulated gene of interest (for examples oncogenes like *myc*, *ras*, *BCR-ABL1,* genes involved in various diseases or cell signaling). Tc or Dox can be supplied in the drinking water to mice [162,163].

1.4.2 ESTABLISHED VECTORS FOR REGULATION OF GENE EXPRESSION

In original Tet-systems, the tTA and the gene of interest are provided on separate plasmids. The separation on two plasmids confers a tight regulation and high transcription level. Disadvantage is that two vectors have to be transferred into one cell which is not achievable for all target cells unless the transfer is done one after the other with a subcloning step in between. For primary cells this is not convenient [164]. All-in-one vectors which harbor all components of the Tet-system are more practical since a single transduction and selection round are sufficient. But these vectors conferred a higher background level and regulation of maximal 500-fold, even after clonal selection [165,166,167]. There are two types of All-in-one vectors. Either both elements are driven by a separate promoter or the transactivator is regulated by a positive feedback loop. In the first case, promoter interference can lead to low expression and regulation level and in the second case, a read-through is needed to start expression which interferes with a tight regulation. The first All-in-one vector was a γ-retroviral vector [168]. Here, the tTA was driven by the simian virus (SV) 40- or JC virus promoter and the responsive transgene cassette was either located directly downstream of the tTA in opposite direction or located in the U3 region of the 3'-LTR. Last mentioned option leads to a two copy provirus, since the U3 region is transferred to the 5'-LTR after reverse transcription. In an auto-regulatory All-in-one self-inactivating vector, the transgene is driven by a minimal CMV promoter

fused to the tandem TRE. The tTA is linked by an IRES site to the transgene. Basal transcription level of the promoter leads to minimal transcription of the gene cassette. tTA binds to the TRE sequences which leads to stronger transcription. In the presence of Tc, tTA does not bind to the promoter anymore and transcription is stopped [169]. Many modifications have been made to the Tet-system. The spacing of the *tetO* sequences could be reduced from 42 to 36 nucleotides which provided a better regulation [170]. By applying mutations an improved rtTA could be identified, rtTA2^{5}-M2, which has a 10-fold higher sensitivity to Dox, higher stability in eukaryotic cells and no background expression [171]. It was fused to a minimal domain derived from the transactivation VP16 domain. Also, retroviral or adenoviral vectors are available for both elements. There are several variants on the market of these systems, providing marker or selection genes, Tags, bidirectional gene expression [168] and reduced leakiness. New bidirectional All-in-one vectors were developed by Heinz *et al.* [172] comprising of the rtTA2^{5}-M2, new TRE-promoter (Ptet-T2, Ptet-T6, Ptet-T8, Ptet-T11) and with small alterations of the vector architecture which showed improved transgene induction of 220-14000 fold by strongly decreasing the background expression in HT1080 cells as measured by luciferase and GFP expression. The vector with the TRE-promoter Ptet-T2 was used for TCR expression in this work.

For the generation of regulated gene expression the insertion site of the Tet-vector is an important factor for the proper function. Enhancer and promoter region near the integration sites can lead to a background activity of the transgene or the insertion site negatively influences the regulation level of the transgene. Therefore, a selection of a cell clone can circumvent this problem. Also, the transduction with a low multiplicity of infection (MOI) should be performed [164].

2. OUTLINE OF THIS THESIS

The aim of this thesis was to determine the safety of TCR gene-modifed T cells. Two different safety concerns were approached. The first safety concern concentrated on the expression of two TCRs in gene-modified T cells and its consequences.

For that, an inducible transgene expression system should be analyzed for the suitability of TCR expression and its regulation in single TCR T cells.

Afterwards, a second TCR should be applied for the establishment of dual TCR T cells. The influence of the transgenic TCR on the endogenous TCR was to be characterized in terms of

- surface expression,
- expression level,
- functionality,
- TCR chain mispairing of both TCRs.

To improve safety of dual TCR T cells by avoiding mispaired TCR chains, a second cysteine bridge was applied in the constant regions of the examined TCRs. Its effect was analyzed by measuring the TCR surface expression, the functionality as well as the pairing of the TCR chains.

The effect of the cysteine bridge was to be determined not only in the established cell line clones with regulated TCR expression but also in primary transgenic and wild-type cells.

The second safety issue of TCR gene-modified T cells concerned the stability of the phenotype *in vivo*, since vector transduction harbors the risk of insertional mutagenesis. This risk should be analyzed in combination with repeated stimulation of TCR-transduced T cells *in vivo*. The transferred T cell populations was to be analyzed in regard to

- phenoytype before transfer,
- activation status after stimulations,
- functionality,
- proliferation capacity,
- vector integrations.

The recipient mice should be observed for occurring malignancies caused by the T cell transfer.

3. MATERIAL AND METHODS

3.1 MATERIAL

Table 1 Media

Medium	Content
CMM	RPMI 1640+GlutaMax1 (Gibco), 10 % heat-inactivated fetal calf serum (FCS, PAN Biotech), 100 U/ml penicillin/ streptomycin (Pen/ Strep, GIBCO), 1 mM N-2-hydroxyethylpiperazine-N'-2-ethanesulfonic-acid (Hepes) pH 7.25 (Sigma-Aldrich), 1 % sodium pyruvate (Gibco), 1 % non-essential amino acids (Gibco), 50 µM β-mercaptoethanol (Sigma-Aldrich)
PlatE medium	Dulbecco's modified Eagle's medium (DMEM, GIBCO), 10 % heat-inactivated FCS (Biochrom), 100 U/ml Pen/ Strep, 1 µg/ml puromycin (Sigma-Aldrich), 10 µg/ml blasticidin (MP Biomedicals)
T cell medium	RPMI 1640+GlutaMax1, 10 % FCS (PAN Biotech), 100 U/ml Pen/ Strep, 10 mM Hepes pH 7.25
LB agar	1.5 % agar (Roth) in LB medium
LB medium	1 % tryptone, 1 % NaCl, 0.5 % yeast extract (all Roth)
Soc medium	20 mM glucose, 2 % tryptone, 0.5 yeast extract, 10 mM NaCl, 2.5 mM KCl, 10 mM $MgCl_2$, 10 mM $MgSO_4$ (all Roth)

Table 2 Buffers

Buffer	Content
ACK lysis	150 Mm NH_4Cl (Merck), 1 mM $KHCO_3$ (Roth), 0.1 mM Na_2EDTA (Roth), pH 7.5
ELISA wash	1 x PBS, 0.05 % Tween-20 (Sigma-Aldrich)
FACS staining	1 x PBS, 0.01 % albumin from bovine serum (BSA, Sigma-Aldrich)
10 x phosphate-buffered salines (PBS)	80 g NaCL (Merck), 2 g KCl (Roth), 14.4 g Na_2HPO_4 (Merck), 2.4 g KH_2PO_4 (Roth)
RetroNectin(RN) wash	1 x PBS, 2,5 % 1 M Hepes
Transfection	1 % Hepes, 1.5 mM Na_2HPO_4, 270 mM NaCl, 10 mM KCl, pH 6.75

Table 3 Interleukine

Interleukine	Concentration used	Company
Human IL-2 (hIL-2)	40 U/ml	Chiron
Recombinant human IL-15 (hIL-15)	10/50 ng/ml	Preprotec

Table 4 Peptides

Peptide name	Amino acid sequence	Presented by	Antigen	Company
gp33	KAVYNFAT**M** (**M** is modified compared to wild-type)	H-2D_b	lymphochoriomeningitis virus glycoprotein gp_{33-41}	Biosynthan
Ova	SIINFEKL	H-2K_b	Ovalbumin$_{257-264}$	Biosynthan

Table 5 Reagents

Reagent cell culture	Concentration used	Company
Antibiotic/fungizide mix	200 U/ml	Gibco
Brefeldin A	10 µg/ml	Biolegend
BSA	0.1, 2 %	Sigma-Aldrich
Calcium chloride dehydrate ($CaCl_2$)	2.5 mM	Sigma-Aldrich
Carboxyfluorescein diacetate succinimidyl ester (CFSE)	5 mM stock	Invitrogen
Dimethyl sufloxide (DMSO)	10 %	Sigma-Aldrich
Ethylendiamin-tetraacetat (EDTA)		Sigma-Aldrich
Doxycycline (Dox)	1 mg/ml stock	Sigma-Aldrich
Gentamycin	10 µg/ml	Gibco
Sulfuric acid (H_2SO_4)	2 N	Roth
Ionomycin	1 µM	Calbiochem
Phorbol-12-myristate-13-acetate (PMA)	5 ng/ml	Sigma-Aldrich

Propidium iodide in PBS	100 ng/µl	Sigma-Aldrich
Protamine sulfate	4 µg/ml	Sigma-Aldrich
RetroNectin CH-296	25 µg/ml	TaKaRa Biomedicals
Trypsin-EDTA	0.05 %	Gibco
Reagent mice work	Concentration used	Company
ABX Vet Pack		Scil animal care
CpG oligodesoxynulceotides (CpG ODN) 1826	10, 50 µg/ml	TIB MOLBIOL
Dulbecco's PBS (DPBS)	1 x	Invitrogen
Endoxan (Cyclophosphamide)	100, 200 mg/kg	Baxter
Freund's adjuvant, incomplete (IFA)	100 µl	Sigma-Aldrich
Reagent molecular work	Concentration used	Company
Agarose	0.8-2 %	Serva
Ampicillin	100 µg/ml	Roth
Deoxynucleotides (dNTP)	200 µM each	Fermentas
Ethidium bromide	0.5 µg/ml	Sigma-Aldrich
DNA-1 kb		Invitrogen
Orange G		Sigma-Aldrich
Reagent LAM-PCR	Concentration used	Company
Aqua ad injectabilia (ddH_2O)		B Braun, Baxter
Dynabeads M-280 Streptavidin		Dynal, Invitrogen
Hexanucleotid mixture (Hexa-Nt)		Roche
LiCl	3, 6 M	Sigma-Aldrich
NaOH	0.1 N	Roth
Spreadex EL1200 precast gel		Elchrom Scientific
Tris-HCL	250 mM; pH 7.5	Sigma-Aldrich

Table 6 Antibodies and Multimeres

Antibody	Fluoro-Phore	Isotype	Clone	Concentration	Company
HA	Biotin	Mouse IgG_{2b},κ	12CA	0.2 mg/ml	Roche

HA	-	Mouse IgG_{2b},κ	12CA	0,2 mg/ml	Roche
Mouse CD3	-	Armenian hamster IgG_1	145-2C11	1 mg/ml	BD Pharmingen
Mouse CD8α	FITC, APC	Rat IgG_{2a},κ	53-6.7	0.2 mg/ml	BD Pharmingen
Mouse CD16/32	-	Rat IgG_{2b}	2.4G2		BD Pharmingen
Mouse CD28	-	Syrian hamster IgG_2	37.51	1 mg/ml	BD Pharmingen
Mouse CD44	PE	Rat IgG_{2b},κ	IM7	0.2 mg/ml	BD Pharmingen
Mouse CD62L	FITC, PE	Rat IgG_{2a},κ	MEL-14	0.2 mg/ml	BD Pharmingen
Mouse CD69	PE	Armenian Hamster IgG1, λ3	H1.2F3	0.2 mg/ml	BD Pharmingen
Mouse CD90.1	PE, PercP	Mouse IgG_1,κ	OX-7	0.2 mg/ml	BD Pharmingen
Mouse/Rat CD90.1	FITC, Biotin	Mouse IgG_{2a},κ	HIS51	0.2 mg/ml 0.5 mg/ml	BD Pharmingen
Mouse CD107α	PE	Rat IgG_{2a},κ	1D4B	0.2 mg/ml	BD Pharmingen
Mouse IFN-γ	APC	Rat IgG_1,κ	XMG1.2	0.2 mg/ml	BD Pharmingen
Mouse IgG (H+L) Fab Fragment	Cy5	Goat		1 mg/ml	Jackson Immunoresearch
Mouse vα2	APC	Rat IgG_{2a}	B20.1	0.1 mg/ml	Caltag
Mouse vβ5.1/5.2	PE	Mouse IgG_1,κ	MR 9-4	0.2 mg/ml	BD Pharmingen
Mouse vβ8.1/8.2	PE	Mouse IgG_{2a},κ	MR 5-2	0.2 mg/ml	BD Pharmingen
Myc	-	Mouse IgG_1	9E10	1 mg/ml	Hybridoma supernatant (ATCC CRL-1729)
Streptavidin	APC			0.2 mg/ml	BD Pharmingen

Tetramer	Fluorophore	Company
H-$2D_b$/KAVYNFATC	APC	Beckman Coulter
H-$2K_b$/SIINFEKL	APC, PE	Beckman Coulter

Table 7 Enzymes

Enzyme	Concentration used	Company

Fast-Link DNA ligation kit	2 U/µl	Epicentre Biotechnologies
Klenow Enzyme	2 U/µl	Roche
Maxima™ SYBR Green qPCR master mix		Fermentas
Phosphatase, alkaline	1 U/µl	Roche
Phusion Taq Polymerase	2 U/µl	Finnzymes
Rapid DNA Ligation Kit	5 U/µl	Roche
Restriction Enzymes	10 U/µl	Fermentas
Restriction enzyme Tsp509I, HpyCH4IV	10 U/µl	New England Biolabs
Taq polymerase	5 U/µl	Genaxxon

Table 8 Preparation kits

Preparation Kit	Usage	Company
Cytofix/Cytoperm™ Kit	Intracellular staining	BD Bioscience
EasyPure DNA Purification kit	DNA clean up from agarose gel	Biozym
Invisorb Spin Blood Mini kit	Mouse blood DNA preparation	Invitek
Invisorb Spin Plasmid Mini Two	DNA plasmid preparation	Invitek
Invisorb Spin Tissue Mini kit	Mammalian cell DNA preparation	Invitek
MinElute PCR Purification kit	Polymerase chain reaction (PCR) mix clean up	Qiagen
Mouse IFN-γ ELISA Set	Mouse IFN-γ detection	BD Bioscience
Mouse IL-2 ELISA Ready-SET-GO!	Mouse IL-2 detection	eBioscience
Plasmid Maxi, Midi kit	DNA plasmid preparation	Quiagen
QuiAmp DNA blood Mini kit	Mouse blood DNA preparation	Quiagen

Table 9 Plasmids

Transgene	Description	Vectors	Cloned by
OT-I-α	OT-I TCRα chain	MP71	Daniel Sommerrmeyer
OT-I-αHA	OT-I TCRα chain with HA tag at N-terminus	MP71; Tet	Simone Reuß
OT-I-β	OT-I TCRβ chain	MP71; Tet	Daniel Sommerrmeyer,

			Simone Reuß
OT-I-β-P2A-αHA	OT-I TCR with HA tag at N-terminus of TCRα chain	MP71; plSN; Tet	Simone Reuß
OT-I-β-P2A-αHAco	Codon-optimized TCR gene	MP71	Provided by Prof. Dr. Ton Schumacher, Simone Reuß
OT-I-β-P2A-αHA-cys -cocys	OT-I TCR with HA tag at N-terminus of TCRα chain; Second cystein bridge in constant region; Codon-optimized	MP71	Simone Reuß
P14-αDAN	P14 TCRα chain with two myc tags at N-terminus	MP71	Elisa Kieback
P14-β	P14 TCRβ chain	MP71	Daniel Sommermeyer
P14-β-P2A-α	P14 TCR	MP71	Elisa Kieback
P14-β-P2A-αDAN	P14 TCR with two myc tags at N-terminus of TCR α chain	MP71, plSN, Tet	Elisa Kieback, Simone Reuß
P14-β-P2A-αDANco	Codon-optimized TCR gene	MP71	Provided by Dr. Jehad Charo, Simone Reuß
P14-β-P2A-αDAN-cys -cocys	P14 TCR with two myc tags at N-terminus of TCRα chain; Second cystein bridge in constant region; Codon-optimized	MP71, plSN	Simone Reuß

Table 10 Primers

Primer Name	Usage	Primer Sequence 5'-3'
HA-fwd	OT-Ivα2HA	CCA TAT GAC GTC CCA GAT TAC GCG CAG CAG CAG GAG AAA CGT GAC CAG C
HA-rev	OT-Ivα2HA	GTA ATC TGG GAC GTC ATA TGG GTA GCC ATT CAC CCC AGC TAG GTG AAG G

OT-Ivα2-P2A-fwd	OT-Ivα2-P2A-fwd	AAC TTC TCT CTG TTA AAG CAA GCA GGA GAC GTG GAA GAA AAC CCC GGT CCC ATG GAC AAG ATT CTG ACA GCA ACG
vα2-NotI-fwd	OT-I/P14vα2	TTT GCG GCC GCC ATG GAC AAG ATT CTG ACA G
1. vα2-EcoRI-rev	OT-I/P14vα2	CCG GAA TTC TCA ACT GGA CCA CAG CCT CAG
2. vα2-EcoRI-rev	OT-I/P14vα2	TTA CTG AAT TCT CAA CTG GAC CAC AGC CTC
vα-cys-fwd	Cysteine bridge cα	CAC TGA CAA ATG TGT GCT GGA CAT G
vα-cys-rev	Cysteine bridge cα	CAT GTC CAG CAC ACA TTT GTC AGT G
vβ-NotI-fwd	OT-Ivβ5/ P14vβ8	CTG GCG GCC GCC ATG TCT AAC ACT GCC
vβ-P2A-rev	OT-Ivβ5/ P14vβ8-P2A-rev	TTC CAC GTC TCC TGC TTG CTT TAA CAG AGA GAA GTT CGT GGC GCC GCT TCC GGA ATT TTT TTT CTT GAC CAT GGC C
vβ-cys-fwd	Cysteine bridge cβ	ACA GTG GGG TCT GCA CGG ACC CTC AG
vβ-cys-rev	Cysteine bridge cβ	CTG AGG GTC CGT GCA GAC CCC ACT GT
Leader-fwd	Sequencing	CAG CAT CGT TCT GTG TTG TCT
PRE-rev	Sequencing	CAT TTA AAT GTA TAC CCA AAT CAA
β-Actin-fwd	Real-time PCR	ACC CAC ACT GTG CCC ATC TA
β-Actin-rev	Real-time PCR	CTC AGC TGT GGT GGT GAA GC
GFP-fwd	Real-time PCR	ACG TAA ACG GCC ACA AGT TC
GFP-rev	Real-time PCR	AAC TCC AGC AGT ACC ATG TG
M2-fwd	Real-time PCR	CGG CTG GGA GCA TGT CTA AG
M2-rev	Real-time PCR	GTC GGT ATC GAA GGC CTG AC
Neo-fwd	Real-time PCR	GGA TTG CAC GCA GGT TCT CC
Neo-rev	Real-time PCR	CGG CCA CAG TCG ATG AAT CC
vα2-fwd	Real-time PCR	CAT GAC CAG CAT CAG GTG AG
vα2-rev	Real-time PCR	CAG TCA ACG TGG CAT CAC AG
LC1	Linker cassette	GACCCGGGAGATCTGAATTCAGTGGCACAGCAGTTA GG
LC3	Linker cassette-Tsp509I	AATTCCTAACTGCTGTGCCACTGAATTCAGATC
LC5	Linker cassette-HpyCH4IV	CGCCTAACTGCTGTGCCACTGAATTCAGATC
LCI-fwd	Linker-fwd	GAC CCG GGA GAT CTG AAT TC
LCII-fwd	Linker-fwd	GAT CTG AAT TCA GTG GCA CAG
LTRa-bio-rev	5'LTR-rev, biotinylated	TGC TTA CCA CAG ATA TCC TG

LTRb-bio-rev	5'LTR-rev, biotinylated	ATC CTG TTT GGC CCA TAT TC
LTRII-bio-rev	5'LTR-rev, biotinylated	GAC CTT GAT CTG AAC TTC TC
LTRIII-rev	5'LTR-rev	TTC CAT GCC TTG CAA AAT GGC

Table 11 Handling material

Material	Volume/Size	Company
Cell strainers	40 µm	BD Flacon
Cryo-tubes	2 ml	Greiner
Culture flasks	25 cm^2, 75 cm^2, 150 cm^2	BD Flacon
Culture flasks	150 cm^2	Techno Plastic Products
FACS tubes		BD
Filters	0.2, 0.45 µm	Whatman
MaxiSorp plates	96-well	Nunc
Microcon YM-30	30 kDa nominal molecular weight limit	Millipore
Needle	0.4 x 20 mm, 27 G	B Braun
PCR tubes	100 µl	NeoLab
Pipettes	5, 10, 25 ml	
Plates, flat bottom	6-, 24-well	Greiner
Plates, round & flat bottom	96-well	Corning Costar
Polystryene tubes	15 ml	Greiner
Syringes	2, 5, 10, 30, 50 ml	B Braun
Tips	10, 200, 1000 µl	Eppendorf
Tips, filtered	10, 200, 1000 µl	Sorenson BioScience
Tubes	0.5, 1.5, 2 ml	Eppendorf
Tubes	15, 50 ml	BD Falcon

Table 12 Equipment

Equipment	Description	Company
Biofuge Pico	Centrifugation	Heraeus
Centrifuge 5810R	Centrifugation	Eppendorf
Centrifuge 5804R	Centrifugation	Eppendorf

Centrifuge 6K10	Centrifugation	Sigma
Centrifuge 3K12	Centrifugation	Sigma
Cryo-container	Freezing cells	Nalgene
Electrophoresis chamber	Agarose gel electrophoresis	Bio-Rad
FACSAria flow cytometer	Cell sorting	BD
FACSCalibur flow cytometer	Cell analysis	BD
FACS Lyse/Wash Assitant	Red blood cell lysis	BD
Gel documentation system	Ultraviolet light (UV) gel analysis	PeqLab
Gel electrophoresis apparatus SEA 2000	Electrophoresis	Elchrom Scientific
GeneRay UV-Photometer	DNA measurement	Biometra
HERA cell 240 incubator	37 °C, 5 % CO_2, 95 % humidity	Kendro Laboratory Products
Horizontal shaker KS 260 basic	Shaker	IKA
Lumi-Imager F1	UV light gel analysis	Roche
Microscope	Inverted micrscopy	Olympus
NanoDrop	DNA measurement	Thermo Scientific
Neubauer chamber	Cell counting	
Power Pac Universal	Electrophoresis, power supply	Bio-Rad
7300 Real-time PCR system	PCR	Applied Biosystems
Scil Vet abc	Murine blood cell counting	Scilvet
Thermocycler	PCR	Biometra
Vortex Genie 2	Vortexing	Bender & Hobein AG
µQuant	Enzyme-linked immune-sorbent assay (ELISA)	BioTek

3.2 METHODS

3.2.1 CELL CULTURING AND CELL PREPARATION

58 cells derived from the T cell lymphoma BW5147 were cultured in T cell medium. Cells were diluted 1:5 in fresh medium three times a week. PlatE cells derived from the 293T cell line expressing *gag-pol* and ecotrophic *env* genes [173]. Cells were cultured in DMEM and 10 % inactive FCS and used for ecotrophic virus production. MC57^{gp33high} clone 1 expresses a fusion gene of gp33 and GFP and is derived from MC57^{gp33low} fibrosarcoma cells treated with 200 nM 4-hydroxytamoxifen [174]. Cells were grown in DMEM with 5 % FCS. Adherent cells were trypsinated with 0.05 % trypsin-EDTA in PBS for 5 minutes (min) at 37 °C and then taken up 1:10 diluted in fresh medium. Murine splenocytes were cultured in CMM.

Freezing and thawing of cells

Frozen cells were kept at -80 °C or in liquid nitrogen in cryo-tubes. For freezing, cell lines were taken up in 500 µl T cell medium with 20 % FCS and 10 % DMSO, primary cells in 500 µl FCS and 10 % DMSO and then slowly cooled down to -80 °C in a cryo-container for 24 h. For thawing, cyro-tubes were shortly incubated at 37 °C; cells were washed with medium and taken up in medium for culturing.

Cell counting

Cells were counted in a 1:10 or 1:4 dilution with 10 µl cells, 30 µl (10 µl) trypan blue and 60 µl (20 µl) PBS in a Neubauer chamber.

Preparation of splenocytes, lymphnodes and bone-marrow

The spleen was cut out and smashed in a cell strainer with a plunger. Cells were washed through the cell strainer with 20 ml PBS and if needed, a second cell strainer was used. After centrifugation for 5 min at 400 g and 4 °C, cells were resuspended in 3 ml ACK lysis buffer and incubated for 3 min. 20 ml PBS was added and cells were centrifuged for 5 min at 400 g and 4 °C. The cells were washed a second time with PBS and then resuspended in CMM medium and activated as mentioned below. Lymphnodes (LN) were pooled and smashed in a cell strainer with a plunger. If necessary, red blood cells were lysed with ACK lysis buffer. Lymphnode cells were resuspended in PBS.

Bone-marrow (BM) was prepared by flushing the *femur* and *tibia* bones with PBS supplemented with 1 mM EDTA and 2 % FCS. Red blood cells were lysed with ACK lysis buffer. Cells were resuspended in PBS.

3.2.2 DNA TRANSFECTION BY CALCIUM PHOSPHATE PRECIPITATION

PlatE cells (1 x 10^6) were plated in 3 ml per well in a 6-well plate 24 h before transfection to obtain 80 % confluency of the cells. 18 µg of the transgene vector DNA was mixed in 150 µl destilled water (dH_2O) containing 15 µl calcium chloride dihydrate (2.5 mM). 150 µl of transfection buffer was added in drops during vortexing the DNA-water-$CaCl_2$ mix to generate DNA-calcium-phosphat-complexes. The transfection mixture was incubated for 15 min at room temperature (RT) and then added in drops on the plated cells. After 6 h incubation, the medium was carefully replaced by fresh medium. 48 h later, viral supernatant was harvested and filtered through a 0.45 µm filter. A second harvest of virus supernatant was done 24 h later.

3.2.3 VIRAL TRANSDUCTION

For transduction with viral particles, cells were seeded on RN-coated plates. For coating, 400 µl RN (25 µg/ml) was used per well on a 24-well plate and 1 ml on a 6-well plate. Coating was done for 2 h at RT. Afterwards; wells were blocked with 2 % BSA for 30 min at RT. Wells were washed with RN wash buffer.

Transduction of cell lines (58 cells)

1 x 10^5 cells were plated in a RN-coated 24-well plate per well and ml. 1 ml viral supernatant was added as well as 4 µg/ml protamine sulfate. The plate was spinoculated for 90 min at 800 g and 37 °C. The transduction was repeated 24 h later in the same way by replacing 1 ml with fresh viral supernatant.

Transduction of murine splenocytes

Freshly prepared splenocytes were activated for 24 h with 1 µg/ml anti-CD3 antibody, 0.1 µg/ml anti-CD28 antibody and 40 U/ml hIL-2. They were seeded in 3 ml CMM with 2 x 10^6 cells /ml per well in a RN-coated 6-well plate. The next day, 3 ml viral supernatant was added per well supplemented with 4 µg/ml protamine sulfate, 1 µg/ml anti-CD3 antibody, 0.1 µg/ml anti-CD28 antibody and 40 U/ml hIL-2. The 6-well plate was spinoculated for 90 min at 800 g and 37 °C. After 24 h, 3 ml was replaced with fresh viral supernatant supplemented with protamine sulfate and hIL-2 and the plate was again spinoculated. After spinoculation, 2 ml fresh medium with hIL-2 was added. For *in vitro* assays, splenocytes were washed and counted the next day. 1 x 10^6 cells /ml were seeded in fresh CMM medium with 10 ng/ml hIL-15 and analysis was done after two days. For the OT-I+P14 I and OT-I+GFP experiment *in vivo*, cells were transferred into mice 24 h after the last transduction. For the OT-I+P14 II experiment, cells were washed after the second transduction and resuspended in fresh CMM medium supplemented with 50 ng/ml rhIL-15. Three days later, cells were transferred into mice.

Determination of virus titer

For the safety analysis of transduced T cells *in vivo* the virus titer was determined by transducing 58 cells. GFP-virus was diluted 1:200 and P14 TCR-virus 1:100 in 2 ml and supplemented with 4 µg/ml protamine sulfate. The RN-plate was spinoculated. After 72h, the cells were analyzed for GFP or TCR expression, respectively. The calculation of the virus titer was as followed:

Virus titer/ ml = number of cells * GFP/P14-TCR-positive cells * dilution factor * division factor / volume

The division factor is 2 since cells had to divide for virus infection.

3.2.4 FUNCTIONAL ASSAYS

In a 96-well plate 1 x 10^5 effector cells and 1 x 10^5 peptide-loaded target cells were added in a volume of 200 µl. As a positive stimulation control 5 ng/ml Phorbol-12-myristate-13-acetate (PMA) and 1 µM Ionomycin was added. The negative control included target cells without peptide. Peptides were added directly to the coculture. After 4 or 24 h incubation at 37 °C, the supernatant was harvested for cytokine secretion analysis by enzyme-linked immune-sorbent assay (ELISA) or cells were harvested for intracellular cytokine staining, respectively. Experiments were repeated at least once.

Determination of secreted IL-2 or IFN-γ

Mouse IL-2 and IFN-γ were measured by an ELISA according to the manufacturer's manual but half of the volumes were used. A 96-well plate was coated with purified anti-mouse IL-2 or IFN-γ antibody in 1 x coating buffer (50 µl/ well) over night at 4 °C. Wells were washed three times with 300 µl ELISA wash buffer. Wells were then blocked with 100 µl 1 x assay diluent diluted in dH_2O for 1 h at RT. After the blocking step and a washing step as mentioned above, 50 µl of the cocultivation supernatant and standard dilutions of recombinant mouse IL-2 (200, 100, 50, 25, 12.5, 6.25 pg/ml) or mouse IFN-γ (2000, 1000, 500, 250, 125, 62.5 pg/ml) in 50 µl 1 x assay diluent were added in doublets and the plate was incubated for 2 h at RT. The plate was washed five times with 300 µl/ well ELISA wash buffer. For IL-2 detection, 50 µl of the detection antibody (biotinylated anti-mouse IL-2) diluted in 1 x assay diluent was added and incubated for 1 h at RT. After washing, 50 µl of streptavidin-horseradish peroxidase diluted in 1 x assay diluent was added and incubated for 30 min at RT. For IFN-γ detection, biotinylated anti-mouse IFN-γ and streptavidin-horseradish peroxidase was added in 50 µl 1 x assay diluent and incubated for 1 h at RT. The wells were washed again and then 50 µl of the substrate (1 x tetramethylbenzidine solution) was added. Incubation was done in the dark, and the

time of reaction was individually decided by judging the developing colour of the standard wells but was maximally 15 min. 50 µl 2 N H_2SO_4 solution stopped the reaction, and the plates were measured with the µQuant at 450 nm and 570 nm for background absorption. Values of 570 nm and the blank value were subtracted from values of 450 nm. A standard curve was drawn with the titrated standard protein concentrations and 450 nm-values. Unknown concentrations were calculated with help of the standard curve.

3.2.5 ANTIBODY-STAINING AND FLOW-CYTOMETRIC MEASUREMENT

Cell staining for fluorescence activated cell sorting (FACS) analysis

0.5 - 1 x 10^6 cells were harvested and resuspended in 50 µl FACS buffer with 0.5-1 µl antibody. The staining was done for 15 - 30 min at 4 °C. The stained cells were washed twice in FACS buffer and if necessary stained with a secondary antibody. The stained cells were analyzed with the FACSCalibur.

Quantification of TCR chains

To quantify TCR chains on the cell surface the Qifikit® from DAKO was used. Cells were stained with primary antibodies. Afterwards, they were stained with 1 µl anti-mouse IgG-FITC antibody in 50 µl FACS buffer. In parallel, 50 µl of set-up beads and of calibration beads were washed in 3 ml FACS buffer and then stained with 1 µl anti-mouse IgG-FITC antibody in 50 µl FACS buffer. After washing twice, the stained cells and beads were measured with the FACSCalibur. The stained set-up beads and unstained cells were used to adjust the photomultiplier tube (PMT) voltage to see the positively and negatively FITC-labeled fractions. Calibration beads were measured with excluding debris and doublets in the forward scatter versus side scatter. Without changing the settings the samples were measured afterwards. For the calculation of the antigen density per cell a calibration curve was determined. The mean fluorescence intensity (MFI) of the bead populations was determined with help of FloJo software and plotted against the antibody-binding capacity (ABC) of each bead population as indicated in the manufacturer's manual (Table 13). The MFI of the samples were determined and the antigen density was calculated with help of the equation of the calibration curve. The MFI of negatively stained cells was used for calculation of the background antibody equivalent (BAE) and subtracted from the ABCs of the samples. The experiment was repeated once.

Table 13 Antibody-binding capacity of bead populations

Calibration Bead	ABC
B	1600

C	10000
D	49000
E	184000
F	543000

DAKO Qifikit® REF K0078 LOT 00046689

FRET analysis

This technique is used to analyze the regional proximity of two molecules by labeling these with suitable fluorophores. One fluorophore serves as donor which transmits its energy after excitation to a nearby acceptor fluorophore which gets excited by non-radiative energy. Prerequisite for this energy transfer is the proximity of 10 nm of donor and acceptor molecule. The donor fluorophore emits light of a different wave length after this energy transfer which can be measured (Figure 5).

For FRET analysis, unstained cells were measured for calculation of the background MFI, single stained cells with the donor fluorophore and acceptor fluorophore for the determination of the correction factors S1-S4 and double stained cells for the calculation of the FRET efficiencies. For the FRET measurement, cells were stained with PE-labeled anti-TCRvβ chain antibodies and primary Tag antibodies (anti-Myc or anti-HA) in combination with an anti-mouse IgG-Cy5-labeled secondary antibody. The PE-fluorophore served as the donor molecule whereas the Cy5-fluorophore functioned as acceptor molecule. The cell clones were cultured with the indicated Dox concentrations and 24 h later stained for the above mentioned combinations. The stained cells were analyzed using a FACSCalibur without compensation. The FACS files were then analyzed with the FRET software Aflex, and FRET efficiencies were calculated. The same correction factors and the α-factor of 1 were used for all analyzed measurements. Stainings were repeated several times.

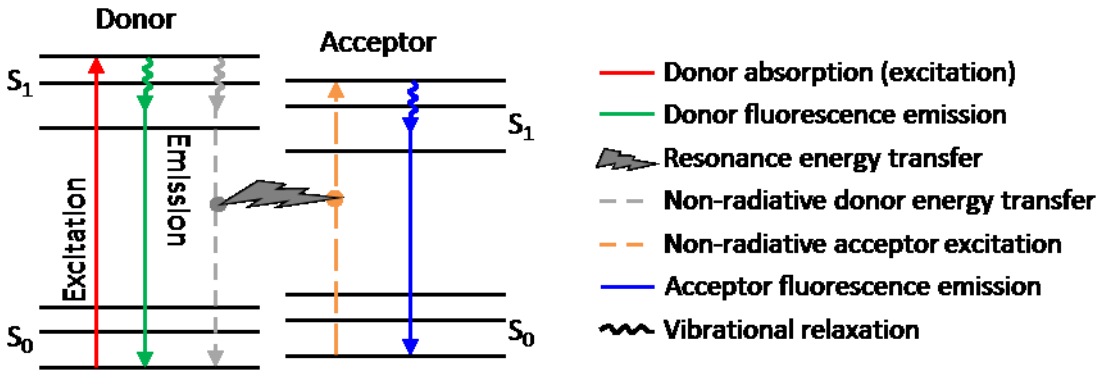

Figure 5 Jablonski Diagramm

Donor and acceptor energy levels are shown. S_0: the unexcitated status of the fluorohore electrons, S_1: excitated status of the fluorohore electrons. Donor fluorophore electrons can transmit energy in a non-radiated form to nearby acceptor fluorophore electrons. Diagram was adapted from the Olympus website.

IFN-γ-/CD107α-staining

Antibody against CD107α as well as Brefeldin A (10 µg/ml) and GolgiStop™ (1 µl/200 µl) was directly added to the cocultivation which was incubated for 4 h at 37 °C. Stimulated cells were harvested and stained first for surface antigens as described above. Then, intracelluar staining for IFN-γ was done with the Cytofix/Cytoperm™ kit. Cells were resuspended in 100 µl Cytofix/Cytoperm supplemented with 1 µl GolgiStop™ and incubated for 30 min at 4 °C. Cells were washed twice with 100 µl 1 x Perm/Wash buffer. Then IFN-γ antibody was added in 50 µl Perm/Wash buffer to the cells and cells were incubated for 20 min at 4 °C. After washing twice with 100 µl Perm/Wash buffer, cells were resuspended in 100 µl FACS buffer.

3.2.6 GENERATION OF TCR EXPRESSING CELL CLONES

The 58 T cell line was used for TCR expression since it does not express an endogenous TCR. To test functionality of MHC class I-restricted TCRs it was engineered to express the CD8α receptor. For the generation of cell clones, 1 x 10^6 transduced cells were stained with an antibody directed against the relevant antigen (TCR chain) as mentioned above. If necessary, the TCR expression was induced by adding 1 µg/ml Dox to the cell culture 24 h before the staining. Stained cells were resuspended in 500 µl PBS with 10 % FCS, 200 U/ml antibiotic/fungizide mix and 10 µg/ml gentamycin and given through a cell strainer into the sterile FACS tube. 96-well round-bottom plates were prepared with 1 x 10^3 irradiated unstained cells in 200 µl T cell medium with 200 U/ml antibiotic/fungizide mix and 10 µg/ml gentamycin. Before, cells were irradiated with 63 gray and washed twice with T cell medium. The single cell sorting of positively stained cells was performed with the FACSAria and one cell was added per well. After approximately 14 days, 100 µl medium was replaced with fresh T cell medium in wells with growing clones. 3 days later, 100 µl cell suspension was transferred into a new 96-well plate and used for antibody staining. Positively stained cells were expanded in culture for further analysis.

3.2.7 ANIMAL EXPERIMENTS

C57BL/6N mice were purchased from Charles River or Janvier. B6.PL-*Thy1*^{a}/CyJ mice were purchased from The Jackson Laboratory. This mouse strain is congenic for the T cell marker *Thy1*^{a} (Thy1.1= CD90.1), and T cells can be differentiated from T cells of C57BL/6 mice which have the congenic

marker CD90.2. B6.PL-*Thy1*^{a}/CyJ mice were bred to OT-I/Rag$^{-/-}$ mice (originating from C57BL/6-Tg(TcraTcrb)1100Mjb/J) to obtain OT-I/CD90.1/Rag$^{+/-}$ mice. Mice of the first generation which expressed both CD90.1 and CD90.2 and of the second generation which only expressed CD90.1 were used for donor cell preparation. Breeding and experiments were done in the animal facility of the Max Delbrück Center for Molecular Medicine, Berlin, Germany. Animal experiments were officially approved and permitted by the institute and the regional authority.

Adoptive T cell transfer

Cells were washed twice in DPBS and counted. 5 x 10^6 cells in 200 µl DPBS were injected intravenously into the tail vein, *vena caudalis mediana*, with a 0.4 x 20 mm needle.

Stimulation *in vivo*

The MC57^{gp33high} tumor cell line was trypsinated and washed twice with DPBS. 3 x 10^6 cells in 300 µl DPBS were injected subcutaneously with a 0.4 x 20 mm needle, 150 µl on each side.

Peptide (50 or 10 µg) and CpG ODN 1826 (50 or 10 µg) was mixed with 100 µl incomplete Freund's adjuvant (IFA) and adjusted to a volume of 200 µl with DPBS. To obtain a homogenous mixture a syringe with a 0.6 x 20 mm needle was used. 200 µl was injected subcutaneously, on each side 100 µl with a 0.4 x 20 mm needle.

Blood withdrawal and blood processing

Blood was taken with a Goldenrod animal lancet (MEDIpoint) from the *Vena facialis* which is located in the submandibular area without anesthesia. 50 - 100 µl blood was taken for DNA preparation with the QuiAmp DNA blood Mini kit or Invisorb Spin Blood Mini kit according to the manufacturer's manuals. Elution of the DNA was done in 200 µl dH_2O. For flow cytometry staining, 30 - 50 µl blood was incubated with 30 - 50 µl PBS and 0.3 - 0.5 µl antibody and anti-CD16/CD32 for FC-receptor blocking for 20 min in the dark at RT. Blood was either lysed with help of the FACS lysis /wash assistant or by adding 500 µl ACK lysis buffer. After 30 min incubation with ACK lysis buffer, cells were washed with 2 ml PBS and resuspended in 200 µl PBS.

***In vivo* proliferation**

5 mM carboxyfluorescein diacetate succinimidyl ester (CFSE) stock solution was diluted 1:500. 1 x 10^7 cells were resuspended in 900 µl PBS. 100 µl of CFSE was added to the cells (CFSE final: 1 µM), and cells were incubated for 15 min at 37 °C. CMM medium was added, and cells were washed. Cells

were resuspended in medium and incubated for 30 min at 37 °C. After washing with DPBS, cells were counted and CFSE-labeling was analyzed by FACS measurement. 3 x 10^6 cells in 200 µl DPBS were injected into the mouse tail vein. Stimulations were done right after as described above. After 4 days, spleens were processed and stained for CD90.1. CFSE dilution was measured by FACS on CD90.1-positive cells.

3.2.8 RETROVIRAL VECTORS

Tetracycline-regulated vector system

The used retroviral vector for inducible gene expression is a MLV SIN vector, where part of the U3 region of the 3'-LTR, which harbors promoter and enhancer functions, was deleted. This region is transferred to the 5'-end of the provirus during the reverse transcription process in the host cell and drives viral gene expression. In the tet-regulated vector transgene expression is driven by the T2-modified minimal CMV promoter (T2) which was constructed to harbor a *tetO* heptamer binding sequence (tetO7) (Figure 6). The M2 transactivator gene expression is constitutively driven by the human Pgk promoter in reverse direction to the transgene. When Dox binds to the M2 transactivator, it can bind to the *tetO* heptamer sequence of the CMV minimal promoter and transcription of the transgene is initialized. The tet-regulated vector was provided by Rainer Löw from the Euffets GmBH and from Niels Heinz from the lab of Christopher Baum at the Medical School Hannover [172].

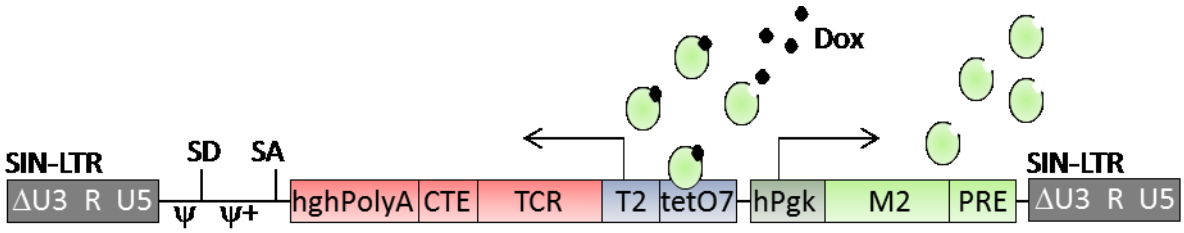

Figure 6 Schematic picture of the tet-regulated retroviral vector

SIN-LTR: deletions in Mo-MLV-3´-LTR: border (-448/-412; -74/-1, TATA-box mutated in core promoter); ψ, ψ+: Psi-binding signal for packaging of viral RNA into the viral particles; SA, SD: splice acceptor, splice donor; PRE: posttranscriptional regulatory element of the woodchuck virus; modified "atg" of ´X´-protein; M2: reverse transactivator; M2 variant; hPgk: human phosphoglycerate kinase promoter; tetO7: tet-operator heptamer, wt-DNA-sequence, 36 nt spacing from core to core, asymmetric operator fusion points; TCR: T cell receptor gene in the formation of TCRvβ chain-P2A-TCRvα chain; CTE: constitutive transport element of the simian retrovirus type 1; hghpA: human growth hormone polyA signal.

MP71 retroviral vector

The MP71 retroviral vector contains LTRs of the MPSV and a PRE of the woodchuck hepatitis virus. It also contains a modified mRNA splice site [92].

LXSN retroviral vector

The LXSN retroviral vector contains the promoter-enhancer elements of the Mo-MLV LTR which drive transgene expression. The SV40 promoter drives neomycin resistance [175].

3.2.9 T CELL RECEPTORS

The P14 TCR is specific for the lymphochoriomeningitis virus glycoprotein peptide gp_{33-41} (gp33) (KAVYNFATM) in a H2-D_b-restricted manner. It consists of the P14vα2 and P14vβ8 chain. The OT-I TCR is specific for the H2-K_b-restricted peptide $ova_{257-264}$ (ova) (SIINFEKL) of the antigen ovalbumin and harbors the OT-Ivα2 and OT-Ivβ5 chain. TCRs were cloned as a transgene into the tet-regulated vector, LXSN vector or MP71 vector in the formation of TCRvβ chain linked by a P2A element of the porcine teschovirus which then enables expression of the followed TCRvα chain.

Since the OT-I and P14 TCR harbor a TCRvα chain of the same family, the antibody directed against the TCRvα2 chain cannot distinguish between the OT-Ivα2 and the P14vα2 chain in dual TCR T cells. Therefore, the TCRvα2 chains were tagged with a short sequence at the N-terminus of the protein. The P14vα2 chain was tagged with two Myc sequences (EQKLISEEDL EQKLISEEDL) by Elisa Kieback and the OT-Ivα2 chain with the HA sequence (YPYDVPDYA). The additional sequences do not interfere with protein functionality and do not disturb the proper pairing of the corresponding TCRvβ chains. These modifications made it possible to distinguish the TCRvα chains by staining with antibodies directed against the Tags.

3.2.10 MOLECULAR CLONING OF GENES

Gene cloning by polymerase chain reaction

Polymerase chain reactions (PCRs) were conducted as stated in Table 14 and run as noted in Table 15. Annealing temperature was adjusted to the used primers. 1 µl 5 x loading buffer was added to 5 µl PCR reaction and the mixture as well as 8 µl of DNA-1 kb marker was applied on a 1 % agarose gel which was prepared with 0.5 µg/ml ethidium bromide. The gel was run at 120 V and bands were visualized by ultraviolet light (UV). PCR reaction products were purified using the MinElute PCR Purification kit and DNA was eluted in 10 µl elution buffer.

Table 14 PCR reaction mix

Reagents	Concentration used	Volume (µl)
Phusion polymerase buffer (Finnzymes)	10 x	5
dNTPs	200 µM each	1
Primer fwd	20 pmol/µl	1
Primer rev	20 pmol/µl	1
Phusion polymerase (Finnzymes)	2 U/µl	1
Template DNA	100 ng	
dH_2O		ad 50

Table 15 PCR cycles

Cycle number	Time and temperature
1	5 min 95 °C
2-35	1 min 95 °C, 45 s 58-64 °C, 45 s 72 °C
36	10 min 72 °C
Hold	4°C

PCR products were annealed as stated in Table 16 and Table 17 and amplified in following PCR cycles (Table 15) by adding 2 µl of 20 pmol/µl primer fwd and rev.

Table 16 Annealing reaction

Reagents	Concentration used	Volume (µl)
Phusion polymerase buffer (Finnzymes)	10 x	10
dNTPs	200 µM each	2
PCR product 1		4
PCR product 2		4
Phusion polymerase (Finnzymes)	2 U/µl	2
dH_2O		ad 100

Table 17 Annealing cycles

Cycle number	Time and temperature
1	5 min 95 °C
2	1 min 95 °C
3	Cool down from 95 °C - 45 °C, 5 °C in 30 s
4	1 min 72 °C
2-4	5 x
Hold	4 °C

PCR reaction product was purified with MinElute PCR purification kit and DNA was digested with restriction enzymes NotI and EcoRI. DNA was eluted in 32 µl dH_2O and 4 µl restriction buffer and 2 µl of each restriction enzyme was added. Digestion was done for 1 h at 37 °C. DNA was precipitated with 10 fold volume of 100 % ethanol by centrifugation at maximal speed at 4 °C. After washing with 2 fold volume 70 % ethanol, the dried DNA was dissolved in 10 µl dH_2O.

The MP71 vector DNA (4 µg) was digested as mentioned above and cohesive ends of the DNA were dephosphorylated with alkaline phosphatase to prevent re-ligation of vector DNA. To 40 µl digestion mix 6 µl 10 x dephosphorylation buffer, 53 µl dH_2O and 1 µl alkaline phosphatase was added and the mixture was incubated for 1 h at 37 °C. After 30 min, again 1 µl alkaline phosphatase was added. Vector DNA was analyzed by agarose gel electrophoresis. Under UV light the correct band was cut out and purified using the EasyPure DNA purification kit.

DNA concentrations of PCR fragment and vector DNA were estimated on a 1 % agarose gel with help of a DNA marker. For ligation, the ratio of vector and fragment size was calculated and a molar ratio of 1:3 was used with 100 ng vector DNA. In a 20 µl ligation mix, 10 µl 2 x ligation buffer, 4 µl 5 x ligation buffer, 1 µl rapid ligase, DNA and dH_20 was added and incubated for 5 min at RT. 10 µl of ligation mix were given to 100 µl chemically prepared competent Mach1^{TM} *E. coli* (Invitrogen) and incubated for 20 min on ice. Heat shock was done with the bacteria for 45 seconds at 42 °C. After incubation for 1 min on ice, 1 ml Soc medium was added to the bacteria and the mix was incubated for 1 h at 37 °C and 220 rpm. Bacteria were plated on a LB agar plate supplemented with 100 µg/ml ampicillin. The plate was incubated over night at 37 °C.

Bacterial colonies were isolated and incubated in 3 ml LB medium over night at 37 °C. Plasmid DNA was prepared using the Invisorb Spin Plasmid Mini Two kit according to the manual. Control digestion was done with purified DNA. DNA was sequenced using primers Leader-fwd and PRE-rev by the

company Eurofins MWG Operon. Correct plasmid DNA (100 ng) was transformed in Mach1™ *E. coli* as described above. A colony culture was set up for a Maxi DNA preparation. The quality of plasmid DNA preparation was checked by control enzymatic digestion.

In Table 18 plasmids are listed which were generated as described above by PCR with stated primers.

Table 18 Plasmids generated by PCR

Generated plasmid	Template DNA	PCR1, PCR2, PCR3	Annealing PCR
MP71-OT-IαHA	MP71-OT-Iα	vα2-NotI-fwd, HA-rev	vα2-NotI-fwd, 1. vα2-EcoRI-rev
	MP71-OT-Iα	HA-fwd, vα2-EcoRI-rev	
MP71-OT-I-β-P2A-αHA	MP71-OT-Iβ	vβ-NotI-fwd, vβ-P2A-rev	vβ-NotI-fwd, vα2-EcoRI-rev
	MP71-OT-IαHA	OT-Ivα2-P2A-fwd, vα2-EcoRI-rev	
MP71-OT-I-βcys-P2A-αHAcys	MP71-OT-I-β-P2A-αHA	vβ-NotI-fwd, vβ-cys-rev	vβ-NotI-fwd, vα2-EcoRI-rev
	MP71-OT-I-β- P2A-	vβ-cys-fwd, vα-cys-rev	
	αHA		
	MP71-OT-I-β- P 2A-αHA	vα-cys-fwd, vα2-EcoRI-rev	
MP71-P14-βcys-P2A-αDANcys	MP71-P14-β-P2A-αDAN	vβ-NotI-fwd, vβ-cys-rev	vβ-NotI-fwd, vα2-EcoRI-rev
	MP71-P14-β-P2A-αDAN	vα-cys-fwd, vα-cys-rev	
	MP71-P14-β-P2A-αDAN	vα-cys-fwd, vα2-EcoRI-rev	

Gene cloning by enzymatic digestion

The cloning of genes into the pLXSN vector and the Tet vector was done by enzymatic digestion as shown in Table 19. For generating the Tet vectors (Tet) an intermediate plasmid with the M2 promoter (M2) was used in a first cloning step. Afterwards, the transgene with the M2 promoter cassette was excised and inserted into the final Tet vector.

Table 19 Plasmids generated by enzymatic digestion

Generated Plasmid	Template Plasmid	Cut with	Target Plasmid	Cut with
pLSN-OT-I-β-p2a-αHA	MP71-OT-I-β-P2A-αHA	NotI, EcoRI; Klenow-Fillin	pLSN	Hpa1 (blunt)
pLSN-P14-β-P2A-αDAN	MP71-P14-β-P2A-αDAN	NotI, EcoRI; Klenow-Fillin	pLSN	Hpa1 (blunt)
M2-OT-I-β-P2A-αHA	MP71-OT-I-β-P2A-αHA	NotI, EcoRI; Klenow-Fillin	M2	Bsp1407I, NcoI; Klenow-Fillin
M2-P14-β-P2A-αDAN	MP71-P14-β-P2A-αDAN	NotI, EcoRI; Klenow-Fillin	M2	Bsp1407I, NcoI; Klenow-Fillin
Tet-OT-I-β-P2A-αHA	M2-OT-I-β-P2A-αHA	NotI, XhoI	Tet	NotI, XhoI
Tet-P14-β-P2A-αDAN	M2-P14-β-P2A-αDAN	NotI, XhoI	Tet	NotI, XhoI
M2-OT-I-β	MP71-OT-I-β	NotI, EcoRI; Klenow-Fillin	M2	Bsp1407I, NcoI; Klenow-Fillin
M2-OT-αHA	MP71-OT-I-αHA	NotI, EcoRI; Klenow-Fillin	M2	Bsp1407I, NcoI; Klenow-Fillin
Tet-OT-I-β	M2-OT-I-β	NotI, XhoI	Tet	NotI, XhoI
Tet-OT-αHA	MP71-OT-I-αHA	NotI, XhoI	Tet	NotI, XhoI

Digested DNA which did not have the same overhangs as the target plasmid was filled up with the Klenow enzyme. Digested DNA was precipitated with ethanol and dissolved in 16.6 µl H_2O, 0.4 µl dNTP, 2 µl Klenow puffer and 1 µl Klenow enzyme. The reaction was incubated for 10 min at RT and for 20 min at 37 °C. Target plasmid was filled up to 100 µl with H_2O for dephosphorylation reaction and purified after agarose gel electrophoresis with the EasyPure DNA purification kit. Insert-DNA was purified by ethanol precipitation or after agarose gel electroporesis.

3.2.11 Determination of vector copy number integration by real-time PCR

The determination of the number of integrated vectors per cell was performed by means of real-time PCR. Vector specific primers (Table 10) were used to detect the proviral DNA, and normalisation was done with detection of the housekeeping gene β-actin. A calibration curve of detected DNA was done with titrated plasmid in untransduced cells. For all samples, 10 ng DNA was used and vector-specific and β-actin detection was done in triplets ,and the PCR was repeated once. 20 µl of the MaximaTM SYBR Green qPCR master mix was used, and 5 µl of DNA was added. The PCR was run with the 7300

Real-time PCR system. ΔCT values were determined with help of the system software. In the calibration curve ΔCT values ($CT_{\beta\text{-actin}}$- $CT_{plasmid}$) were calculated and plotted against copy number in a log scale. ΔCT values were calculated for the samples ($CT_{\beta\text{-actin}}$- CT_{vector}) and solved for the copy number with help of the equation of the calibration curve. For the calculation it was assumed that one cell contains 6,81 pg DNA. The copy number integration was calculated per cell and the transduction efficiency was taken into account. For the Tet vector cell clones a factor of 1 was taken for the transduction efficiency since ~100 % TCR-positive cell clones were used.

3.2.12 LINEAR AMPLIFICATION-MEDIATED PCR

Linear PCR

Linear amplification-mediated (LAM) PCR was performed after the protocol by Schmidt *et al*. [176] and done in the lab of Prof. von Kalle, NCT, Heidelberg. The LAM-PCR protocol was developed for the determination of vector integration sites in the target genomic DNA (Figure 7).

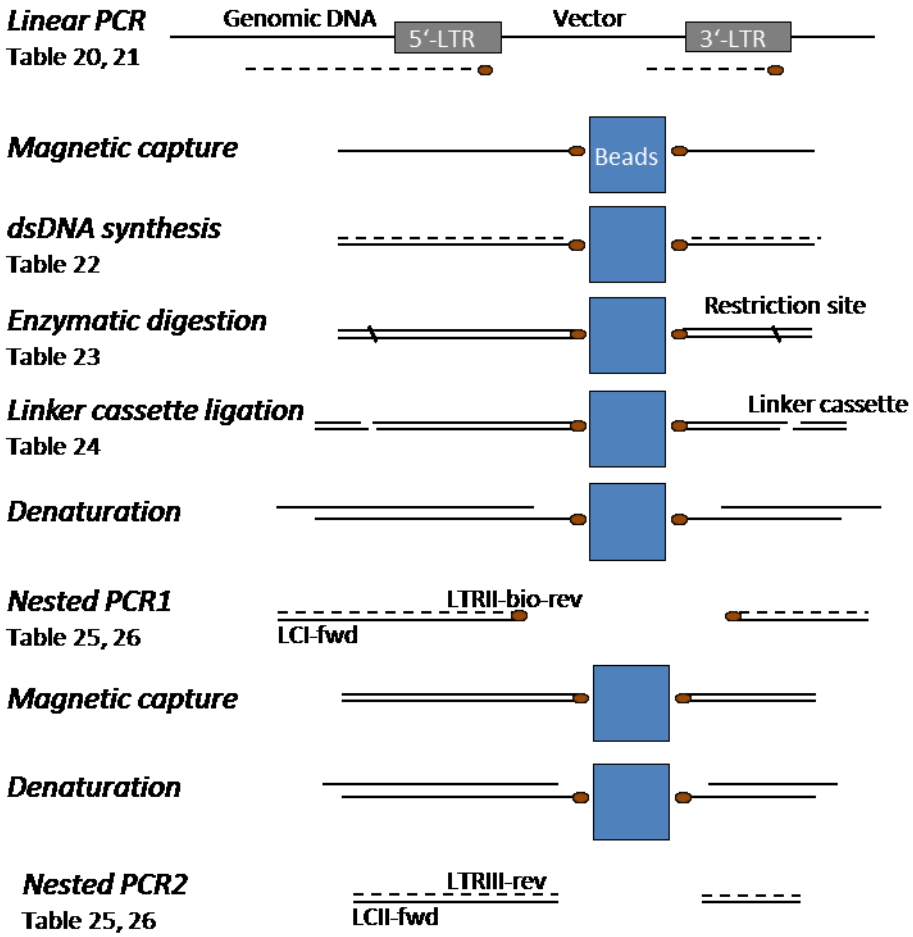

Figure 7 LAM-PCR

Experimental set-up of the LAM-PCR. Adapted from [176]. Blue quadrates represent the beads. In brown Biotin bound to DNA is shown.

100 ng DNA was used in a volume of 50 µl for a linear PCR with 5'-biotinylated primers which bind in the 5'-LTR. After the first run, 0.25 µl Taq polymerase was added to each tube and a second round of PCR cycles was done (Table 20, Table 21).

Table 20 Linear amplification mix

Reagents	Concentration used	Volume (µl)
Taq polymerase buffer (Quiagen)	10 x	5
dNTPs	200 µM each	1
Primer LTRa-bio-rev	0.5 pmol/µl	0.25
Primer LTRb-bio-rev	0.5 pmol/µl	0.25
Taq polymerase (Genaxxon)	5 U/µl	0.5
Genomic DNA	100 ng	
ddH_2O		ad 50

Table 21 PCR cycles

Cycle number	Temperature
1	5 min 95 °C
2-51	1 min 95 °C, 45 s 60 °C, 90 s 72 °C
52	10 min 72 °C
Hold	4 °C

Magnetic capture

Magnetic beads were prepared. 20 µl per reaction was taken and put on a magnet. Supernatant was taken, and beads were diluted in 40 µl PBS with 0.1 % BSA. The washing step was repeated once. Then, beads were washed with 20 µl 3 M LiCl and resuspended in 50 µl 6 M LiCl. Beads were mixed with 50 µl PCR reaction mixture and incubated over night at RT and 300 rpm.

dsDNA synthesis

The PCR-bead mix was washed with 100 µl ddH_2O on the magnet and then resuspended in 20 µl Hexa-Nt priming mix. The reaction was done for 1 h at 37 °C (Table 22).

Table 22 Hexanucleotid priming

Reagents	Concentration used	Volume (µl)
Hexa-Nt	10 x	2
dNTPs	200 µM each	0.5
Klenow enzyme	2 U/µl	1
ddH_2O		16.5

80 µl ddH_2O was added to the reaction and put on the magnet. Supernatant was withdrawn and samples were washed with 100 µl ddH_2O.

Enzymatic digestion of DNA

The DNA was then digested with either HypCH4IV or Tsp509I restriction enzyme in a 20 µl reaction volume for 1 h at 37 °C (Table 23).

Table 23 Enzymatic digestion

Reagents	Concentration used	Volume (µl)
Restriction buffer	10 x	2
Enzyme	10 U/µl	0.4
ddH_2O		17.6

Ligation of the linker cassette to the DNA

DNA-bead mix was washed with 80 µl and 100 µl ddH_2O as described above. In a 10 µl volume a linker cassette was ligated to the digested DNA. The ligation was performed for 5 min at RT (Table 24).

Preparation of the linker cassette

The linker cassette had to be prepared in advance. 40 µl of LC1 (100 pmol/µl), 40 µl of LC2 (100 pmol/µl), 10 µl of $MgCl_2$ (100 mM) and 110 µl of annealing buffer (Tris-HCL (250 mM; pH 7.5)) was mixed and incubated for 5 min at 95 °C. The reaction mixture was then cooled slowly to 4 °C. After 6 - 24 h, 300 µl ddH_2O was added and the mixture was transferred to a Microcon-30 column which was centrifuged for 12 min at 15000 g and RT. The reversed column was placed on a new 1.5 ml tube and centrifuged for 3 min at 1000 g and RT. The dropped-down volume was adjusted to 80 µl with ddH_2O. The linker cassette was frozen in aliquots of 10- 20 µl each and only used once.

Table 24 Ligation

Reagents	Concentration used	Volume (µl)
Ligation buffer	10 x	1
ATP	10 mM	1
Ligase	2 U/µl	1
Linker cassette	n.d.	2
ddH_2O		5

Denaturation of DNA

The DNA was washed with 90 µl and 100 µl ddH_2O on the magnet and then denaturated with 5 µl 0.1 N NaOH for 10 min at RT and 300 rpm on a horizontal shaker.

Nested PCRs

The denaturated DNA was placed on the magnet and 2 µl of the supernatant which contained single-stranded unbiotinylated DNA was used for a nested PCR with primer LCI-fwd and LTR-bio-rev (Table 25, Table 26).

Table 25 Nested PCR

Reagents	Concentration used	Volume (µl)
Taq polymerase buffer (Quiagen)	10 x	5
dNTPs	200 µM each	1
Primer LCI-fwd/LCII-fwd	16.67 pmol/µl	0.5
Primer LTRII-bio-rev/LTRIII-rev	16.67 pmol/µl	0.5

Taq polymerase (Genaxxon)	5 U/µl	0.5
Denaturated DNA		2/1
ddH_2O		40.5

Table 26 PCR cycles of nested PCR

Cycle number	Temperature
1	5 min 95 °C
2-35	1 min 95 °C, 45 sec 60 °C, 90 s 72 °C
36	10 min 72 °C
Hold	4 °C

20 µl beads were prepared as described above, except that they were taken up in 20 µl 6 M LiCl. Beads were mixed with 20 µl of the PCR reaction mixture and incubated over night at RT and 300 rpm on a horizontal shaker. After incubation, DNA was washed with 60 µl and 2 x 100 µl ddH_2O on the magnet and denaturated with 20 µl 0.1 N NaOH for 10 min at RT and 300 rpm on a horizontal shaker. 1 µl of the supernatant was used for a second nested PCR with primers LCII-fwd and LTRIII-rev as stated in Table 25 and Table 26. For analysis 5 µl of the PCR reaction was mixed with loading buffer and run on an agarose gel or spreadex gel.

3.3 COMPANIES

Table 27 Companies

Company	City, Country
Applied Biosystems by Life Technologies	Carlsbad, USA
ATCC	Manassas, USA
Baxter	Unterschleissheim, Germany
BD Bioscience	Heidelberg, Germany
BD Falcon	Franklin Lakes, USA
BD Pharmingen	Heidelberg, Germany
Beckman Coulter	Krefeld, Germany
Bender & Hobein	Zurich, Switzerland
Biochrom	Berlin, Germany
Biolegend	Fell, Germany
Biometra	Goettingen, Germany
Bio-Rad	Munich, Germany
Biosynthan	Berlin, Germany
BioTek	Bad Friedrichshall, Germany
Biozym	Hessisch Oldendorf, Germany
B Braun	Melsungen, Germany
Calbiochem by Merck	Darmstadt, Germany
Caltag Laboratories	Karlsruhe, Germany
Charles River	Sulzfeld, Germany
Chiron	Marburg, Germany
Corning Costar	Munich, Germany
Chiron	Marburg, Germany
Dako by Biozol	Eching, Germany
eBioscience	San Diego, USA
Elchrom Scientific	Cham, Switzerland
Epicentre Biotechnologies	Madison, USA
Eppendorf	Hamburg, Germany
Eurofins MWG Operon	Martinsried, Germany
Fermentas	St. Leon-Rot, Germany

Finnzymes	Lafayette, USA
Genaxxon	Ulm, Germany
Gibco	Karlsruhe, Germany
Greiner Bio-One	Frickenhausen, Germany
Heraeus	Buckinghamshire, UK
Invitek	Berlin, Germany
Invitrogen by Life Technologies	Darmstadt, Germany
Jackson Immunoresearch	West Grove, USA
Kendro Laboratory Products	Langenselbold, Germany
MEDIPoint	New York, Germany
Merck	Darmstadt, Germany
Millipore	Schwalbach/TS., Germany
MP Biomedicals	Illkirch Cedex, France
Nalgene	Rochester, USA
NeoLab	Heidelberg, Germany
New England Biolabs	Ipswich, USA
Nunc	Langenselbold, Germany
PAN Biotech	Aidenbach, Germany
Peprotech	Hamburg, Germany
Quiagen	Hilden, Germany
Roche Diagnostics	Mannheim, Germany
Roth	Karlsruhe, Germany
Scil animal care	Viernheim, Germany
Serva	Heidelberg, Germany
Sigma-Aldrich	Taufkirchen, Germany
Sorenson BioScience	Salt Lake City, USA
TaKaRa Biomedicals	Otsu, Japan
The Jackson Laboratory	Bar Harbor, USA
Techno Plastic Products	Trasadingen, Switzerland
Thermo Scientific	Karlsruhe, Germany
TIB MOLBIOL	Berlin, Germany
Tree Star	Ashland, USA
Whatman	Middlesex, UK

4. RESULTS

4.1 SAFETY ANALYSIS OF T CELLS EXPRESSING TWO TCRS

4.1.1 CHARACTERIZATION OF THE TETRACYCLINE-REGULATED TCR EXPRESSION

For the safety analysis of TCR gene-modified T cells a model was established in which the regulation of TCR expression was possible. The influence on the endogenous TCR by different amounts of transgenic TCR molecules should by analyzed. The regulated TCR-transgene expression was conferred by a tet-regulated vector.

TCR expression could be induced

Clones of 58 cells were generated either expressing the P14 or the OT-I TCR in a tet-regulated fashion. The inducibility of the TCR gene expression was analyzed by adding different Dox concentrations. Cells were analyzed by staining of the TCR chains with TCRα- and TCRβ-antibodies 24 h later (Figure 8A). A clear TCR-positive population appeared with 0.01 µg/ml Dox (58+P14tet: 17 ± 7 %; 58+OT-Itet: 9 ± 6 %). For 58+P14tet TCR-positive cells increased from 60 ± 1 % with 0.05 µg/ml Dox to 88 ± 9 % with 0.1 µg/ml Dox which already indicated maximal TCR expression (Figure 8A, white bars). The clone 58+OT-Itet had an increase in TCR-positive cells from 55 ± 9 % to 69 ± 16 % with 0.05 to 0.1 µg/ml Dox. With 0.5 µg/ml Dox, the 58+OT-Itet cells clearly reached its maximal TCR expression with 86 ± 5 % TCR-positive cells (Figure 8A, black bars). When comparing the two cell clones 58+P14tet cells showed slightly more TCR-positive cells with 1 µg/ml (91 ± 7 %) than 58+OT-Itet cells (88 ± 7 %).

The expression level of the transgenic TCR was determined by the mean fluorescence intensity (MFI) of both TCR chains. TCR expression level was only slightly over background with 0.01 µg/ml Dox but was well detectable with 0.05 µg/ml Dox. It increased from 0.05 to 1 µg/ml Dox differently for each TCR chain in both cell clones (Figure 8B and C). In 58+P14tet cells the P14vα2 chain increased in its expression level as measured by MFI between 0.05 and 0.1 µg/ml Dox from 9 ± 1 to 19 ± 6 and the P14vβ8 chain from 12 ± 4 to 24 ± 9 (Figure 8B). Whereas the MFI of the P14vα2 chain did not further increase, the P14vβ8 chain did increase to 38 ± 11 with 0.5 µg/ml Dox. The MFI of the OT-I TCR chains in the 58+OT-Itet cells had an increase between 0.05 and 0.1 µg/ml from 7 ± 1 to 13 ± 5 for OT-Ivα2 chain and from 9 ± 1 to 17 ± 4 for the OT-Ivβ5 chain (Figure 8C). The OT-Ivα2 chain increased further in its MFI with 0.5 µg/ml Dox to 21 ± 7 but did not further increase with 1 µg/ml Dox (22 ± 6). The OT-Ivβ5 chain showed higher MFI of 22 ± 5 and 32 ± 8 for 0.5 and 1 µg/ml Dox, respectively. The expression level as measured by the MFI of the TCR chain stainings indicated for both cell clones the

lowest expression level with 0.05 µg/ml Dox. Although the TCRα and TCRβ chains should be expressed equally on the cell surface, differences in MFI were detected which might be due to properties of the antibodies used.

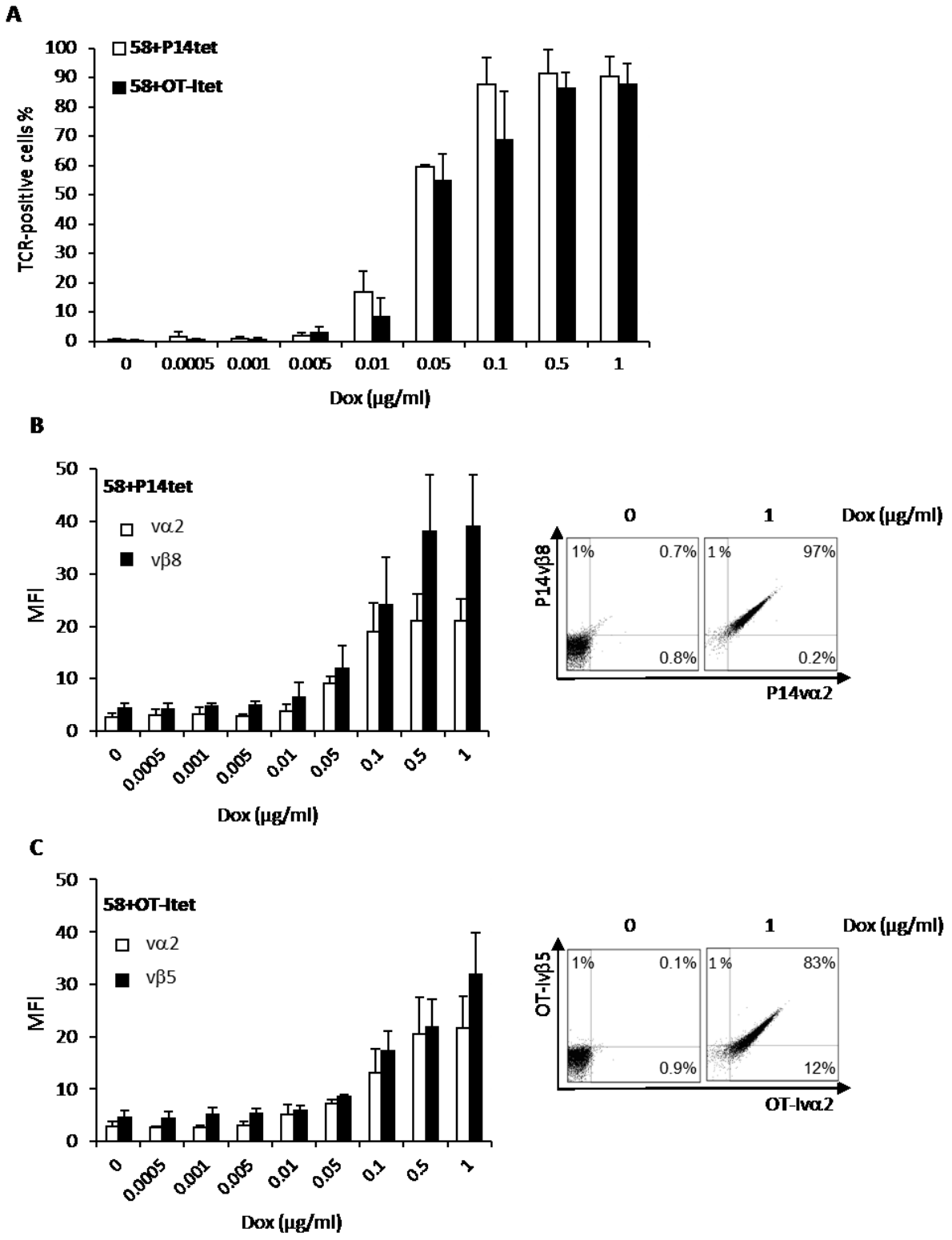

Figure 8 Characterization of tet-inducible P14 and OT-I TCR expression

Cells were incubated for 24 h with different concentrations of Dox. The TCRvβ chains were stained with anti-vβ5-PE for the OT-I TCR and anti-vβ8-PE for the P14 TCR. TCRvα2 chains were stained with an APC-labeled antibody. A: Percentages of TCRvα2 and TCRvβ chain-positive cells are shown of 58+P14tet and 58+OT-Itet cells. B: left side: MFI of each TCR chain of 58+P14tet cells, right side: representative TCR staining of 58+P14tet cells incubated without or with 1 µg/ml Dox. C: left side: MFI of each TCR chain of 58+OT-Itet cells, right side: representative TCR staining of 58+OT-Itet cells incubated without or with 1 µg/ml Dox.

High TCR expression was obtained already after 13 hours in 58+P14tet cells or 15 hours in 58+OT-Itet cells and was lost again after 72 hours

Cells were analyzed for the time needed to express the TCR on the cell surface after induction with 1 µg/ml Dox. Cells were taken after indicated hours for TCR staining. After 3 h, first TCR expression could be detected (Figure 9). After 8 h, 58+P14tet cells already showed 89 ± 3 % TCR-positive cells which increased to 95 % after 13 h and 97 ± 2 % after 24 h. In 58+OT-Itet cells, high TCR expression was reached after 13 h with 88 %. It slightly increased to 95 ± 3 % TCR-positive cells after 15 h and 93 ± 3 % after 24 h. Therefore, maximal TCR expression was reached after 13 h or 15 h in 58+P14tet cells or 58+OT-Itet cells, respectively. After deprivation of Dox the TCR expression was lost after 72 h in both cell clones.

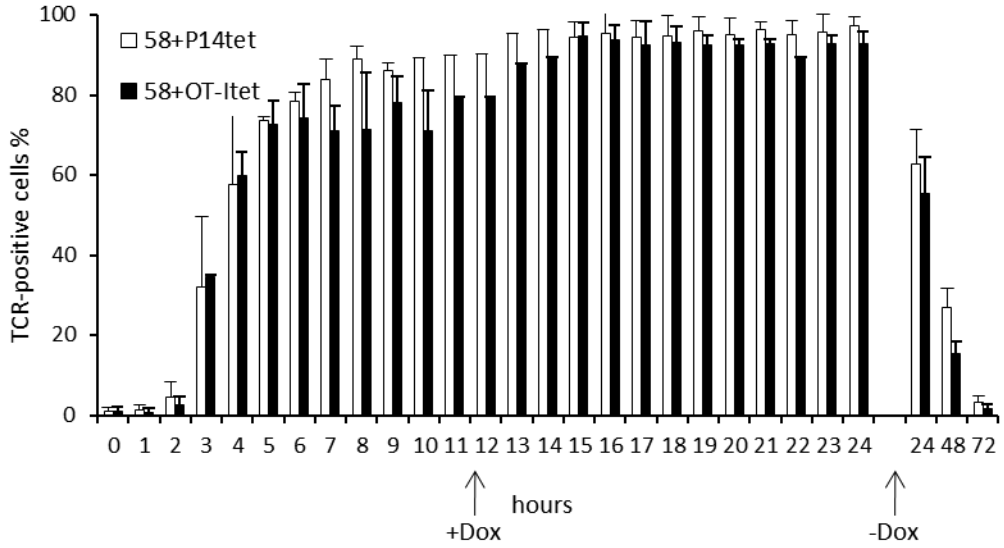

Figure 9 Percentage of TCR-positive cells after different time points of Dox treatment

Cells were incubated for different hours with 1 µg/ml Dox and then stained for TCR chains. Staining was done with anti-vα2-APC for both vα TCR chains, anti-vβ8-PE for the P14 TCR and anti-vβ5-PE for the OT-I TCR.

TCR expression conferred functionality corresponding to percentage of TCR-positive cells

The induced TCR expression was tested for functionality. The 58 cell line is a hybridoma originating from a CD4 T cell and is therefore capable of IL-2 secretion. The OT-I and P14 TCR are originated from CD8 T cells and only function in combination with the co-receptor CD8. The CD8α chain is sufficient for these TCRs to maintain their functionality, therefore the CD8α chain was introduced into the 58 cells used in this work.

Cell clones were incubated with stated Dox concentrations to induce different amounts of TCR expression. 10 µM of cognate peptide, gp33 or ova, was loaded on irradiated splenocytes as APCs which were cocultured with the cell clones 58+P14tet and 58+OT-Itet, respectively. The amount of secreted IL-2 increased mostly with the Dox concentration (Figure 10) due to the induced TCR expression of both cell clones (see Figure 8A). First TCR expression was seen with 0.01 µg/ml Dox in Figure 8A which is also indicated by IL-2 secretion of 58+P14tet cells in this experiment, whereas 58+OT-Itet cells already secreted IL-2 with 0.005 µg/ml Dox. In 58+P14tet cells, IL-2 secretion increased thereafter until treatment with 0.5 µg/ml Dox. The IL-2 amount in 58+OT-Itet cells increased only subtle. In conclusion, induced P14 TCR expression led to slightly higher IL-2 secretion when treated with high concentrations of Dox whereas the level of IL-2 secreted by 58+OT-Itet cells did not further increase with more than 0.01 µg/ml Dox. As a control unloaded splenocytes (w/o) were used which did not trigger IL-2 secretion. The maximal stimulus was given by PMA and Ionomycin (Max) which led to high amounts of secreted IL-2.

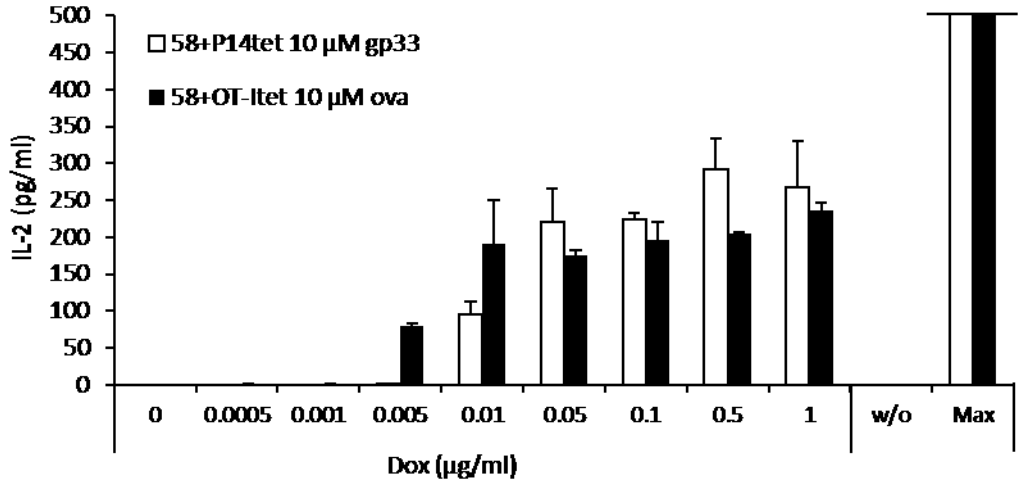

Figure 10 Inducible TCR expression resulted in Dox-dependent IL-2 secretion

Cell clones were cocultivated with irradiated splenocytes loaded with 10 µM peptide (gp33 for P14 TCR and ova for OT-I TCR) and different concentrations of Dox as indicated. As control no peptide (w/o) or an unspecific

stimulus with PMA and Ionomycin (Max) was added. Supernatant was taken 24 h later and employed in an anti-mouse IL-2 ELISA. Max values were 728 ± 6 pg/ml IL-2 for 58+P14tet cells and 740 ± 76 pg/ml IL-2 for 58+OT-Itet cells.

4.1.2 DUAL TCR EXPRESSING T CELLS

In TCR gene therapy, T cells which already express an endogenous TCR are transduced with a therapeutic TCR. To analyze the properties of those T cells the two TCR-tet-regulated cell clones were transduced with a second TCR representing the endogenous one. The 58+P14tet clone was transduced with the OT-I TCR and the 58+OT-Itet clone with the P14 TCR. As a transfer system the LXSN vector was chosen. This vector supports a constitutive TCR expression level which allows simultaneous inducible TCR expression. The inducible TCR represents here the transgenic TCR. Cell clones transduced with the LXSN vector were taken for further analysis after subcloning. The cell clones were named as 58+OT-I+P14tet and 58+P14+OT-Itet (Table 28).

Table 28 Designation of Dual TCR expressing T cells

Cell designation	TCR expression	
	Endogenous (Constitutive)	Inducible (Transgenic)
58+OT-I+P14tet	OT-I	P14
58+P14+OT-Itet	P14	OT-I

After second TCR induction both TCRs were coexpressed on the cell surface

The generated cell clones were incubated with different amounts of Dox and 24 h later analyzed for constitutive and induced TCR expression by flow cytometry. In the 58+OT-I+P14tet clone, the transgenic P14 TCR could be induced with 1 µg/ml Dox in up to 96 % cells as measured by TCRα- and β-positive cells. At the same time, the endogenous constitutive OT-I TCR stayed on the cell surface of all cells (Figure 11A). In the 58+P14+OT-Itet clone, the inducible OT-I TCR expression was measured on 87 % cells whereas the endogenous P14 TCR surface expression was slightly reduced from 99 % down to 93 % TCR-positive cells with 1 µg/ml Dox (Figure 11B).

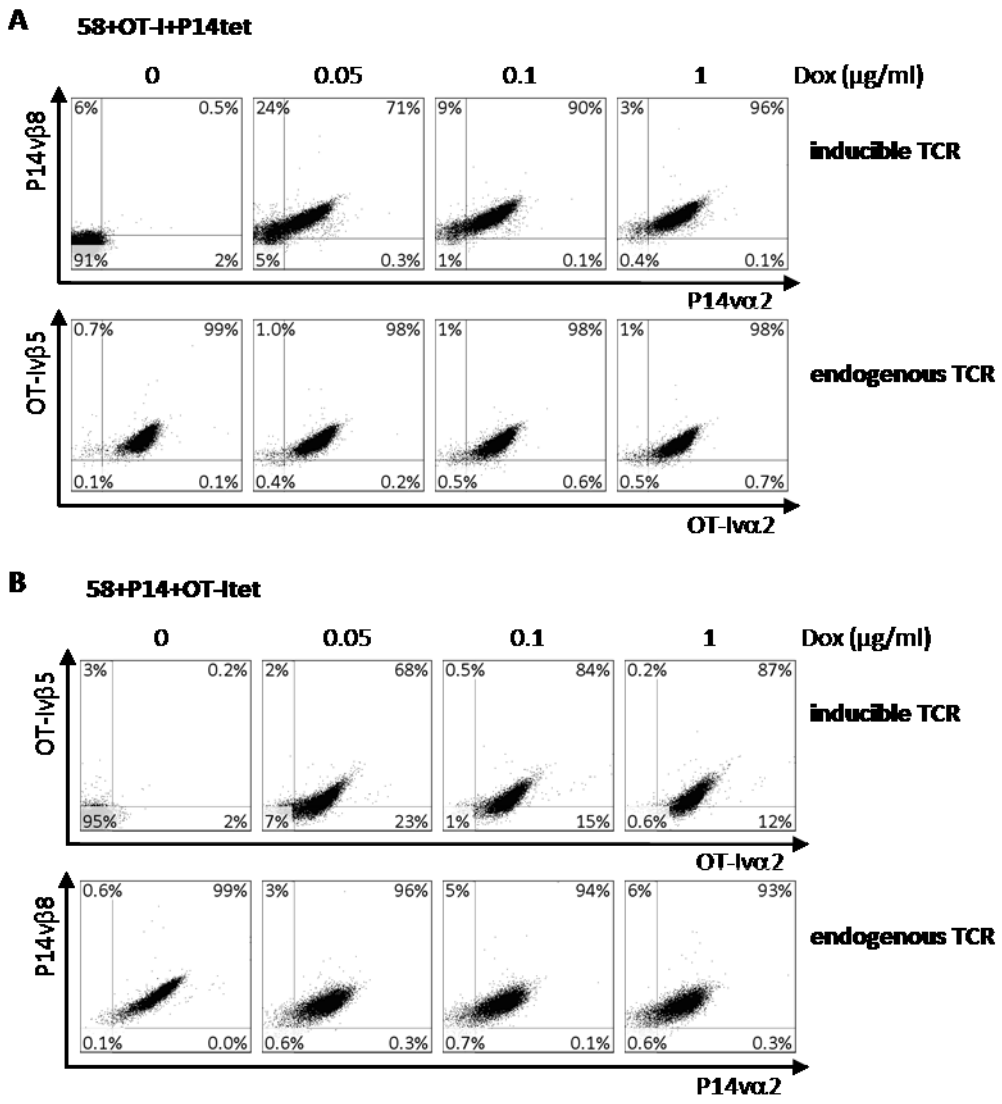

Figure 11 Induction of TCR expression led to coexpression with the endogenous TCR

After 24 h with Dox, A: 58+OT-I+P14tet; B: 58+P14+OT-Itet cells were taken for staining of the induced and the endogenous TCR. The sequential staining was done with anti-HA antibody for the OT-Ivα2 chain and anti-Myc antibody for the P14vα2 chain, the tag primary antibodies were then labeled with anti-mouse IgG-Cy5. Finally, the TCRvβ chains were stained with anti-vβ5-PE for the OT-I TCR and anti-vβ8-PE for the P14 TCR.

Inducible TCR expression effected the expression level of the endogenous TCR

Although the percentage of cells expressing the endogenous TCR did not change, when the inducible TCR came to the surface, the expression level of the endogenous TCR chains partially changed (Figure 12). The induced TCR of both cell clones increased in its TCR chain fluorescence intensity with increasing Dox concentration, although between 0.1 and 1 µg/ml Dox no difference was seen (Figure 12 upper row). In the 58+OT-I+P14tet clone, the endogenous OT-Ivα2 TCR chain decreased but not

the vβ5 TCR chain. In the 58+P14+OT-Itet cells, both endogenous P14 TCR chains were reduced in their expression level as determined by their mean fluorescence intensity (MFI) (Figure 12 lower row).

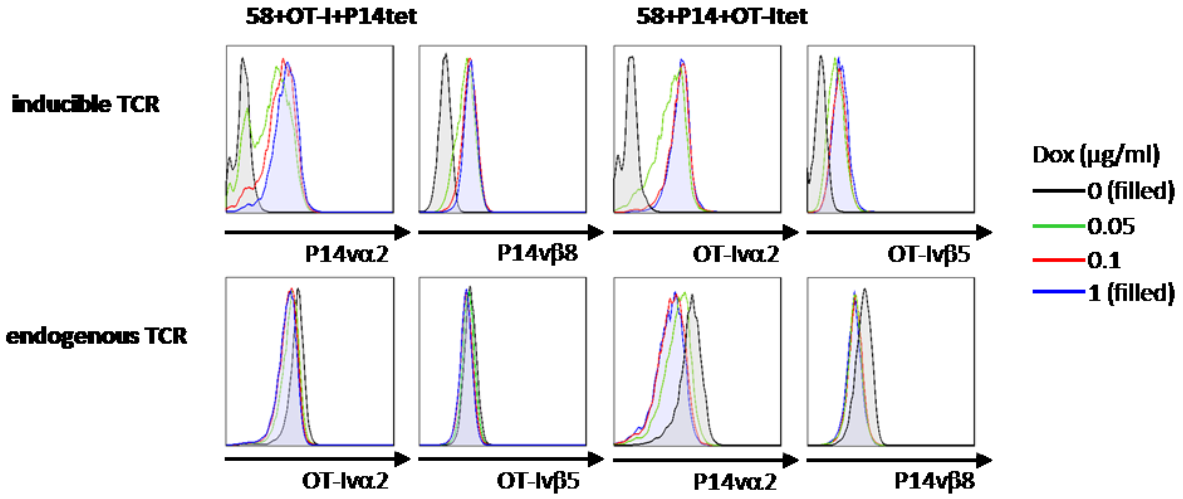

Figure 12 Inducible TCR expression lowered the MFI of endogenous expressed TCR chains

TCR stainings from Figure 11 were analyzed as histograms for each TCR chain.

Quantification of endogenous TCR chains showed a reduction of surface expression level

The reduced surface TCR expression level of the endogenous TCRs after induction of the tet-regulated TCR was analyzed in more detail. The staining shown in Figure 11 and Figure 12 was biased by the used antibodies and different fluorophores. To obtain equal conditions for the staining of all TCR chains primary antibodies were used which were then labeled with a FITC-labeled secondary antibody directed against the murine IgG region. For the quantification of the FITC-signal beads with different amounts of IgG were labeled with the FITC antibody. The measured MFI were correlated to the antibody-binding capacity (ABC) of the beads as stated by the manufacturer (Figure 13A). With help of a calibration curve (Figure 13B) the antigen density per cell was determined with the measured MFI of each TCR chain.

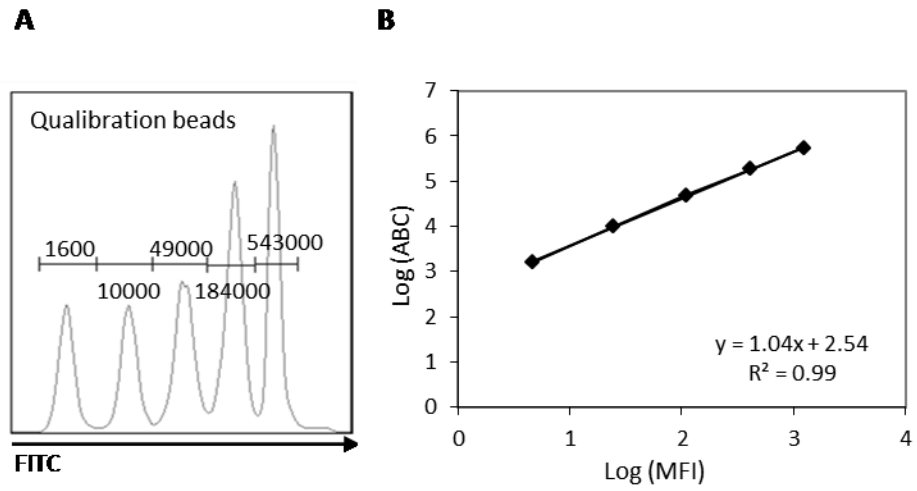

Figure 13 FITC-labeled beads for quantification of FITC fluorescence intensity

A: Histogram of FITC-labeled beads. Indicated numbers show antibody-binding capacity per bead (ABC) as given by the manufacturer. B: MFI of the gated bead populations plotted against the ABC values in a calibration curve.

The endogenous TCRs (in blue) of both cell clones were reduced in surface expression when the inducible TCR expression was induced, although differences between Dox concentrations were only subtle (Figure 14). The amount of the endogenous OT-I TCR chain molecules in 58+OT-I+P14tet cells was 1830 ± 480 for the OT-Ivα2 chain and 1910 ± 210 for the OT-Ivβ5 chain without Dox (Figure 14A). The total amount of the induced P14 TCR chains was more (P14vα2: 1670 ± 460 and P14vβ8: 1850 ± 560) as for the OT-I TCR (OT-Ivα2: 940 ± 360 and OT-Ivβ5: 820 ± 130) with 1 µg/ml Dox. By setting the antigen density of the endogenous TCR chains without Dox as 100 % the decrease of each TCR chain on the cell surface could be calculated in percentage. In the 58+OT-I+P14tet clone, the OT-Ivα2 chain was decreased by 49 % and the OT-Ivβ5 chain by 57 % with 1 µg/ml Dox. In the other cell clone, the endogenous P14 TCR had 4360 ± 1080 of P14vα2 chain molecules and 3200 ± 440 P14vβ8 chain molecules on the cell surface (Figure 14B). The amount of the P14 TCR chains stayed at higher levels (P14vα2: 1600 ± 780 and P14vβ8: 1970 ± 400) as compared to the induced OT-I TCR (OT-Ivα2: 1280 ± 680 and OT-Ivβ5: 830 ± 50). In 58+P14+OT-Itet cells, the P14vα2 chain was stronger decreased (63 %) as the P14vβ8 chain (39 %) when the antigen density without Dox was set as 100 %. The quantified staining confirmed the results of the staining presented in Figure 12 but here, the reduction of the TCR β chains was also seen.

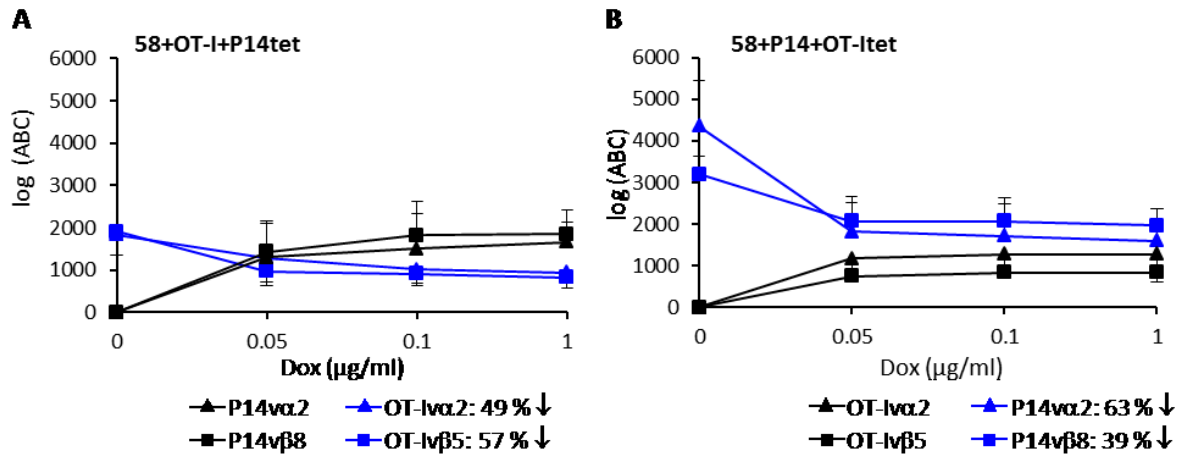

Figure 14 Quantified TCR staining of TCR chains showed a reduction of cell surface expression of the endogenous TCR

After 24 h Dox, A: 58+OT-I+P14tet; B: 58+P14+OT-Itet cells were taken for staining, either with anti-vβ8-Biotin, anti-vβ5-Biotin, anti-Myc or anti-HA-Biotin. In a second staining step, cells were labeled with anti-IgG-FITC. TCR chain amounts were calculated with help of a calibration curve determined by staining of calibration beads. Background staining with each antibody was subtracted. The reduction of the endogenous TCR chains was calculated in percentage by setting the ABC values without Dox as 100 %.

Functionality of the endogenous TCR was lost when the expression of the second TCR was induced

To analyze the functionality of the dual TCR T cells cocultivations with peptide-loaded splenocytes were done. The peptide amounts were titrated from 10^{-5} M to 10^{-9} M. The cell clones were simultaneously incubated with a low (0.05 µg/ml) and a high Dox concentration (1 µg/ml). In 58+OT-I+P14tet cells, the induced P14 TCR led to IL-2 secretion which was according to TCR-positive cells higher for 1 µg/ml as for 0.05 µg/ml Dox (Figure 15A). At the same time, the endogenous OT-I TCR led to a reduced secretion of IL-2 when the P14 TCR expression was induced with 0.05 µg/ml and was even more reduced with 1 µg/ml Dox. For both TCRs the amount of IL-2 secreted was titrated by the peptide concentrations. In 58+P14+OT-Itet cells, the inducible OT-I TCR led to IL-2 amounts according to TCR-positive cells with the low and high Dox supply (Figure 15B). The IL-2 amount was according to the peptide concentration from 10^{-7} to 10^{-10} M. With both Dox concentrations the endogenous P14 TCR lost its function and did hardly lead to IL-2 secretion after stimulation.

The endogenous TCR had a reduced functionality in 58+OT-I+P14tet cells and even lost its functionality in 58+P14+OT-Itet cells, although TCR expression was still observed on the cell surface as shown before in both cell clones.

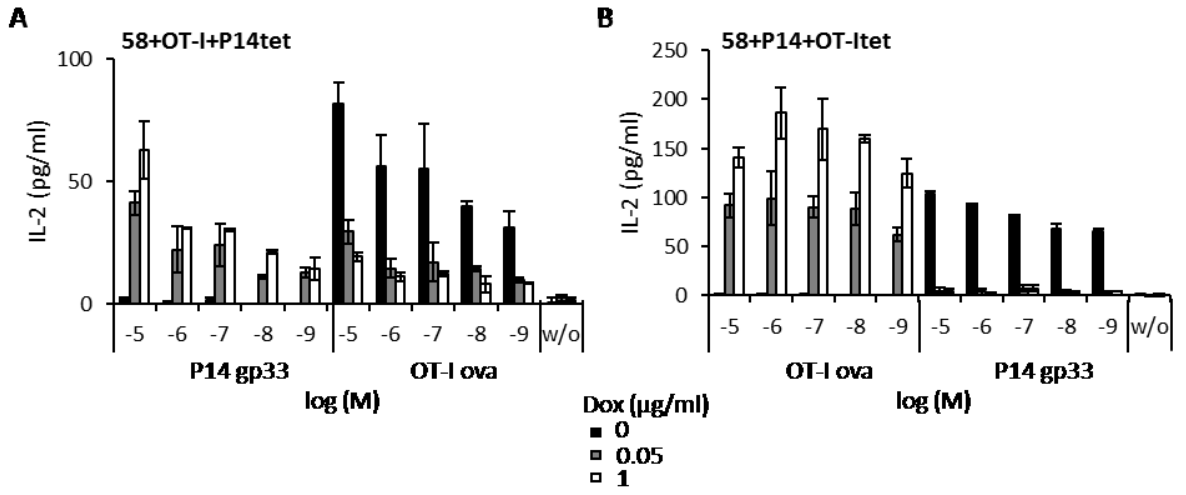

Figure 15 IL-2 secretion analysis showed functionality loss of the endogenous TCR when the expression of the second TCR was induced.

A: 58+OT-I+P14tet; B: 58+P14+OT-Itet cells were cocultivated with irradiated splenocytes loaded with indicated peptide concentrations (gp33 for P14 TCR and ova for OT-I TCR). Indicated Dox concentrations were added to the coculture. As control no peptide (w/o) was added. Supernatant was taken 24 h later and employed in an anti-mouse IL-2 ELISA.

4.1.3 TCR CHAIN INTERACTIONS

The lost functionality of the endogenous TCR led to the question why surface expression, although reduced in expression level, was still detectable on the cell surface of both cell clones. We hypothesized that the TCR chains of the one TCR could form a TCR dimer with the chains of the other TCR. The mispaired TCR dimers could be another reason beside the reduced surface expression for the loss of functionality of the endogenous TCR. To investigate this hypothesis FRET measurements were done in collaboration with Zolt Sebestyén (Erasmus University Rotterdam, Netherlands).

On dual TCR T cells mispaired TCR dimers could be detected by FRET

FRET measurements were done with the cell clones 58+OT-I+P14tet and 58+P14+OT-Itet without and with Dox. All possible combinations were stained when the expression of the second TCR was induced: P14vα2 and P14vβ8 for the correct pairing of the P14 TCR, OT-Ivα2 and OT-Ivβ5 for the correct pairing of the OT-I TCR, OT-Ivα2 and P14vβ8 for a mispaired TCR dimer and P14vα2 and OT-Ivβ5 for the second possible mispaired TCR dimer. For all combinations FRET efficiencies could be calculated. In 58+OT-I+P14tet cells, the FRET efficiency of the constitutively expressed OT-I TCR did not change when P14 TCR expression was induced (without Dox: 34 ± 5 %, with Dox: 32 ± 8 %) (Figure 16A). The induced P14 TCR had a lower FRET efficiency (23 ± 8 %) as the OT-I TCR but which

was as high as the mispaired TCR combination of OT-Ivα2 chain and P14vβ8 chain (23 ± 8 %). The FRET efficiency of the second mispaired TCR dimer of P14vα2 and OT-Ivβ5 was the lowest (12 ± 7 %). In the other cell clone, the constitutive P14 TCR dropped in its FRET efficiency when the second TCR was induced in its expression (without Dox: 35 ± 3 %, with Dox: 19 ± 6 %) (Figure 16B). The FRET efficiency for the induced OT-I TCR was 25 ± 6 % which was also here similar to the mispaired TCR combination of OT-Ivα2 chain and P14vβ8 chain (21 ± 8 %) The second mispaired TCR version of P14vα2 and OT-Ivβ5 had a lower FRET value (12 ± 3 %). The detected mispaired TCR dimers in both cell clones and the reduced FRET efficiency of the endogenous P14 TCR in 58+P14+OT-Itet cells explained the lost or reduced functionality of the endogenous TCRs.

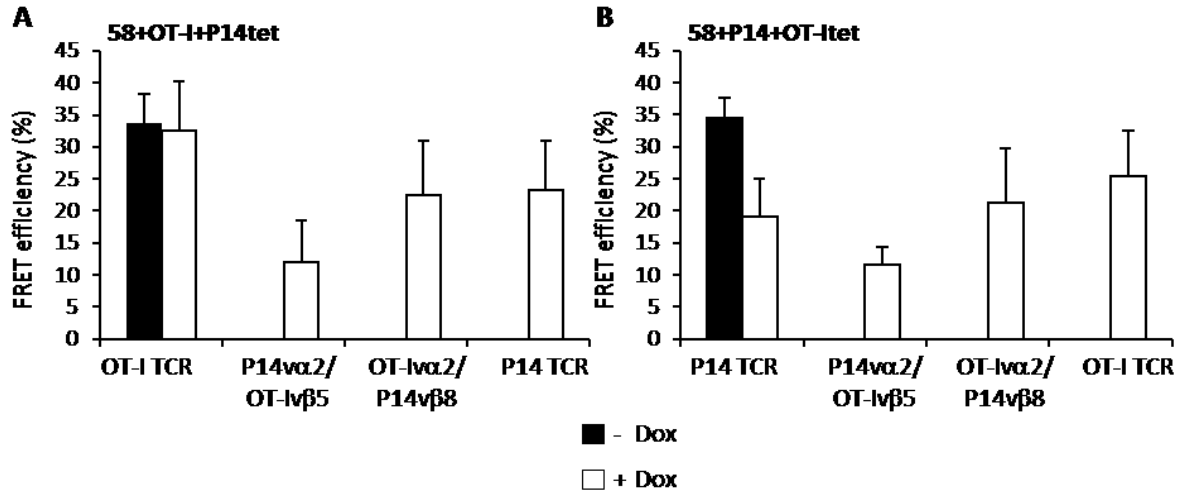

Figure 16 Mispaired TCRs could be detected by FRET

58+OT-I+P14tet cells (A) and 58+P14+OT-Itet cells (B) are shown without (black bars) or with 1 µg/ml Dox (white bars) after 24 h. All possible TCR chain combinations were measured. The staining was done as described in Figure 11.

Mispaired TCR dimers could be confirmed by tet-inducible single TCR chain expression in a T cell clone

To verify the FRET measurements shown in Figure 16 cell clones were constructed which expressed the endogenous P14 TCR and either the OT-Ivα2 or the OT-Ivβ5 chain as inducible transgenic TCR chain. TCR expression was determined without and with Dox by TCR staining and FRET efficiencies were calculated. When the OT-Ivα2 chain expression was induced the P14 TCR-positive cell population decreased from 96 % to 76 % which was due to the partial loss of P14vα2 chain expression (Figure 17A, left). Also, the MFI of P14vα2 chain was decreased as seen in the histogram

(Figure 17A, right). The induced OT-Ivα2 chain formed a double-positive TCR cell population of 89 % with the P14vβ8 chain which even had an increased MFI in this situation. These FACS stainings showed that the P14vα2 chain was displaced by the OT-Ivα2 chain. In the other cell clone, the expression of the OT-Ivβ5 chain was turned on by Dox. Here, the P14 TCR surface expression dropped from 96 % to 46 % TCR-positive cells (Figure 17B, left). The regulated OT-Ivβ5 chain formed a double-positive cell population of 59 % with the P14vα2 chain. Therefore, the P14vβ8 chain was partially replaced by the expression of the OT-Ivβ5 chain which was also indicated by the lower MFI of the P14vβ8 chain shown in the histogram. For the P14vα2 chain there was no difference in MFI seen in these cells (Figure 17B, right).

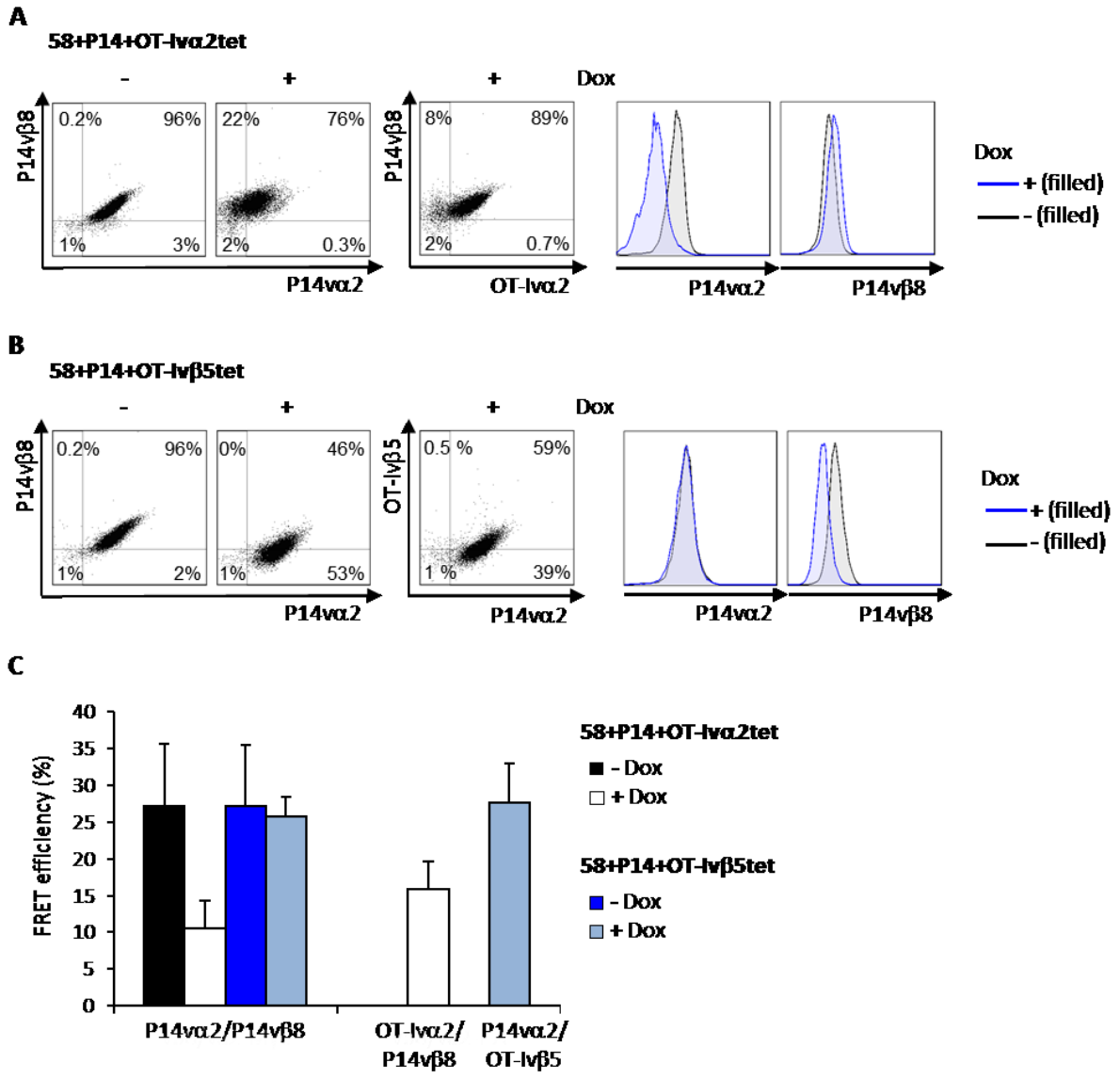

Figure 17 Induction of only one TCR chain led to mispaired TCR dimers with the constitutive P14 TCR chains

A: TCR staining of 58+P14+OT-Ivα2tet and B: 58+P14+OT-Ivβ5tet after 24 h TCR induction with 1 µg/ml Dox. C: FRET efficiencies of 58+P14+OT-Ivα2tet without (black bar) or with 1 µg/ml Dox (white bar) and of 58+P14+OT-Ivβ5tet without (dark blue bar) and with 1 µg/ml Dox (light blue bar). TCR staining was done as described in Figure 11.

FRET measurements showed that the FRET efficiency of the endogenous P14 TCR was clearly reduced when the OT-Ivα2 chain was induced (from 27 ± 8 % to 10 ± 4 %) but only slightly when the OT-Ivβ5 chain came to the cell surface (from 27 ± 8 % to 26 ± 3 %) (Figure 17C). The mispairing of the OT-Ivα2 chain with the P14vβ8 showed a FRET efficiency of 16 ± 4 % and mispairing of the P14vα2 chain with the OT-Ivβ5 resulted in a FRET value of 28 ± 5 %. These results indicated that the OT-Ivα2 chain had a higher potential to pair with the P14vβ8 as the corresponding P14vα chain. But both inducible OT-I TCR chains could reduce the percentage of P14 TCR-positive cells.

4.1.4 TCR WITH A SECOND CYSTEINE BRIDGE IN THE CONSTANT REGION

Mispairing of TCR chains can lead to severe problems if it occurs in a clinical setting. A new unknown reactivity arises which could lead to autoimmunity. Besides that it diminishes the functionality of the therapeutic TCR. As shown by Kuball *et al.*, the modification of the constant region by introducing cysteines which form a cysteine bridge between the constant region of both TCR chains lead to preferential pairing of the TCR chains and an increase in cell surface expression of the modified TCR [113]. Since we clearly detected mispairing between the OT-I and P14 TCR chains, it was tested if introduction of an additional cysteine bridge could diminish the observed mispaired TCR versions. The setting of induced OT-I TCR and endogenous expressed P14 TCR was chosen because the P14 TCR chain pairing was strongly impaired by the induced OT-I TCR. The P14 TCR chains were modified with a cysteine in both constant regions and cell clones were generated.

Depending on the TCR induction rate the P14cys TCR was lost on part of the cells

Two 58+P14cys+OT-Itet cell clones were chosen for detailed analysis. In the first analyzed clone 7, the OT-I TCR was induced to a lower percentage (57 %) (Figure 18A). The P14 TCR with the second cysteine bridge (P14cys) was not affected by the OT-I TCR, neither in percentage of TCR-positive cells nor in the MFI. The second chosen clone 9 showed an induction of the OT-I TCR in 96 % of the cells. The high OT-I TCR expression led to a reduction of P14cys TCR-positive cells from 96 % to 68 % and also resulted in a strongly decreased MFI of the P14vα2 chain and a fewer decreased MFI of the P14vβ chain (Figure 18B). Here, a partial replacement of the P14cys TCR was observed, which was not the case in the described clone with endogenous P14 TCR without a cysteine bridge.

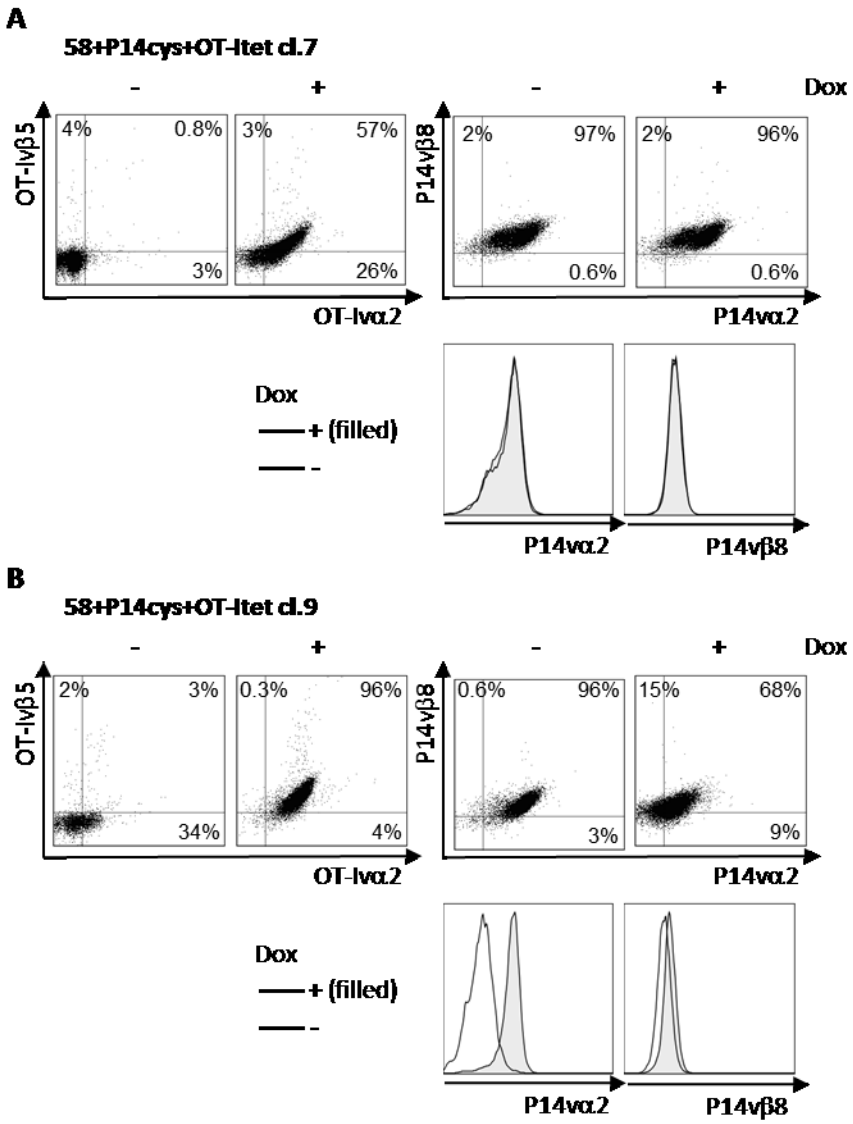

Figure 18 Characterization of 58+P14cys+OT-Itet clones

A. TCR stainings of 58+P14cys+OT-Itet clone (cl.) 7 and B: cl. 9 after 24 h induction with 1 µg/ml Dox. The staining was done as described in Figure 11.

Functionality of the endogenous P14 TCR is lost despite of the second cysteine bridge in its constant region

To test the functionality of the cysteine-modified P14 TCR a cocultivation was done with irradiated splenocytes which were loaded with different amounts of gp33 or ova peptide. The 58+P14cys+OT-Itet cl. 7 and 9 were simultaneously incubated with Dox. Secreted IL-2 was measured 24 h later by an ELISA. The induced TCR showed IL-2 secretion, and the IL-2 amount was depending on the peptide concentration in both cell clones (Figure 19). On the other side, the constitutively expressed P14 TCR

with the cysteine bridge in cl. 7 and cl. 9 did not maintain its functionality as already seen for the P14 TCR without the cysteine bridge. Thus, the additional disulfide bond did not rescue the functionality of the P14 TCR.

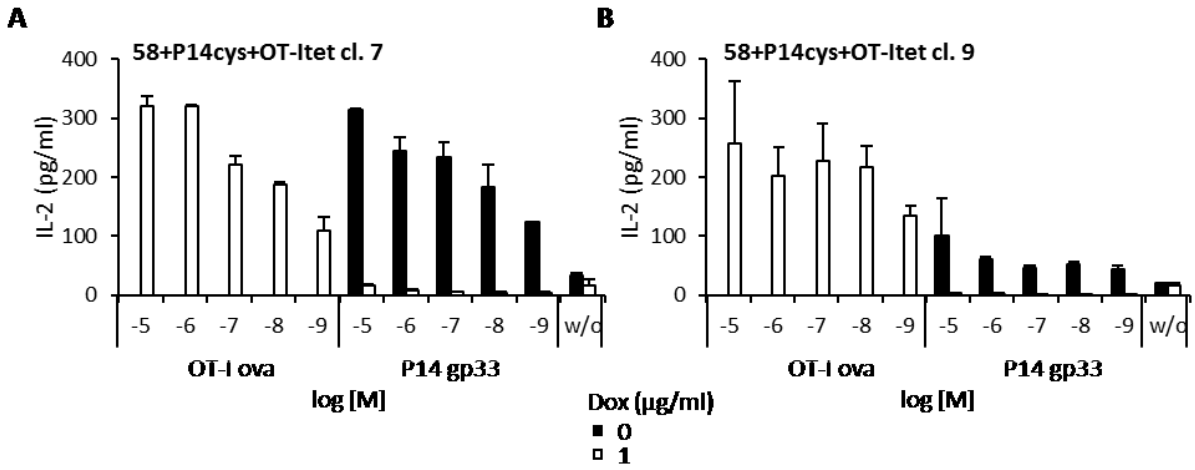

Figure 19 IL-2 secretion analysis showed functionality loss of the endogenous P14 TCR when the second TCR was induced despite of the cysteine bridge

---

A: 58+P14cys+OT-Itet cl. 7; B: 58+P14cys+OT-Itet cl. 9 were cocultivated with irradiated splenocytes loaded with indicated peptide concentrations (gp33 for P14 TCR and ova for OT-I TCR). 1 µg/ml Dox was added to the coculture. As control no peptide (w/o) was added. Supernatant was taken 24 h later and employed in an anti-mouse IL-2 ELISA.

The second cysteine bridge in the TCR constant region did not prevent mispairing

FRET analysis was done to see if one can detect a difference between the pairing behavior of the P14 TCR with or without a cysteine bridge. Both cell clones of 58+P14cys+OT-Itet cells were stained for their TCR chains. The cl. 7 showed a small reduction of the P14cys TCR FRET efficiency when the OT-I TCR expression was induced (from 20 ± 5 % to 15 ± 4 %) (Figure 20A). The mispairing of the P14vα2 chain and the OT-Ivβ5 chain reached a FRET efficiency of 15 ± 6 %, whereas the TCR dimer of OT-Ivα2 and P14vβ8 had a lower one (10 ± 6 %). The induced OT-I TCR showed pairing with 26 ± 4 %. The reduction in FRET efficiency of the P14cys TCR was stronger in cl. 9 (from 25 ± 6 to 11 ± 5 %) (Figure 20B). The mispaired TCR dimers had different FRET values compared to cl. 7 (P14vα2/OT-Ivβ5: 6 ± 3 %; OT-Ivα2/P14vβ8: 19 ± 3 %). The induced OT-I TCR showed a similar FRET efficiency as in cl. 7 (25 ± 7 %). In both cell clones, mispaired TCR chain combinations could be detected. Therefore, the cysteine bridge did not diminish the mispaired TCR dimers between the P14 and the OT-I TCR.

The two clones showed different reduction of the P14 TCR FRET efficiency when the transgenic OT-I TCR was expressed. As seen in the TCR stainings of Figure 18 this effect was related to the amount of induced TCR expressed. In cl. 7 OT-I TCR was only inducible in 46 % of the cells and the pairing of the P14 TCR was not as drastic reduced as in cl. 9 in which OT-I was induced in 90 % of the cells.

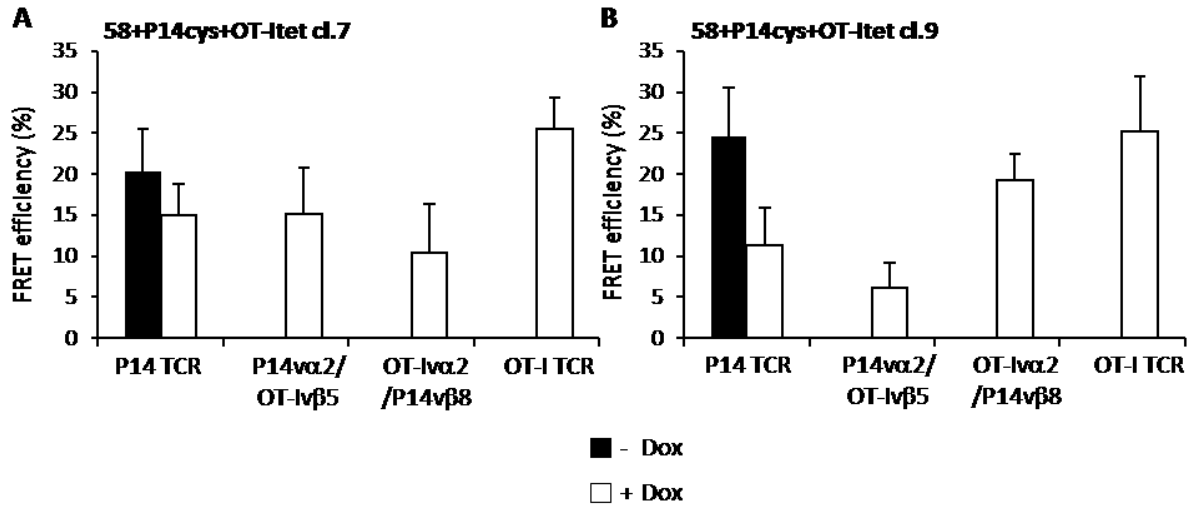

Figure 20 Cysteine bridge of the P14 TCR did prevent mispairing of TCR chain combinations

58+P14cys+OT-Itet cl. 7 (A) and cl. 9 (B) are shown without or with 1 µg/ml Dox after 24 h. All possible TCR chain combinations were measured. The sequential staining was done as described in Figure 11.

Different copy number integrations of the endogenous TCR correlated with FRET efficiencies

To further analyze the shown effect that the pairing of the P14 TCR independent of the cysteine bridge was impaired when the OT-I TCR expression was induced the copy number of integrated vectors of all cell clones was determined by real-time PCR.

Indeed, there was a different copy number for the endogenous TCR found in 58+OT-I+P14tet (16.2), 58+P14+OT-Itet (5.2), 58+P14cys+OT-Itet cl. 7 (11.4) and 58+P14cys+OT-Itet cl. 9 (5.4) which might influence the FRET efficiencies of the endogenous TCR, simply because different amounts were available when the transgenic TCR was induced (Table 29). In cell clones with a lower number of copies of the endogenous TCR gene, the TCR chains were eventually easier displaced. But, T cell clones were mostly still over 90 % positive for the endogenous TCR chains, and FRET efficiencies should be independent of TCR molecule amounts.

The copy number of the induced TCR was the same (1 copy per cell) for all clones except for 58+P14cys+OT-Itet cl. 9 which was 2.6 copies per cell. In 58+P14cys+OT-Itet cl. 7 the copy number of

the endogenous TCR expressing vector was 11.4 which might explain the low induction of the expression of the OT-I TCR.

Table 29 Vector copy number integration

Vector	58+OT-I+P14tet	58+P14+OT-Itet	58+P14cys+OT-Itet cl.7	58+P14cys+OT-Itet cl.9
Endogenous TCR (pLSN)	16.2 ± 0	5.2 ± 0	11.4 ± 0	5.4 ± 0
Transgenic (Tet)	1.1 ± 0.001	0.9 ± 0.001	1.1 ± 0.002	2.6 ± 0.001

4.1.5 ANALYSIS OF DUAL TCR PRIMARY T CELLS

So far, cell lines expressing two TCRs were analyzed. To broaden the analysis primary cells were used to determine the influence of the cysteine bridge on the P14 TCR. Transgenic OT-I cells were transduced with the MP71 vector encoding the P14 or the P14cys TCR. TCR stainings were undertaken to determine the transduction and FRET efficiencies between the P14vα2 chain and P14vβ8 or OT-Ivβ5 TCR chains. The FRET efficiency between OT-Ivα2 chain and the TCRvβ chains could not be done, since the transgenic OT-Ivα2 chain does not harbor the HA tag.

P14 TCR transduced cells showed similar gp33 tetramer binding and FRET efficiencies independent of a second cysteine bridge in the constant region

Primary OT-I T cells transduced with the P14 or P14cys TCR were stained with the gp33-tetramer for P14 TCR expression and with the ova-tetramer for the OT-I TCR expression. OT-I+P14 cells showed 77 % gp33-tetramer binding and OT-I+P14cys 81 % (Figure 21A). The expression level as determined by MFI of gp33-tetramer-positive cells did not reveal differences between the transduced cells. All cells still bound the ova-tetramer (OT-I+P14 95 % and OT-I+P14cys 94 %).

The staining used to calculate the FRET efficiencies are shown in Figure 21B. In OT-I+P14 cells 87 % were P14vα2- and P14vβ8-positive, in OT-I+P14cys 88 % were positive. FRET efficiencies between these two TCR chains was 9 ± 3 % for OT-I+P14 and 12 ± 2 % for OT-I+P14cys cells (Figure 21C). In the second possible FRET staining OT-I+P14 cells were 81 % and OT-I+P14cys cells 83 % positive for P14vα2 and OT-Ivβ5. The staining with P14vα2 and OT-Ivβ5 showed a low correlation between the two TCR chains. FRET efficiencies of these stainings were 5 ± 3 % for both cell populations. As seen for the cell line clones, there was not a clear advantage of the P14 TCR with the second cysteine bridge than without. Only the FRET efficiency of P14vα2 and P14vβ8 was slightly higher for OT-I+P14cys but this was not significantly different.

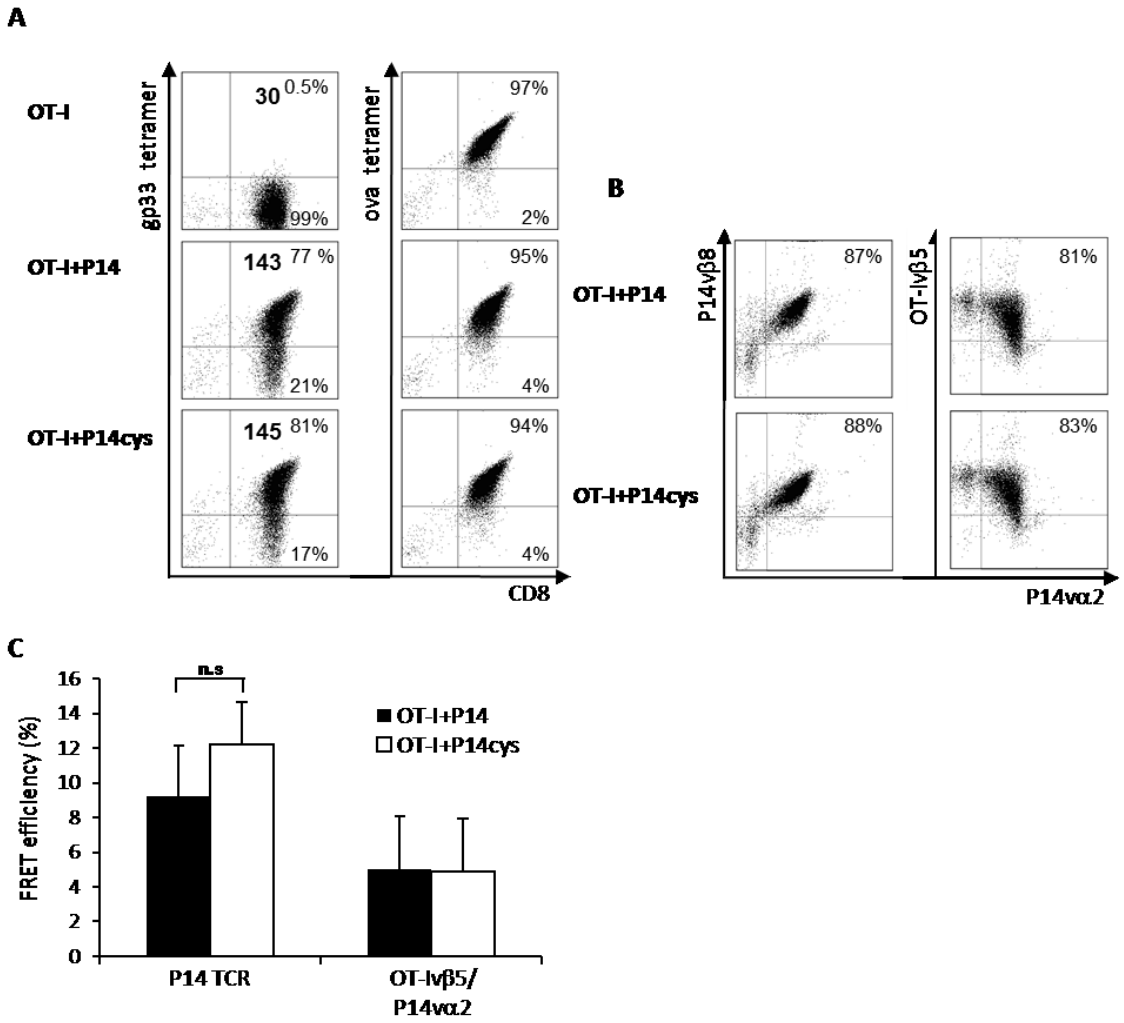

Figure 21 Transduction and FRET efficiencies of OT-I+P14 and OT-I+P14cys cells

A: TCR stainings of P14 TCR-transduced or untransduced OT-I splenocytes labeled with anti-CD8-FITC and gp33-tetramer-APC or ova-tetramer-APC. MFI values of gp33-tetramer-positive cells are given in black and bold in the middle of the FACS dot plot. B: FRET stainings were done as described in Figure 11. C: FRET efficiencies of stainings in B.

P14 TCR and P14cys TCR transduced OT-I cells showed same functionality

The functionality of P14 TCR-transduced OT-I cells was tested to see if the P14 TCR with the cysteine bridge has an advantage. Transduced and untransduced cells were incubated with irradiated splenocytes loaded either with gp33 or ova peptide, and the supernatant was tested for IFN-γ. All cell populations showed reactivity down to 10^{-11} M peptide (Figure 22). No differences could be seen between cell populations incubated with gp33 peptide or with ova peptide. The functional assay confirmed the results of the TCR stainings and FRET measurements.

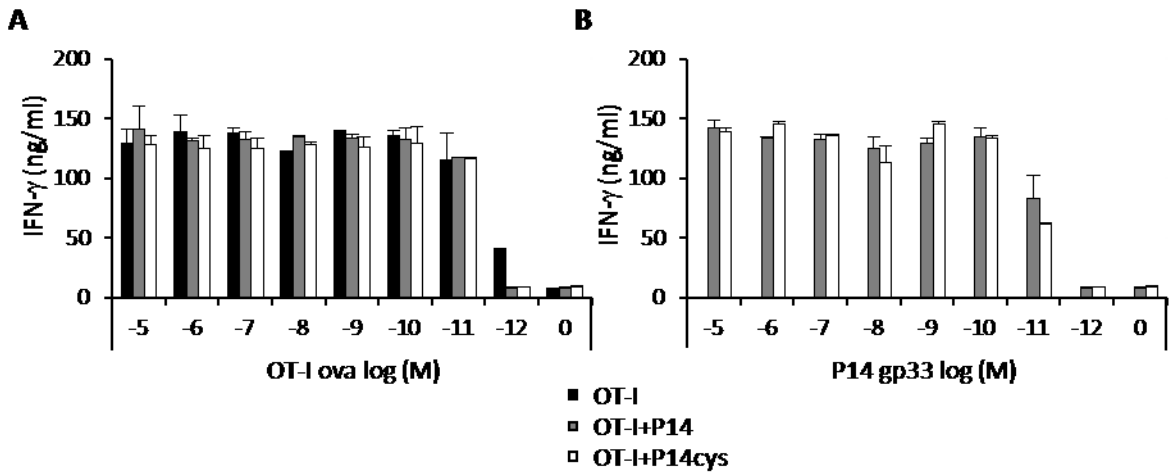

Figure 22 IFN-γ secretion of primary OT-I cells transduced with the P14 or P14cys TCR was not different

Transduced T cells were cocultivated with irradiated splenocytes loaded with indicated peptide concentrations (A: ova for OT-I TCR and B: gp33 for P14 TCR). Supernatant was taken 24 h later and employed in an anti-mouse IFN-γ ELISA.

In wild-type cells differences in FRET efficiency could be detected between different TCR formats

The obtained results indicated that the second cysteine bridge in the constant region did not prevent mispairing of the P14 TCR with the OT-I TCR chains. To exclude that this situation only holds true for this setting primary wild-type cells were transduced with different TCR formats of the P14 and the OT-I TCR (with and without the second cysteine bridge in non- and codon-opitmized TCRs). As expected TCRs encoded by codon-optimized DNA yielded higher transduction rates as shown by TCRβ and TCRα staining, but differences between cys-formats could not be confirmed (Figure 23A). Only the OT-Icys TCR had a higher expression rate of 30 % than the OT-I TCR which was due to a higher virus titer. Calculated FRET efficiencies revealed a tendency between the P14 TCRs (Figure 23B). With TCR optimization the FRET efficiency increased. Also for the OT-I, OT-Icys, OT-Ico TCR this increase could be seen, but no differences was caclulated between the OT-Ico and OT-Icocys TCR. Therefore, the cysteine bridge might only have an effect on certain TCRs and formats, but the differences in FRET efficiencies were not significant.

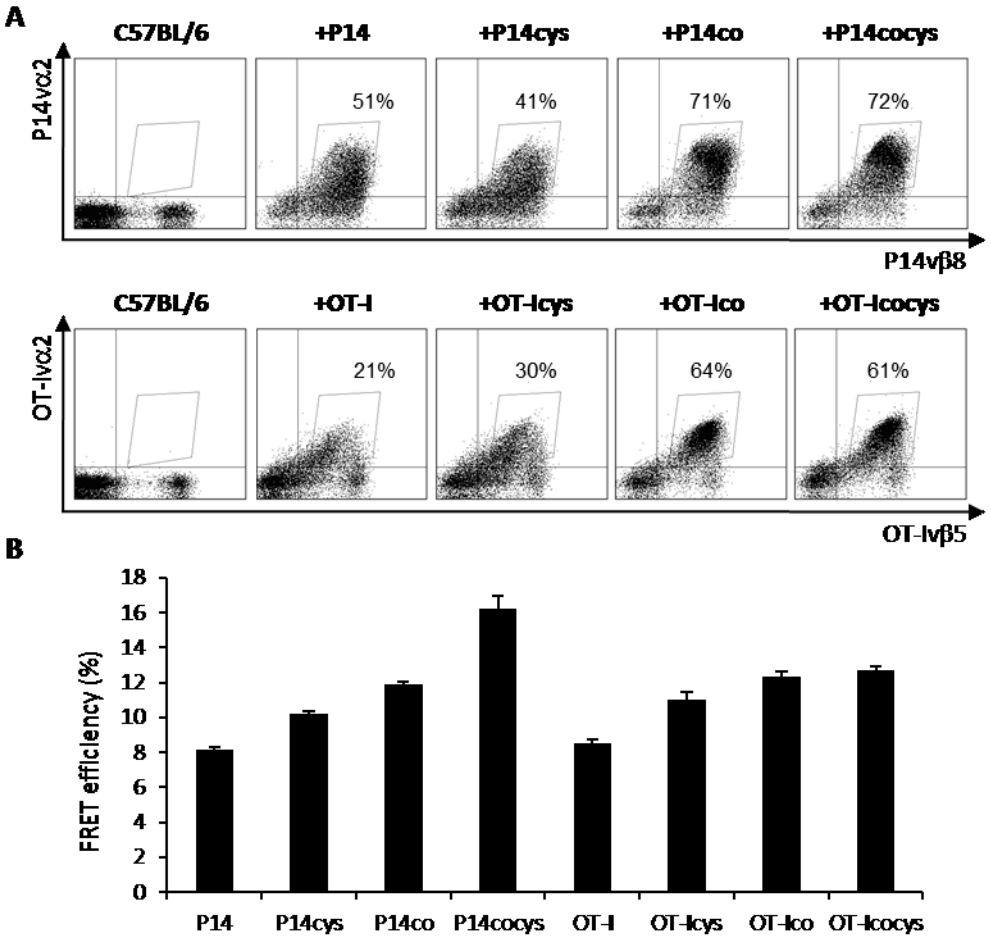

Figure 23 Primary C57BL/6 cells transduced with the P14 or OT-I TCRs revealed small differences in TCR pairing behavior

---

A: C57BL/6 splenocytes were transduced with different formats of the P14 and OT-I TCR and transduction rates were determined by staining as described in Figure 11. B: FRET efficiencies of stainings in A.

Only with a small amount of antigen differences in functionality between different TCR formats could be detected

Small differences in FRET efficiencies between TCR formats could be detected. To see if these differences also apply to functionality of the transgenic TCR a cocultivation of equilibrated numbers of TCR-positive cells with peptide-loaded splenocytes was done. Only for 10^{-12} M and $10^{-12.3}$ M peptide different amounts of IFN-γ could be seen in the order of optimization (Figure 24). These small differences could also be due to the different transduction rates despite of usage of equilibrated TCR-positive cell numbers.

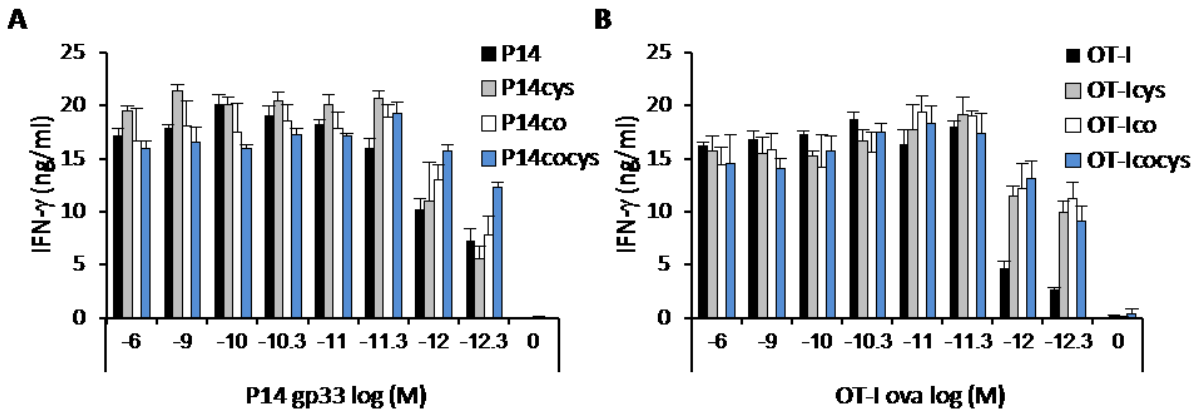

Figure 24 IFN-γ secretion of primary C57BL/6 cells transduced with the P14 or OT-I TCRs was only different for small amounts of antigen

---

Transduced C57BL/6 splenocytes were cocultivated with irradiated splenocytes loaded with indicated peptide concentrations (A: gp33 for P14 TCR and B: ova for OT-I TCR). Supernatant was taken 24 h later and employed in an anti-mouse IFN-γ ELISA.

4.2 SAFETY ANALYSIS TCR GENE-MODIFIED T CELLS *IN VIVO*

The second part of the dissertation deals with the long-term analysis of TCR-transduced T cells *in vivo*. Vector transduction leads to integration into the cell genome which results in changes at the integration site, like changed expression of surrounding genes or disruption of genes. Potentially changed expression of genes involved in the regulation of the cell cycle could lead to an advantage of proliferating cells or survival of cells. This potential risk was combined with a regularly stimulation of transduced T cells. Stimulation of T cells leads to proliferation and mutated cells might have a proliferation advantage. In the following described experiment OT-I T cells were transduced with the P14 TCR and transferred into non-myeloablative treated mice. In the recipient mice the transferred cells were stimulated either with gp33 peptide, ova peptide, each combined with an adjuvant, or with a gp33-positive tumor cell line. The experiment was repeated once with a milder non-myeloablative treatment and stimulation was done with the gp33-positive tumor cell line. One control experiment was carried out with adoptive transfer of GFP-transduced OT-I T cells into lymphodepleted mice but without stimulation of transferred cells.

4.2.1 CHARACTERIZATION OF TCR- AND GFP-TRANSDUCED OT-I SPLENOCYTES BEFORE ADOPTIVE TRANSFER

OT-I splenocytes were highly transduced with the P14 TCR or with GFP

OT-I splenocytes were transduced with the MP71 vector encoding the P14 TCR. Transduced cells and recipient mice of the first experiment were named as OT-I+P14 I whereas of the second experiment OT-I+P14 II. Tetramer staining of the P14 TCR was done 72 h after transduction. OT-I+P14 I cells were highly transduced with 73 % and OT-I+P14 II with 49 % gp33-tetramer-positive cells (Figure 25A). Transduction of OT-I T cells with the MP71 vector encoding GFP led to 66 % GFP-positive cells (Figure 25A).

The activation status of the OT-I+P14 I cells was analyzed by the activation marker CD44, the early activation marker CD69 and the homing marker CD62L and compared to naive splenocytes which revealed an activated phenotype with up-regulated CD44 and CD69 and down-regulated CD62L (Figure 25B).

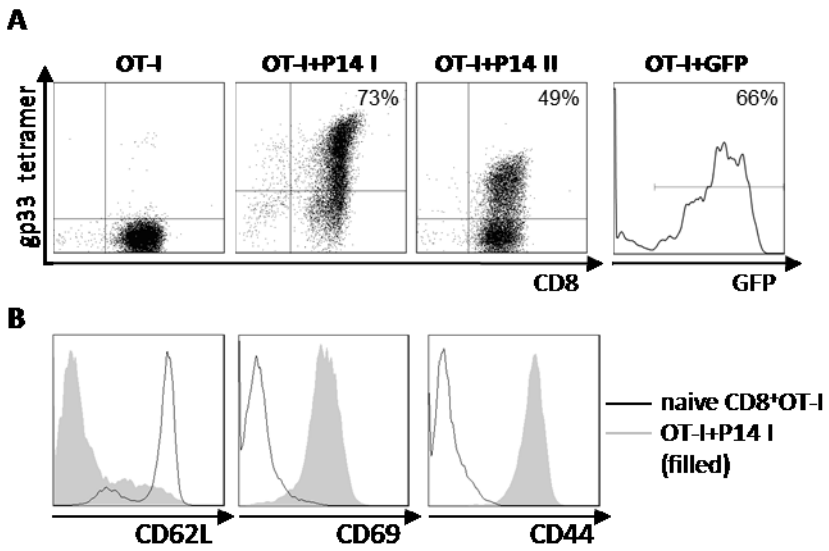

Figure 25 Transduced OT-I splenocytes showed P14 TCR or GFP expression and an activated phenotype

---

A: Tetramer stainings showing transduction efficiency of OT-I splenocytes transduced with P14 TCR stained with anti-CD8-FITC and gp33-tetramer-APC. As control untransduced OT-I cells are shown. GFP-transduced OT-I cells are shown as a histogram. B: Activation status of OT-I+P14 I cells (filled histogram) compared to naive CD8-positive OT-I cells (black line). Staining was done with anti-CD62L-PE, -CD69-PE, -CD44-PE. Naive cells were gated on CD8-positive cells stained with anti-CD8-APC.

P14 TCR-transduced and GFP-transduced OT-I T cells harbor high virus copy number integrations

To determine the copy number of integrated provirus per cell Real-time PCR was done with DNA from transduced cells. P14vα2- and GFP-specific primers were used to detect the proviral DNA and a calibration curve with P14 plasmid DNA was done for calculations (Figure 26). The transduction rate measured by TCRvα2 and TCRvβ8 staining or the GFP expression was taken into account. As already indicated by the transduction efficiencies OT-I+P14 I cells had a higher copy number of 3.8 than OT-I+P14 II cells (1.2 copy number) (Table 30). OT-I+GFP-transduced cells had 7.7 copy numbers of provirus per cell. Since the transgene vector with GFP is smaller as the vector with the P14 TCR the virus titer was higher (5.7 and 9 x 10^6/ml for 1st and 2nd GFP virus harvest versus 2-6 x 10^6/ml for P14 TCR virus harvests as measured on 58 cells) which led to a higher copy number integration per cell.

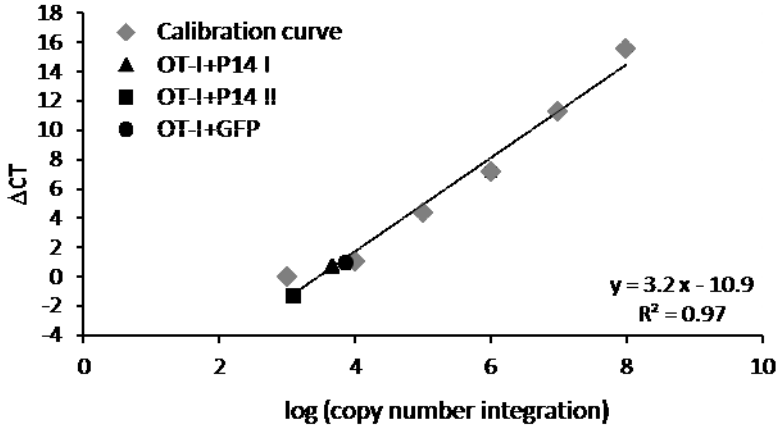

Figure 26 Calibration curve of diluted plasmid DNA and DNA samples detected by real-time PCR

ΔCT values were plotted against the copy number of plasmid DNA used in a Real-time PCR with P14vα2-specific primers. DNA cell samples analyzed resulted in ΔCT values in range of the calibration curve, here shown for average values.

Table 30 Vector copy number integration

Cells	OT-I+P14 I ($v\alpha2^+/v\beta8^+$)	OT-I+P14 II ($v\alpha2^+/v\beta8^+$)	OT-I+GFP (GFP^+)
Transduction efficiency (%)	81	60	66
Copy number integration per transduced cell	3.8 ± 0.5	1.2 ± 0.003	7.7 ± 001

4.2.2 ADOPTIVE TRANSFER OF TCR AND GFP GENE-MODIFIED T CELLS

For the long-term analysis of TCR-transduced T cells recipient mice were lymphodepleted before transfer to ensure the prober engraftment of transferred T cells. For lymphodepletion the chemotherapy agent cyclophosphamide was chosen. This agent is a nitrogen mustard alkylating substance and given as a prodrug which is converted in the liver. Recipient mice were pretreated intraperitoneal with 200 mg/kg cyclophosphamide [177] in the experiment with OT-I+P14 I and OT-I+GFP cells and with 100 mg/kg cyclophosphamide in the experiment with OT-I+P14 II cells one day before adoptive transfer. Mice were either 10 or 12 weeks old in the first or second experiment, respectively. 5 x 10^6 T cells were intravenously transferred.

Peptide-stimulated transferred cells showed a higher activation status than gp33 tumor cell-stimulated or unstimulated transferred cells

One day after transfer, mice of the first experiment were stimulated either with ova peptide (4 mice) gp33 peptide (10 mice) or with a tumor cell line presenting the gp33 peptide (gp33 tumor cells) (5 mice). The tumor cell line does not grow in immune-competent mice. The peptides were combined with CpG ODN 1826 and IFA. One mouse was left unstimulated. The OT-I+GFP transferred T cells were left unstimulated (12 mice). In the second experiment transferred T cells were either left unstimulated (15 mice) or were stimulated with the gp33-positive tumor cell line (14 mice).

Blood was taken on day 7 or day 4 after stimulation in the OT-I+P14 I- or OT-I+P14 II-experiment, respectively. The activation status was analyzed by staining for the congenic marker CD90.1 of transferred T cells, the activation marker CD44 and the homing molecule CD62L which is down-regulated upon activation. Compared to unstimulated or tumor cell-stimulated cells peptide-stimulated cells were stronger activated shown by the higher down-regulation of CD62L (Figure 27).

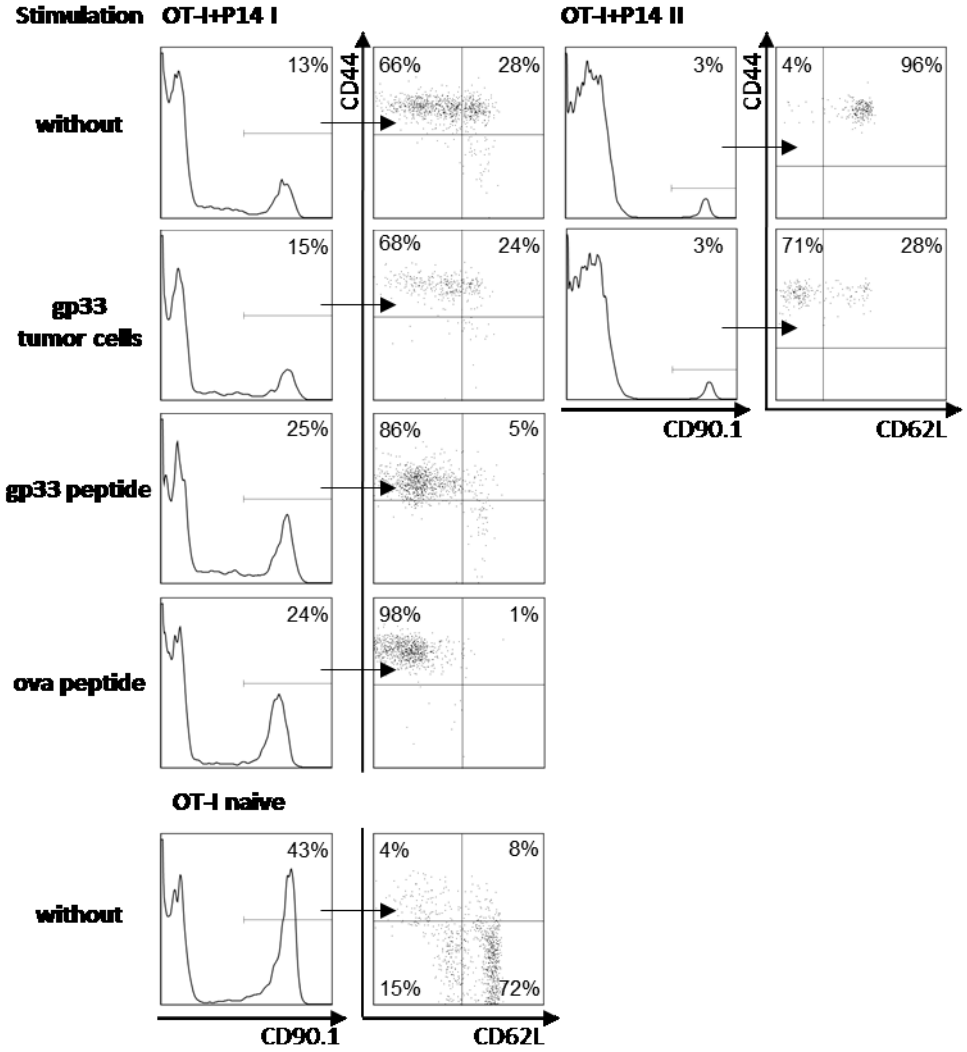

Figure 27 Activation status of transferred cells after first restimulation

OT-I+P14 I: Blood cells were stained with anti-CD90.1-biotin/streptavidin-APC, anti-CD44-PE and anti-CD62L-FITC. OT-I+P14 II: Blood cells were stained with anti-CD90.1-PercP, anti-CD44-PE and anti-CD62L-FITC.The dot plot of CD44 against CD62L is gated on CD90.1-positive cells.

All transferred cells were CD44-positive due to the *in vitro* activation for viral transduction. As control blood of a naive OT-I mouse is shown. In unstimulated mice, 66 % or 3 ± 1 % cells down-regulated CD62L in the first or second experiment, respectively (Table 31). Tumor cell-stimulated cells were 72 ± 6 % or 43 ± 23 % CD62L-negative in the OT-I+P14 I- or OT-I+P14 II- experiment, respectively. The ova peptide-stimulated cells were 95 ± 3 % and the gp33 peptide-stimulated cells 84 ± 14 % CD62L-negative. Differences in the CD62L-down-regulation between the first and second experiment could be due to the different amount of cyclophosphamide used in these mice.

Table 31 Down-regulation of CD62L in stimulated mice

CD90.1: $CD44^+/CD62L^-$ (%)	OT-I+P14 I	OT-I+P14 II	Naive mice
Stimulation	Day 8	Day 4	
Without	66 (n=1)	3 ± 1 (n=3)	10 ± 2 (n=2)
gp33 tumor cells	72 ± 6 (n=2)	43 ± 23 (n=3)	
gp33 peptide	84 ± 14 (n=6)		
ova peptide	95 ± 3 (n=3)		

Toxicity was observed in recipient mice due to cyclophosphamide treatment

The time point of death and its reasons of individual mice are listed inTable 32 as well as the last measured percentage of transferred cells. In the experiment OT-I+P14 I surviving mice were killed individually (indicated as autopsy in Table 32) whereas in OT-I+GFP and OT-I+P14 II surviving mice were killed on day 450 or day 365, respectively.

Between day 30 and 86 after T cell transfer of OT-I+P14 I cells the animal facility was closed due to a suspicion of mouse hepatitis infection. During this time 6 out of 20 mice died and could not be analyzed (Table 32). Since the reason for the early death could not be clarified at this time point, the surviving mice were further analyzed. The control group receiving OT-I+GFP cells started at a later time point. Here 3 out of 12 mice died early (day 48, 75, 112). Death of mice was mainly due to the cyclophosphamide concentration and the young age of mice at the time point of adoptive transfer which led to early toxicity with symptoms like teeth problems or outgrowth of untransduced OT-I cells in two mice with OT-I+GFP cells (70 % and 98 % CD8: CD90.1-positive, 0.4 and 0.03 % CD8:

CD90.1/GFP-positive). Late toxicity occurred around day 200 which might have been caused by a not well enough reconstituted immune system. Three mice died during peptide injection (Handling).

Toxicity could be limited by reducing the cyclophosphamide concentration in the second experiment (OT-I+P14 II). Here, one mouse in the unstimulated group and three mice in the stimulated group died due to early or late toxicity. One mouse was sacrificed shortly before the end of the experiment (day 314) because of sore skin lesions but this mouse had lost the transferred cells (Late toxicity). A second mouse killed on day 209 had a bowel obstruction.

Table 32 Overview of recipient mice and cause of death

Experiment	Stimulation	Death due to	Day after T cell transfer	Transferred T cells CD8: $CD90.1^+$ (%)
OT-I+P14 I	without	Autopsy	460	60
	gp33 tumor cells	Early toxicity	>86	26, 30
		Autopsy/ Old age	410, 557, 557	66, 85, 30
	gp33 peptide	Early toxicity	>86	4, 16, 5
		Late toxicity	262, 310	7, 14
		Autopsy/ Old age	480, 546, 546	29, 28, 41
		Handling	151	1, 5
	ova peptide	Early toxicity	>86	7
		Late toxicity	213	20
		Autopsy	416	39
		Handling	34	3
OT-I+GFP	without	Early toxicity	48, 75, 112	12, 70, 98
OT-I+P14 II	without	Late toxicity	216	7
	gp33 tumor cells	Early toxicity	121	0
		Reason unkbown/ Late toxicity	209, 314	34, 0

Transferred OT-I+P14 cells persisted in most of the recipient mice

Blood analysis of recipient mice showed that the transferred T cells persisted over time in most of the mice (Figure 28). CD8 cells from the peripheral blood were analyzed for CD90.1 expression and TCRvβ8 chain expression of the transduced P14 TCR. On day 8 after transfer, T cells had an expansion peak due to homeostatic proliferation and also due to the stimulation. In the first experiment, the ova peptide-stimulated group had the highest percentage with 58 ± 10 % CD90.1 of CD8 cells, followed by the gp33 tumor cell-stimulated group with 53 ± 12 %, then the unstimulated mouse with 43 % and the gp33 peptide-stimulated group with 40 ± 11 % (Figure 28A). The gp33 peptide-stimulated group had a higher percentage of cells which had down-regulated CD62L than the gp33 tumor cell-stimulated group on day 8 after transfer but had a lower proliferation peak of transferred cells. In the second experiment, OT-I+P14 II blood was taken on day 4 after stimulation and analyzed for transferred cells. Transferred T cells persisted and enriched over time (Figure 28B) with the exception of two mice in the unstimulated group and four mice in the tumor cell-stimulated group. In these mice transferred T cells persisted below 0.5 % of CD8 T cells. The first expansion peak in the second experiment was lower than for the OT-I+P14 I with 8 ± 2 % in the unstimulated group and 11 ± 6 % CD90.1 of CD8 T cells in the gp33 tumor cell-stimulated group. The difference was due to the lower concentration of cyclophosphamide used for the non-myeloablative treatment.

Transferred T cells declined thereafter until the next stimulation which led to a small increase in both experiments. The increase was seen after most of the stimulations in the first and after all stimulations in the second experiment. Since the blood was always checked on day 7 after stimulation in OT-I+P14 I mice, the expansion peak might have occurred before which could also depend on the type of stimulation (peptide versus tumor cell line). The analysis on day 4 after stimulation in OT-I+P14 II mice always revealed an increase of transferred cells. After stimulations the cells normally declined again.

Overall, the transferred T cells enriched over time in the CD8 T cell compartment which became vigorous from day 200 on (Figure 28A and B). In OT-I+P14 I mice, the unstimulated mouse had enriched the transferred T cell up to 60 % on day 416 and the gp33 tumor cell-treated mice up to 44 ± 26 % (three mice) on day 501. Although peptide stimulation led to a higher down-regulation of CD62L, cells did not increase in percentage which might have been due to activation-induced cell death. The transferred T cells in the peptide-stimulated mice stayed on a lower level, for gp33 peptide- 31 ± 9 % on day 416 (three mice) and for ova peptide stimulation 39 % on day 416 (one mouse) (Figure 28A). Similarly, in the OT-I+P14 II experiment in unstimulated mice 28 ± 10 % and in

tumor cell-stimulated mice 58 ± 18 % CD90.1-positive cells of CD8 T cells were found on day 365 after adoptive transfer.

Analysis of vβ8-positive and vβ8-negative cells revealed that the transduced and untransduced cells kept the ratio over time in the gp33 peptide-, gp33 tumor cell-stimulated or unstimulated group (Figure 28A lower figures). In the ova peptide-stimulated group, the proportion of untransduced cells increased a little since here also untransduced cells were addressed by the stimulation. In the second experiment, the ratio of transduced to untransduced transferred cells also stayed the same with mainly over 90 % vβ8-positive cells of CD90.1 cells shown as CD90.1/vβ8-positive cells (Figure 28B lower figure).

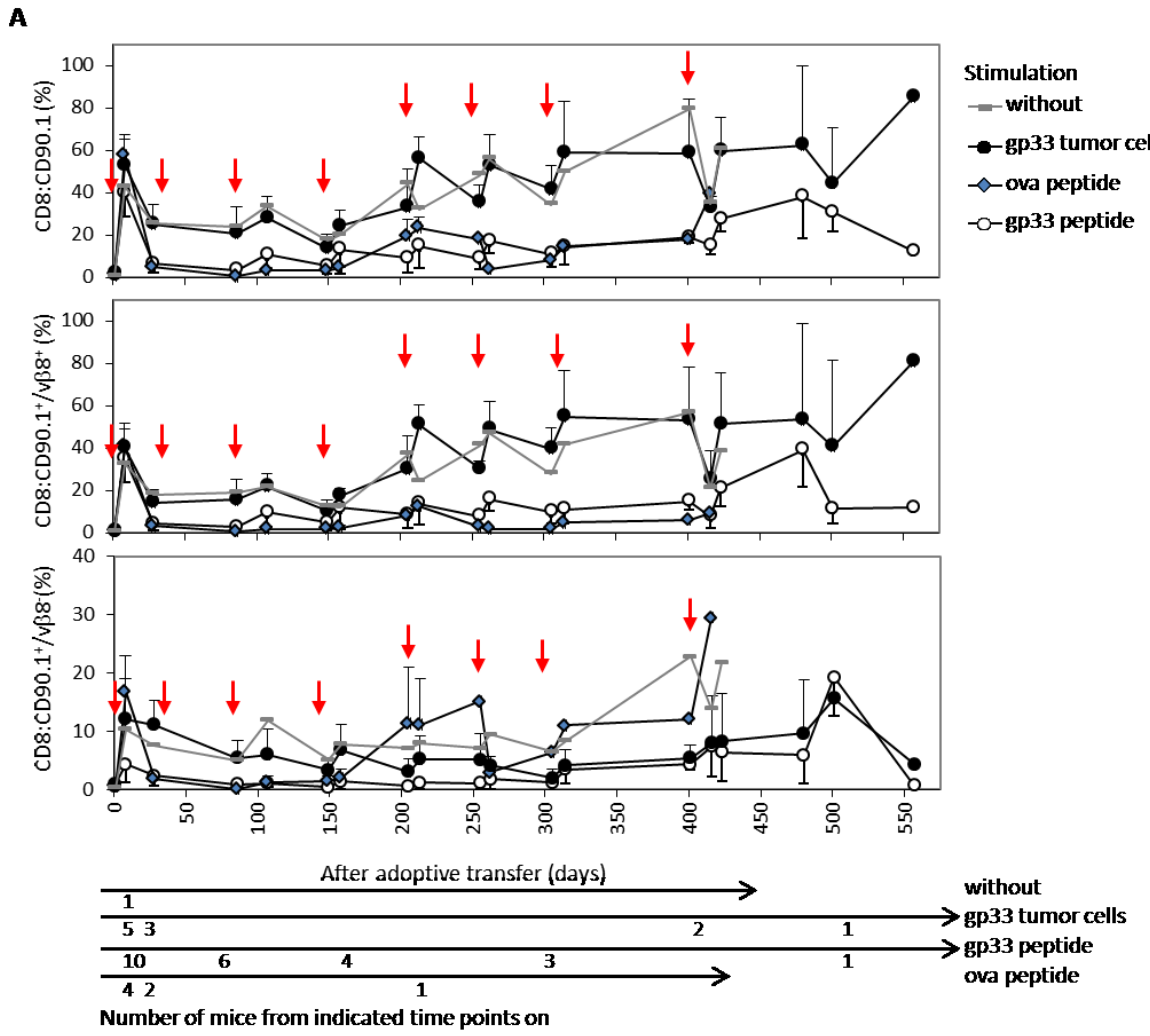

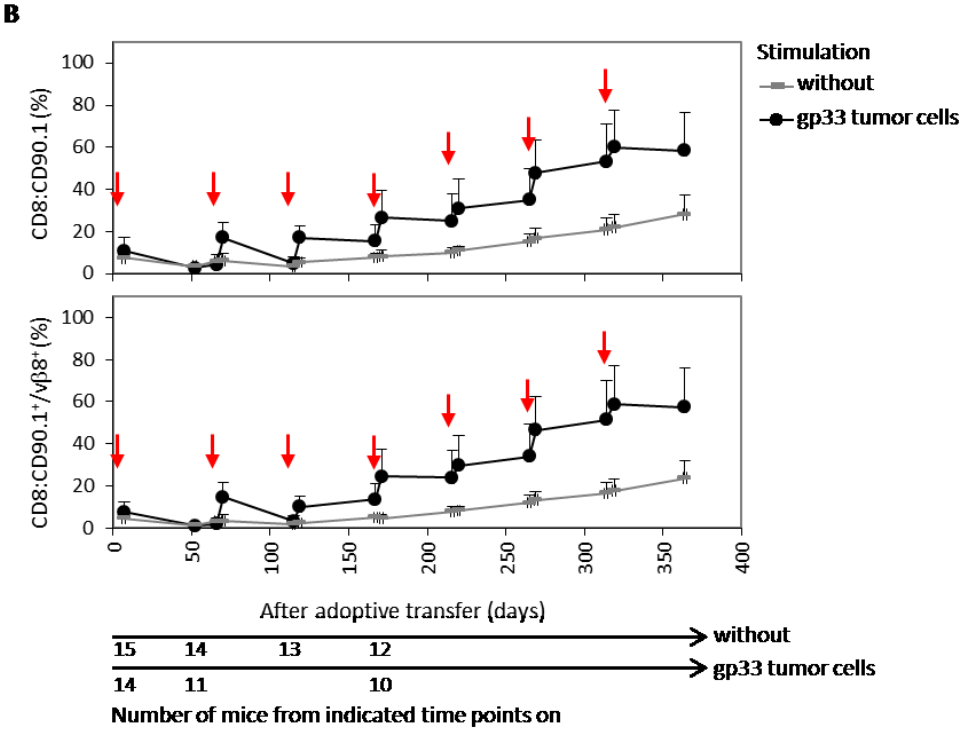

Figure 28 Transferred OT-I+P14 cells persisted long-term in recipient mice

Blood of recipient mice was checked on time points with symbols. A: OT-I+P14 I. Cells were stained anti-CD8-APC, anti-CD90.1-FITC, and anti-vβ8-PE. B: OT-I+P14 II. Cells were stained with anti-CD8-APC, anti-CD90.1-PercP, and anti-vβ8-FITC. Red arrows indicate stimulation time points, for A: day 1, 34 (only #2 and #4), 99, 151, 207, 255, 305, 401, for B: day 1, 66, 115, 167, 216, 265, 314.

Transferred OT-I+GFP cells persisted in recipient over time

The OT-I+GFP mice were bled every 50 days and every second 50 days after 7 days again as done with OT-I+P14 I mice. After a small expansion peak of 13 ± 3 % CD90.1-positive of CD8 T cells which was not as vigorous as for OT-I+P14 I mice the transferred cells declined until day 100 (Figure 29). After day 100, cells enriched slowly as seen in OT-I+P14 I and II mice. At the end of the experiment on day 450, they made up 28 ± 8 % of the CD8 T cells. On day 8 after transfer 11 ± 3 % and on day 450 17 ± 12 % of cells were GFP/CD90.1-positive. In regard to CD90.1-positive cells the percentage of transduced GFP-expressing cells declined from 86 ± 20 % to 53-62 % of CD90.1-positive cells until the end of the experiment on day 450 (Figure 29).

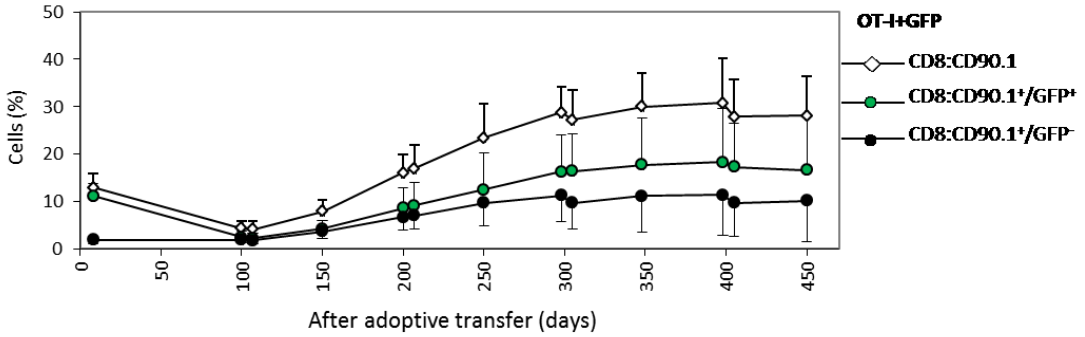

Figure 29 OT-I+GFP cells persisted long-term in recipient mice

Blood of recipient mice was checked on time points with symbols. Cells were stained with anti-CD8-APC and anti-CD90.1-PercP. Number of mice was 12 on day 8 and 9 mice from day 100 on.

Peptide-stimulated transferred T cells showed a stronger activation status than gp33 tumor cell-stimulated or unstimulated T cells over time

Upon activation the CD62L is down-regulated and rises again with memory formation or after repetitive stimulation. Memory T cells are differentiated into effector memory T cells and central memory T cells which differ in CD62L expression. Effector memory T cells are CD62L-negative and central memory T cells are CD62L-positive. Both types of memory T cells are present in the peripheral

blood. The CD62L expression was analyzed on transferred T cells after three stimulation rounds in OT-I+P14 I mice. CD8-gated cells were checked for CD90.1 and CD62L expression (Figure 30).

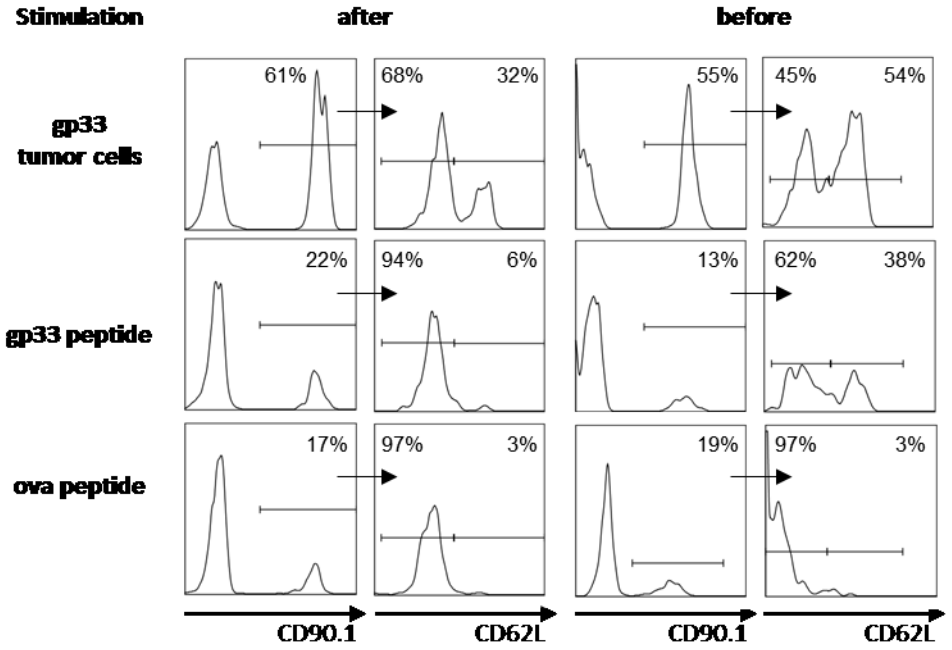

Figure 30 Upon stimulation transferred T cells showed down-regulated CD62L expression which is up-regulated thereafter again

---

A: Examples shown once after stimulation (day 213) and before the next stimulation round (day 305, ova peptide: day 401). Cells were stained with anti-CD8-APC, anti-CD90.1-FITC, and anti-CD62L-PE. Cells were gated on CD8 and in the first histogram CD90.1-positive cells are shown. These were analyzed for CD62L expression shown in the second histogram.

After the third stimulation, tumor cell stimulation led to a down-regulation of CD62L expression in 60 ± 25 % of the cells, whereas gp33 peptide- and ova-peptide stimulation led to a down-regulation in 95 ± 4 % and 98 ± 1 % of the cells, respectively (Table 33). Analyzed samples of two chosen time points, just before stimulation, showed that the tumor cell- and gp33 peptide-stimulated group increased its CD62L expression again but 52 ± 27 % or 58 ± 25 %, respectively, stayed CD62L-negative. In case of the two ova peptide-stimulated mice 95 ± 5 % cells stayed CD62L-negative. The tumor cell stimulation, as already shown on day 7 after the first stimulation *in vivo*, was not as strong as peptide stimulation as shown by weaker CD62L down-regulation. During the memory phase this group showed a higher CD62L expression as the ova-stimulated group but similar to gp33-stimulated mice. This property confers to a central memory phenotype.

Table 33 Activated phenotype of transferred T cells

CD90.1: CD62L$^-$ (%)	After stimulation	Before stimulation
Stimulation	Day 213	Day 305/401
without (naive mice)	10 ± 3 (n= 2)	
gp33 tumor cells	60 ± 25 (n= 3)	52 ± 27 (n= 6)
gp33 peptide	95 ± 4 (n= 5)	58 ± 25 (n= 6)
ova peptide	98 ± 1 (n=2)	95 ± 5 (n= 2)

In OT-I+P14 II mice, peripheral blood cells were regularly checked for CD62L- and CD44 expression. After each stimulation CD62L-negative cells increased indicating the stimulation effect on the transferred cells by tumor cell stimulation (Figure 31). Blood of unstimulated mice was also analyzed for CD44 and CD62L expression, but here CD62L-negative cells decreased over time indicating memory formation of transferred cells.

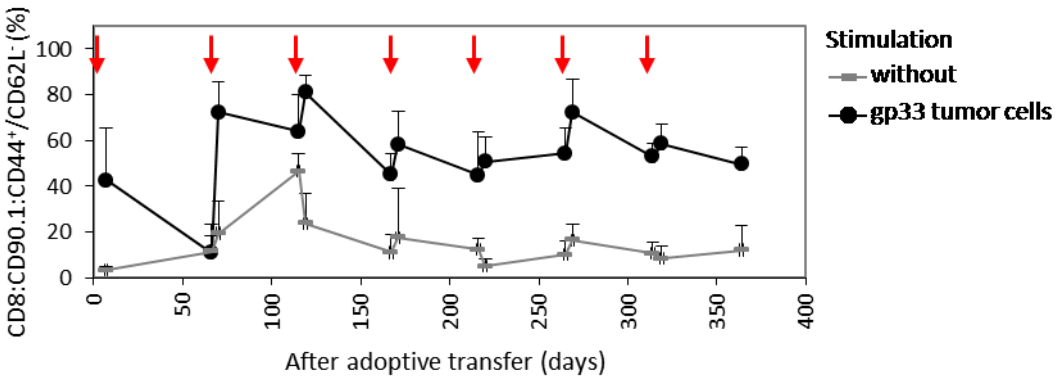

Figure 31 Analysis of CD62L expression over time in transferred T cells

Peripheral blood cells were stained with anti-CD8-APC, anti-CD90.1-PercP, anti-CD62L-FITC, and anti-CD44-PE. Cells were gated on CD8, then on CD90.1 and finally analyzed for CD44-positive and CD62L-negative cells. Red arrows indicate stimulation time points.

4.2.3 *Ex vivo* analysis of transferred T cells

Transferred T cells were able to bind P14 TCR-specific gp33-tetramer

To make sure that vβ8-positive transferred T cells still bound P14 TCR-specific gp33-tetramer, peripheral blood of OT-I+P14 I mice was analyzed on day 262. Transferred cells stained positive for gp33-tetramer (Figure 32**).** Blood of the unstimulated mouse was 62 % positive for gp33-tetramer, of gp33 tumor cell- or peptide-stimulated mice were 76 ± 3 % or 74 ± 4 % positive, respectively (Table

34). The ova-stimulated cells bound 31 % of gp33-tetramer which was less than for the other groups. This correlated with the vβ8 TCR chain expression which was lower for the ova-stimulated group/mouse. In OT-I+P14 II mice, splenocytes were analyzed at the end of the experiment for gp33-tetramer binding. Here, unstimulated cells bound 80 ± 11 % and tumor cell-stimulated cells bound 74 ± 19 % tetramer (Table 34). Between these groups no significant difference was detected.

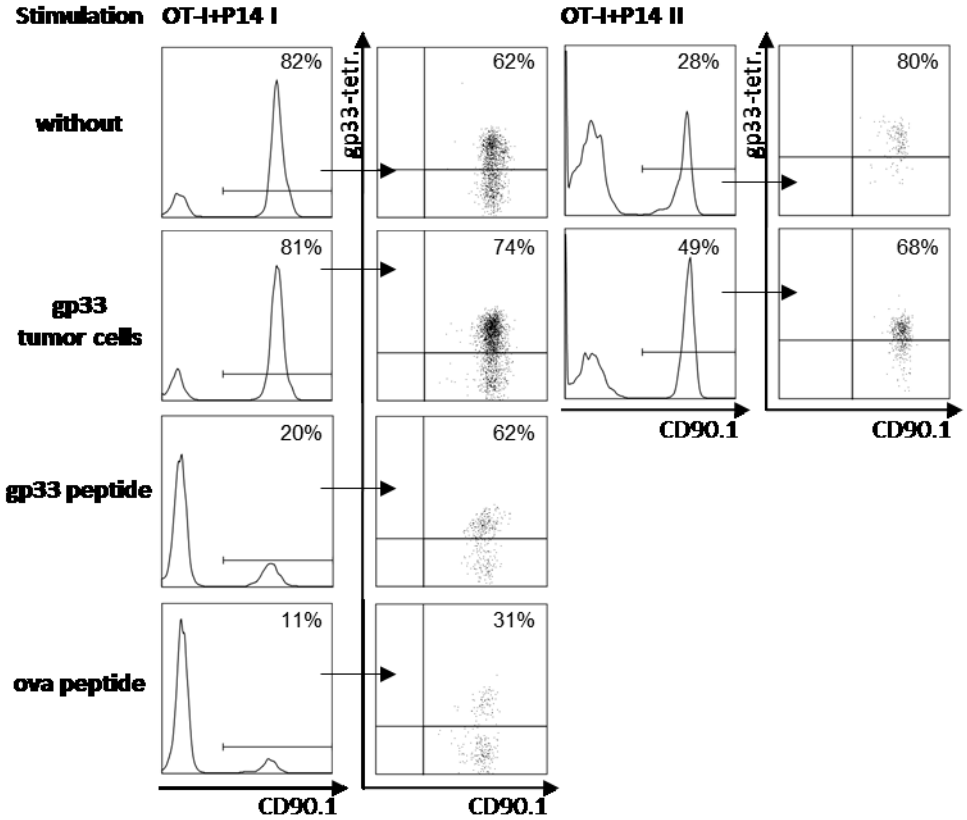

Figure 32 Transferred T cells bound gp33-tetramer

A: Peripheral blood of one mouse is shown per group on day 262 of OT-I+P14 I mice and spleen cells of OT-I+P14 II mice. Blood of OT-I+P14 I mice was stained with anti-CD8-PE, anti-CD90.1-FITC, gp33-tetramer-APC and splenocytes of OT-I+P14 II mice with anti-CD8-FITC, anti-CD90.1-PercP, and gp33-APC. First histogram shows CD90.1-positive cells gated on CD8. CD90.1-positive cells are gated in the dot plot against gp33-tetramer (gp33-tetr.).

Table 34 GP33-Tetramer-binding of transferred T cells

CD90.1: gp33$^+$ (%)	OT-I+P14 I	OT-I+P14 II	
Stimulation	peripheral blood	spleen	
Without	62 (n= 1)	80 ± 11 (n= 12)	n.s.
gp33 tumor cells	76 ± 3 (n= 3)	74 ± 19 (n= 10)	
gp33 peptide	74 ± 4 (n= 4)		

ova peptide	31 (n= 1)

Transferred T cells were present in blood, spleen, LN and BM

After day 365, OT-I+P14 II mice were sacrificed. Lymphoid organs were analyzed for transferred cells. In all lymphoid organs, blood, spleen, LN and BM, the transferred T cells were found at similar levels and were highly positive for P14vβ8 and OT-Ivβ5-TCR chains (Figure 33A).

Transferred T cells in lymphoid organs were also analyzed for CD62L- and CD44 expression. Cells of the unstimulated group were mainly CD62L- and CD44-positive (Figure 33B). Cells from mice which were stimulated with gp33 tumor cells were significantly lower in CD62L expression in the blood, spleen and in the bone-marrow due to the stimulation.

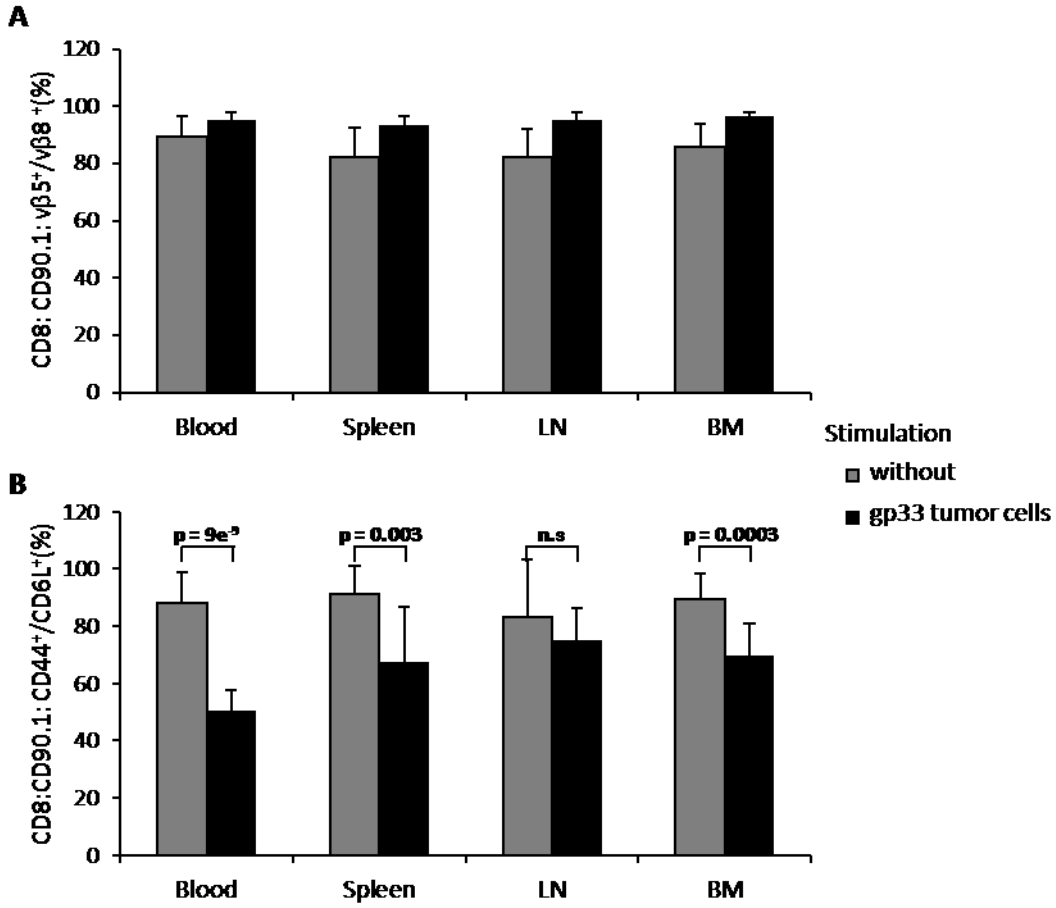

Figure 33 Transferred cells were found in lymphoid organs

Blood, splenocytes, LN and BM were prepared on day 368-371 and stained with anti-CD8-APC, anti-CD90.1-PercP, and A: anti-vβ5-PE and anti-vβ8-FITC or B: anti-CD44-PE and anti-CD62L-FITC. Cells were gated first on CD8, then on CD90.1-positive cells and were finally analyzed for positive vβ5- and vβ8-expression (A) or positive CD62L- and CD44 expression (B).

Transferred T cells still showed proliferation capacity at the end of the experiment upon adoptive transfer into second recipients

Since transferred T cells were regularly restimulated *in vivo*, proliferation capacity was tested at the end of the experiment. Mice were sacrificed and splenocytes were labeled with CFSE. Labeled cells were transferred into second recipients and stimulated as in the first recipients. After 3 - 4 days, splenocytes of second recipients were stained with anti-CD90.1 and analyzed for CFSE labeling which is diluted upon proliferation. The gp33 peptide- and gp33 tumor cell-stimulated cells showed a clear CFSE dilution upon transfer into second recipient and restimulation (Figure 34A). Transduced OT-I+P14 II T cells, which were not used for adoptive transfer into first recipients, were cryopreserved and could be compared to OT-I+P14 II T cells from first recipients (three mice per group) for their proliferation capacity in parallel. Transduced T cells before first adoptive transfer and T cells from unstimulated first recipient mice showed a background proliferation of 39 or 41 ± 6 %, respectively, without stimulation in the second recipient (Figure 34B). For T cells from tumor cell-stimulated mice, the background proliferation was significantly lower with 6 %. Upon stimulation in the second recipient, 91 % of OT-I+P14 II T cells before first adoptive transfer, 75 ± 20 % of T cells from unstimulated first recipient and 45 ± 18 % of gp33 tumor cell-stimulated first recipient mice proliferated. In comparison, T cells from mice which were left untreated showed a similar proliferation capacity as OT-I+P14 II T cells before adoptive transfer. T cells from stimulated first recipients showed a lower proliferation capacity in second recipients upon restimulation, but the difference was not significant. These results showed clearly that, although multiple times stimulated, that the transferred T cells were still able to proliferate upon stimulation and were not exhausted by the chosen stimulation methods.

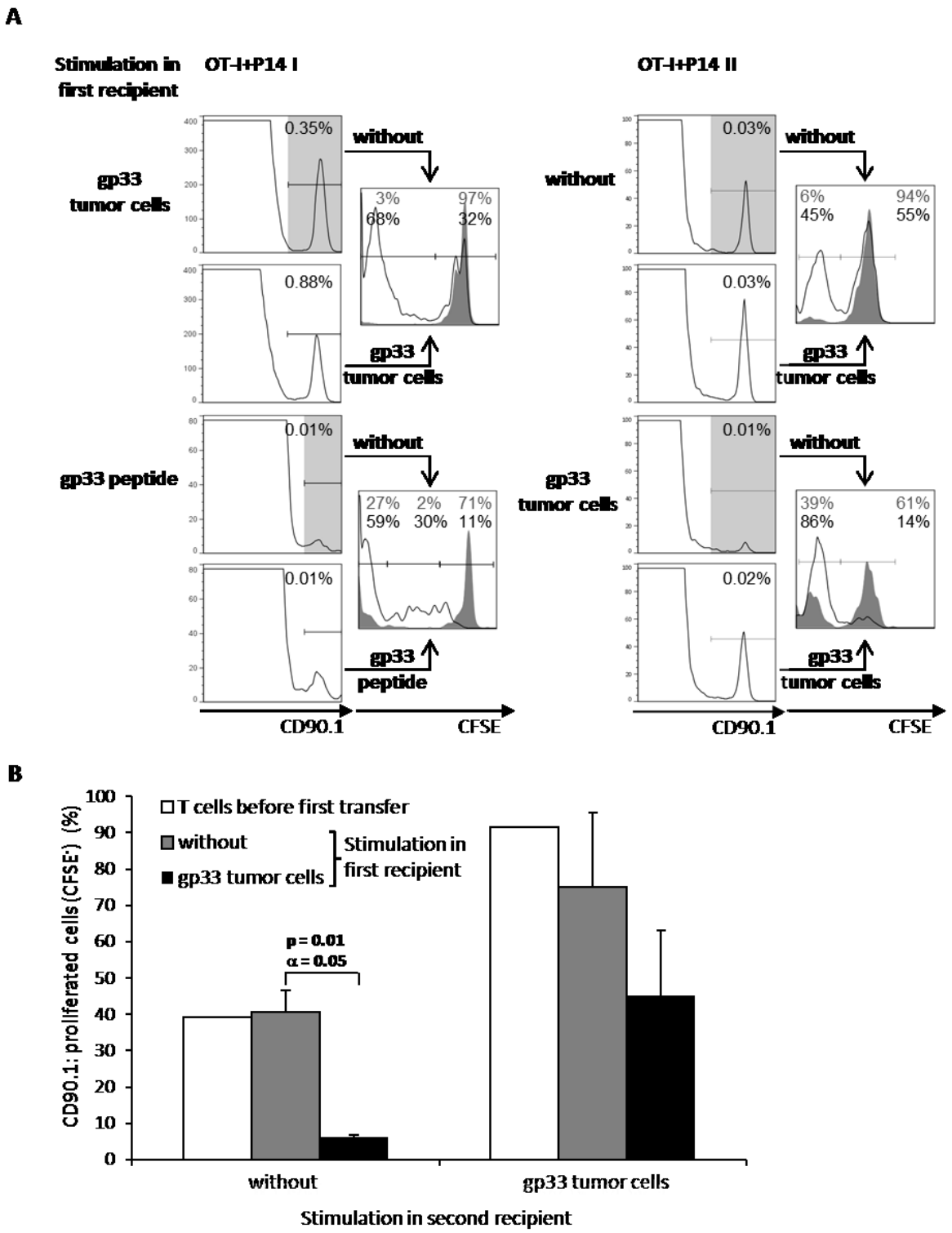

Figure 34 Transferred T cells proliferated upon transfer and stimulation in second recipients

Splenocytes of second recipients were stained with anti-CD90.1-PercP. Cells were gated on CD90.1-positive cells and are shown in an overlaid histogram for CFSE. Filled histograms are cells from unstimulated second recipients, black line from stimulated recipients. Grey numbers on histogram indicate percentage of the CFSE-populations of unstimulated cells. Black numbers indicate CFSE-populations of stimulated cells. OT-I+P14 I:

Splenocytes taken on day 557 after transfer. OT-I+P14 II: Splenocytes taken on day 368-371. B: Summarized results of OT-I+P14 II with three mice per group. Transduced T cells before first transfer were cryopreserved until this assay.

Transferred T cells secreted IFN-γ and degranulated CD107α

At the end of the experiment with OT-I+P14 II mice, transferred T cells were analyzed for the cytokine secretion capacity by staining of IFN-γ as well as their degranulation capacity by staining of CD107α. Splenocytes from OT-I+P14 II mice were incubated for four hours with gp33, ova or no peptide as well as anti-CD107α-antibody. Afterwards, intracellular staining was done for IFN-γ. Splenocytes secreted IFN-γ as well as degranulated CD107α upon stimulation with gp33 or ova peptide (Figure 35). As example CD107α-/IFN-γ-stainings from splenocytes of one mouse of each group are shown (Figure 35A). Splenocytes from mice which were left unstimulated were positive for CD107α/IFN-γ with 37 ± 13 % when stimulated with gp33 peptide, with 47 ± 13 % when stimulated with ova peptide and with 13 ± 10 % without peptide (Figure 35B). Splenocytes from mice which were stimulated with gp33 tumor cells were 44 ± 15 % positive for CD107α/IFN-γ when stimulated with gp33 peptide, 43 ± 16 % when stimulated with ova peptide and 3 ± 8 % without peptide. Between both groups no significance difference could be detected, only without *in vitro* peptide stimulation the background secretion of CD107α/IFN-γ of splenocytes from unstimulated mice was higher as from stimulated mice.

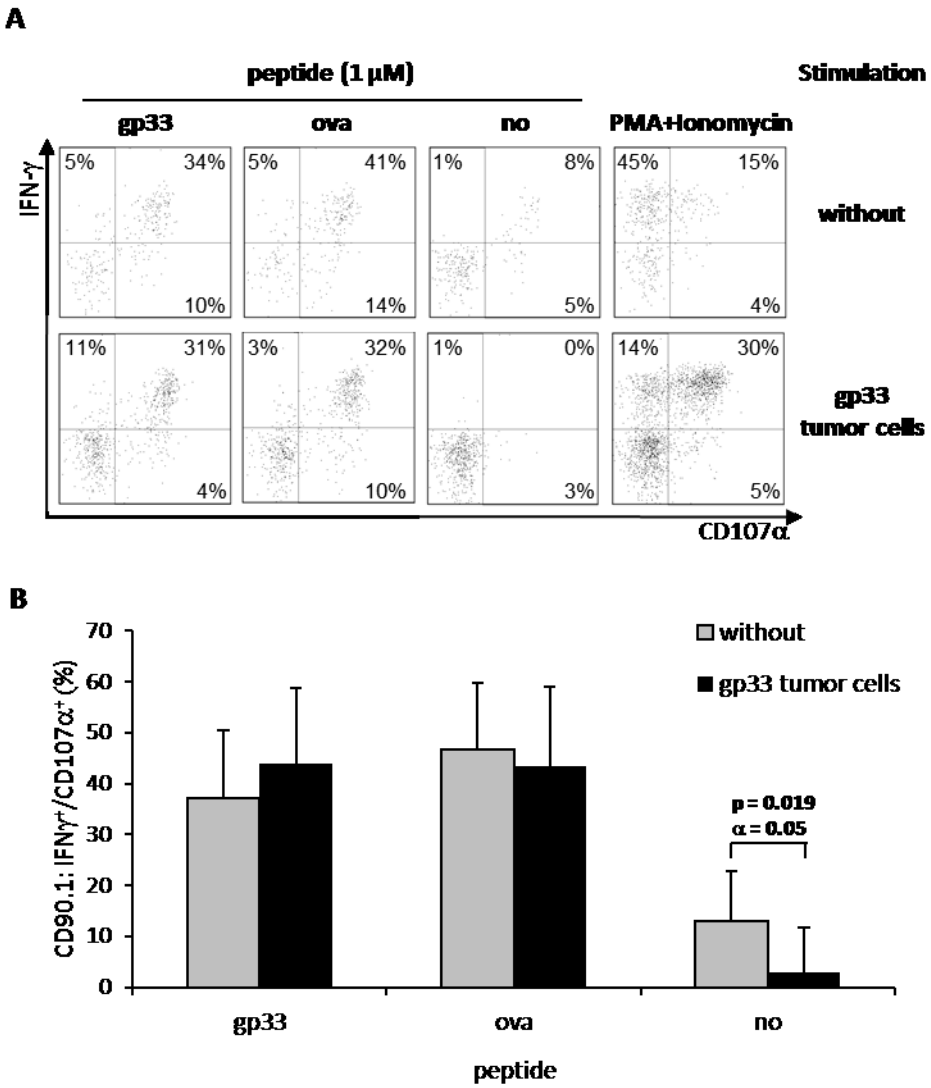

Figure 35 Transferred T cells were still functional at the end of the experiment

Splenocytes were incubated with 1 µM of ova, gp33 peptide or without (no), anti-CD107α-PE, Brefeldin (10 µg/ml) and Golgi-Stop (0.5 µl/200 µl) for 4 h. Cells were stained with anti-CD90.1-PercP and intracellular staining was done with anti-IFN-γ-APC. Cells were gated on CD90.1. A: Dot plots of CD107α- against IFN-γ-expression of two mice are shown. Upper row: splenocytes from a mouse which was left unstimulated (without), lower row: splenocytes from a mouse which was stimulated with gp33 tumor cells. B: Bar diagram shows summarized results of the CD107α-/IFN-γ-stainings of splenocytes from mice which were left unstimulated (12 mice) or which were stimulated with gp33 tumor cells (10 mice).

LAM-PCR revealed polyclonality of the transduced T cells over time

LAM-PCR is used to detect the integration site of the provirus in the cell genome. The analysis was undertaken with DNA from all collected time points and done with two restriction enzymes for the experiment with OT-I+P14 I transferred T cells (Figure 36) and OT-I+GFP transferred T cells (data not

shown). The experiments were carried out in the lab of Christof von Kalle in Heidelberg. Gel electrophoresis showed multiple bands of different size ranging from 100-500 bp (Figure 36A-C). Since the 5'-LTR and 3'-LTR are equal in the provirus, an internal control is also amplified from the 3'-LTR into to the proviral sequence. For the restriction enzyme HpyCH4IV the internal control band has a size of 512 bp if it is cut at the first restriction site. Shortly after, there are two more restriction sites for HpyCH4IV which would lead to band sizes of 525 and 576 bp. Two bands were visible around 500 bp which were seen in all samples representing the internal control bands. For each sample 100 ng was used but band intensities were different between samples which was due to the different percentages of transferred cells in the mice on different time points. Smears indicated many integrations sites. Specific bands did not increase with time, but disappeared again. LAM-PCR experiments of some samples were done at a later time point (Figure 36D-E). Here, LAM-PCR did not give raise to multiple distinct bands but only to a DNA smear and one single band. Reason for that were contaminations with the MP71 plasmid which disturbed the amplification of integration sites. Instead, a plasmid band of a size of 90 bp which had an advantage during the amplification procedure over larger sequences was amplified. In the first LAM-PCR, this contaminated plasmid band was also visible but nevertheless other sequences could be well amplified. Optimization of the DNA preparations to avoid plasmid contaminations was done in the OT-I+P14 II experiment, but LAM-PCR experiments are still ongoing. LAM-PCR products will be sequenced in the future. Nevertheless, the first and also partly the second LAM-PCR experiments showed that multiple integration sites were present in the analyzed DNA samples which suggest that in none of the mice a monoclonal outgrowth could be observed. DNA of the control experiment OT-I+GFP was also analyzed by LAM-PCR but here, also the plasmid contamination dominated the amplification so that other bands were rarely visible or only as a smear (data not shown).

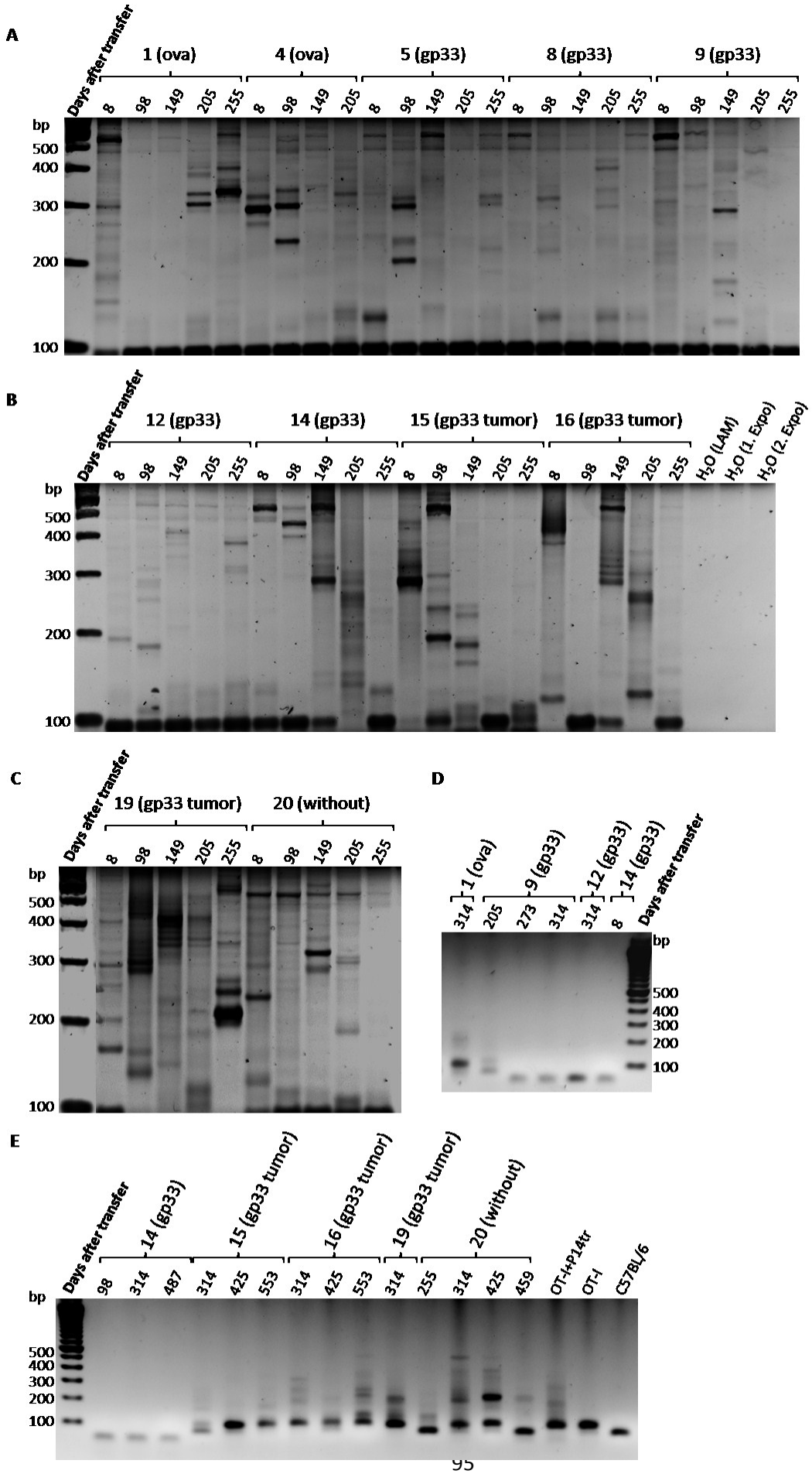
A
Days after transfer
1 (ova)
4 (ova)
5 (gp33)
8 (gp33)
9 (gp33)
8 98 149 205 255 8 98 149 205 8 98 149 205 255 8 98 149 205 255 8 98 149 205 255
bp
500
400
300
200
100
B
Days after transfer
12 (gp33)
14 (gp33)
15 (gp33 tumor)
16 (gp33 tumor)
H2O (IAM)
H2O (1. Expo)
H2O (2. Expo)
8 98 149 205 255 8 98 149 205 255 8 98 149 205 255 8 98 149 205 255
bp
500
400
300
200
100
C
Days after transfer
19 (gp33 tumor)
20 (without)
8 98 149 205 255 8 98 149 205 255
bp
500
400
300
200
100
D
1 (ova)
9 (gp33)
12 (gp33)
14 (gp33)
314 205 273 314 314 8
Days after transfer
bp
500
400
300
200
100
E
Days after transfer
14 (gp33)
15 (gp33 tumor)
16 (gp33 tumor)
19 (gp33 tumor)
20 (without)
98 314 487 314 425 553 314 425 553 314 255 314 425 459
OT-I+P14tr
OT-I
C57BL/6
bp
500
400
300
200
100

Figure 36 LAM-PCR of analyzed blood DNA revealed polyclonal integrations sites

LAM-PCR with the restriction enzyme HpyCH4IV is shown. A-C: Spreadex gels - first LAM-PCR experiment. D-E: 2% agarose gels- second LAM-PCR experiment. Second LAM-PCR experiment was performed on a later time point. 100-bp marker was loaded. On spreadex gels 5 µl and on agarose gel 10 µl of PCR products was loaded. In the second LAM-PCR experiment few samples of the first LAM-PCR were repeated. Numbers above brackets indicate mouse numbers, and beside the stimulation method is indicated. gp33: gp33 peptide-stimulation, ova: ova-peptide stimulation, gp33 tumor: gp33-tumor cell stimulation.

5. DISCUSSION

5.1 INDUCIBLE TCR EXPRESSION AND DUAL TCR T CELLS

5.1.1 INDUCIBILITY OF THE ANALYZED TET-SYSTEM

The TCR complex has a complex structure and biology. The inducibility of the TCR expression is not easily comparable to proteins like luciferase or GFP. The TCR complex consists of two polypeptides which have to be folded in the endoplasmatic reticulum (ER) and associate there with the CD3 complex which also consists of multiple polypeptides. Therefore, the TCR expression in the Tet-system does not only depend on the induction but also on the prober association with the CD3 complex. The fold-induction which is used as a characteristic term for tet-regulated gene expression of indicator genes like luciferase or GFP is not useful for tet-regulated TCR surface expression. The vector used in this work had a 220-fold induction of GFP and luciferase in HT1080 cells [172]. The cell system used in this analysis does not harbor an endogenous TCR in the first place. But TCR expression on the cell surface is limited by the amount of CD3. When all available CD3 complexes are occupied, there is no further increase of TCR expression. Also, one has to take into account that the TCR/ CD3 complexes are cycled between the cell surface and endosomes [178,179,180]. 70 - 85 % of the TCR/ CD3 complexes are on the cell surface while 15 - 30 % are found inside the cell. The cycling time is about 100 min and a TCR is recycled approximately nine times in resting cells before it is degraded [181]. The screening of cell clones showed different expression patterns (data not shown). Some clones did not show good TCR expression but others were > 90 % TCR-positive after Dox induction. As also seen for other transgenes, the different expression patterns can be due to different copy numbers of the vector per cell and also depend on the integration site [164]. In case of TCR expression, other properties of the cell clone could have an influence like the CD3 availability, the protein folding and recycling machinery.

The inducibility of the TCRs P14 and OT-I in the shown 58 cell clones was similar. A small TCR-positive population of 10- 20 % was visible with 0.01 µg/ml Dox which increased to around 60 % with 0.05 µg/ml Dox. The 58+P14tet clone reached the maximal TCR expression with less Dox (0.1 µg/ml) than the 58+OT-Itet clone (0.5 µg/ml). With higher Dox concentrations the differences in TCR-positive cells were small if not absent. The expression levels, studied by the MFI, were the lowest with 0.05 µg/ml Dox. The increase of the expression level was different between the TCR chains which might also have been due to the properties of the used antibodies. Also, the cell number and the fitness of the cells could influence the inducibility and titration. Although the experimental set-up was standardized with usage of the same cell concentrations, variations were seen between experiments.

The functionality of the TCR-positive cells was partially titrated with different Dox concentrations, but also here variability was seen between experiments. IL-2 secretion of 58+P14tet cells increased until a concentration of 0.5 µg/ml Dox, although the maximal TCR expression was already reached with 0.1 µg/ml Dox. The functionality of the 58+OT-Itet cells was not further increased with more than 0.01 µg/ml Dox, but maximal TCR expression was shown to be obtained only with 0.5 µg/ml Dox. For the functionality assay only one experiment was shown, whereas for the TCR expression summarized results were shown which probably causes the discrepancies to the functionality data.

In case of dual TCR T cells, it was possible to generate T cell clones which were over 90 % TCR-positive after induction and kept at the same time the endogenous TCR expression. The induction properties with different Dox concentrations were similar to the Tet clones expressing a single TCR. With 0.05 µg/ml Dox around 70 % cells were TCR-positive. With higher concentrations the percentage was between 80- 90 % for the induced OT-I TCR and 85-98 % for the induced P14 TCR depending on the experiment. The expression level as determined by the MFI was lowest with 0.05 µg/ml Dox and with higher Dox concentrations hardly distinguishable. The differences in expression level were more prominent for the TCRvα chains than for the TCRvβ chains, probably due to the two-step antibody staining which led to an enhancement of the signal and therefore, to an enhancement of MFI differences.

Although the functionality of the induced TCR was seen in dual TCR T cells, the functionality of the endogenous TCR was lost or reduced even with a low concentration of 0.05 µg/ml Dox. The reason for this could be intrinsic factors of the 58 cell line or others as discussed below. With the here described Tet vector, it was not possible to analyze the correlation of TCR amount on the cell surface and function, since the expression level was only lower when only part of the cells expressed the TCR (with 0.05 µg/ml Dox). With higher Dox concentrations differences were too small or absent.

Labrecque *et al.* [16] have genereated a transgenic mouse with a constitutively expressed OT-Ivβ5 chain and a regulable OT-Ivα2 chain by a Tet-off system. After treatment of mice with Tetracycline (Tc), blood was taken on day 4 and stained for CD8 or CD4 and OT-Ivα2. A strong decrease of expression level was seen which further decreased to baseline level on day 14. With help of calibration beads TCR molecules were quantified. The transgenic mouse had 20000 TCR molecules on the cell surface without Tc. After treatment with different doses of Tc (5, 10 and 400 µg/ml) for two weeks, stably reduced expression levels of the OT-Ivα chain was measured corresponding with 5000-6000, 500-1000, 0-200 with stated Tc concentrations, respectively. The functionality of these different T cell populations was dose-dependent of Tc. 1100 TCR molecules were enough to trigger proliferation in 7 % (2 % background) of the cells after immunization with 0.1 µg peptide. With 450

TCR molecules they saw proliferation in 40 % of the cells after immunization with 100 µg peptide. In these transgenic mice, it was possible to determine the functionality of T cells dependent on the TCR density on the cell surface. Although the inducible TCR expression in the presented cell system conferred a lower TCR level with a low Dox concentration (0.05 µg/ml), this effect was concomitant with the lower percentage of cells expressing the TCR.

5.1.2 TCR AMOUNT AND TCR PROPERTIES

The avidity of T cells is reduced when the expression level of the transduced TCR is lower than in the original clone. This can be due to a less efficient expression of one or both TCR chains because of several reasons or mispairing with endogenous TCR chains. It was clearly shown that the T cell avidity is proportional to the expression level of the TCR [16,182].

That the surface expression level of the transgenic TCR depends on the endogenous TCR was shown by several investigators. Heemskerk *et al.* saw that a transgenic TCR is expressed on different levels depending on the T cell clone used for transduction [183]. This effect was independent of the expression system. As Sommermeyer *et al.* [106] showed, certain TCRs can replace endogenous TCRs on the cell surface. The P14 TCR could replace the endogenous TCR of B3Z cells as shown by TCRvβ chain staining and functional analysis. The expressional and functional loss was also the case when a human CMV-specific T cell clone was transduced with the melanoma-specific gp100-TCR. When using the same expression system by using retroviral transduction of human Jurkat76 cells, which do not harbor an endogenous TCR, it was also shown that the strong gp100 TCR replaces a weak renal cell carcinoma-specific TCR. On the other hand, two strong TCRs could be coexpressed as shown for a melan-A-specific T cell clone transduced with the gp100 TCR and also shown in double-transduced Jurkat76 cells.

A study using combinations of 16 different TCRα chains and 15 different TCRβ chains showed that each TCR chain combination had a different capacity to be expressed on the cell surface. This was analyzed in γδ T cells where mispairing with TCRγ and δ chain could be excluded. Expression level was solely dependent on the competition for the CD3 complex with TCRγ and δ chains. This analysis showed that the competence to associate with the CD3 complex was dependent on the variable region, only 5 amino acids in the CDR3 region could make a difference [183].

In the analyzed cell system the P14 and OT-I TCR could be coexpressed. The percentage of cells positive for the endogenous TCR was not or only slightly reduced (Figure 11) but the expression level as measured by MFI was reduced after TCR induction in both cell clones (Figure 12). The quantification of the TCR chains (Figure 13) revealed that the 58+OT-I+P14tet had less TCR molecules of the endogenous OT-I TCR on the cell surface (OT-Ivα2: 1830 ± 480, OT-Ivβ5: 1910 ± 210 molecules)

than the 58+P14+OT-Itet of endogenous P14 TCRs (P14vα2: 4360 ± 1080, P14vβ8: 3200 ± 400 molecules). Normally, on primary mouse T cells 40000 TCR molecules are found [16]. The low amounts of TCRs seen here must be a property of 58 cells. In 58+OT-I+P14tet cells, the endogenous OT-I TCR was equally reduced in its TCR chains (OT-Ivα2 by 49 %, OT-Ivβ5 by 57 %) whereas the transgenic P14 TCR was equally induced. In the second clone, the endogenous P14 TCR chains were reduced to different amounts, the P14vα2 by 63 % and the P14vβ8 by 39 %, but stayed with more molecules on the cell surface as the induced OT-I TCR molecules. The different reduction of endogenous TCR chain molecules correlate with the measured FRET values. The endogenous OT-I TCR did not drop in its FRET efficiency after second TCR expression but the endogenous P14 TCR. Since the molecule amount of the P14vα2 without Dox had a high standard deviation the calculated reduction of 63 % might not be correct. Nevertheless, in the FACS histogram of Figure 12 it was also seen that the P14vα2 chain was strongly decreased in its MFI. Also, by the cell clones with only one inducible OT-I TCR chain it was apparent that the P14vα2 chain was strongly decreased in its MFI when the OT-Ivα2 chain was induced which again led to a drop of FRET efficiency of the P14 TCR. The replacement of P14vα2 by the OT-Ivα2 might be therefore the main reason that FRET efficiency of the P14 TCR decreased after induced OT-I TCR expression.

There was a discrepancy between the measured TCR surface molecules by quantified TCR staining (Figure 13) and detected copy number of integrated vectors (Table 29). The 58+OT-I+P14tet cells showed less OT-I TCR surface expression but had a high copy number of 16 for the pLSN vector expressing the OT-I TCR. The 58+P14+OT-Itet cells had more P14 TCR surface expression but less integrated P14 TCR-pLSN vector (5). This might lead to the conclusion that the P14 TCR is easier expressed on the cell surface despite of less expressing integrated vectors as the OT-I TCR. Integration sites might have an influence on the vector expression, therefore it is not clear how many TCR molecules were really expressed and if, in the one case, just more TCR molecules came to the cell surface. But the lower copy number of the endogenous P14 TCR also would explain that the P14vα2 chain was easily replaced by the OT-Ivα2 chain, since the intracellular storage of TCR molecules was just less as for the endogenous OT-I TCR.

The analysis of the functionality showed a loss or at least reduction of function of the endogenous TCRs in both cell clones. Although, by Labrecque *et al*. it was shown that 500-1000 TCR molecules are enough for T cell reactivity [16], in all analyzed cell clones the functionality of the endogenous TCRs was lost. The reduced TCR surface expression as measured by the MFI and the mispaired TCR dimers could explain this observation. But the observation is also restricted to the 58 cells and the kind of vectors used, since in primary OT-I cells the function was not lost when they were transduced with the P14 TCR, expressed by the strong retroviral MP71 vector.

5.1.3 TCR MISPAIRING

In the clinical trial of Morgan *et al.* the detection of the transduced TCR in the patient's blood by quantitative reverse-transcription PCR (26 %) did not correlate with the TCRvβ staining (8.1 %) and MART-1 tetramer staining (0.8 %) [85]. This discrepancy can be due to mispairing of transduced TCR chains with endogenous TCR chains. By Dossett *et al*. it was observed that P14 transgenic T cells transduced with a TCR specific for the gag antigen of Friend murine leukemia virus showed TCRvα3 expression on around 60 % of cells but TCRvβ12 on only 20 % cells depending on the transgene cassette used. These differences of cell surface expression hinted to a mispairing of the transferred TCRvα3 chain with the endogenous P14vβ8 chain [95]. That TCR chain mispairing can indeed lead to autoreactivities was demonstrated by Bendle *et al* [123]. He transduced OT-I TCR, single OT-I TCR chains or other TCRs into C57BL/6 splenocytes and transferred them into recipient mice by employing a transfer protocol similar to human trials with total body irradiation and high-dose IL-2. Transduced cells induced GVHD by mispaired TCR dimers in this setting whereas transgenic OT-I splenocytes did not. For human TCRs the possible mispairing could be proven by van Loenen [124] by transducing T cell clones with TCRs and testing the transduced cells with autologous or allogeneic LCLs which elicited new reactivities.

Also in nature T cells with mispaired TCRs occur. Due to failure of allelic exclusion it happens that T cells express a second TCR chain as seen for TCRα in up to 10 % of peripheral T cells [184,185]. In animal models it was seen that these dual T cells are involved in alloreactivities [185] and might provide a link between viral and autoimmune diseases [186].

In the presented study, TCR mispairing was quantified by FRET. In the dual TCR T cell clones it was seen, that indeed mispairing occurred; to a lesser extend between the P14vα2 chain and the OT-Ivβ5 chain than between the OT-Ivα2 chain with the P14vβ8 chain. Strikingly, the endogenous P14 TCR was reduced in its FRET efficiency when the OT-I TCR occurred on the cell surface which did not happen the other way around. This effect was mostly due to the displacement of the P14vα2 chain by the OT-Ivα2 chain, which was shown by analyzing cell clones with an endogenous P14 TCR and inducible single OT-I TCR chains. When the OT-Ivα2 chain was induced the FRET efficiency of the P14 TCR dropped vigorously, whereas it dropped only slightly when the OT-Ivβ5 chain was induced. This reduction of the endogenous TCR pairing was not seen for the OT-I TCR in 58+OT-I+P14tet cells. Probably, the available intracellular amount of the endogenous TCR plays a role since a higher copy number of 16 was measured for the endogenous OT-I TCR than only 5 of the endogenous P14 TCR. The copy number of the cell clone with one inducible OT-I chain were not determined but it cannot be excluded that this might influence the result. In conclusion, beside the provided protein amount also the intrinsic properties of the TCR chains determine the cell surface expression when competing

with other TCR chains. That the TCR chain determines its ability to associate with the CD3 complex was also shown by Heemskerk *et al.* [183] which in turn has an influence on the mispairing efficiency.

In vivo Bendle *et al.* [123] saw a difference in GVHD induction between the usage of the OT-I TCR cassette with an IRES site linking the TCR chains and the OT-I TCR cassette with a 2A element linking the TCR chains and a second cysteine bridge. Also, in human TCRs it was shown that the second cysteine bridge has a benefit for the transgenic TCR-mediated functionality and surface expression [113]. In the presented work a second cysteine bridge was employed in the P14 TCR. The mispairing of the TCR chains could not be avoided and also not the reduction of the P14cys TCR FRET efficiency. Although, the reduction was different between the two analyzed cell clones. In cl. 7 the transgenic OT-I TCR was only inducible in 46 % of the cells, whereas in cl.9 in 90 % of the cells. The reduction of endogenous P14cys FRET efficiency was stronger in cl.9 than in cl.7. Here again, the copy number of integrated vectors could be a reason, since cl.7 had 11 P14 TCR vector copies whereas cl.9 had only 5.

But more importantly, the second disulfide bond did not reduce the mispaired TCR formats. Also, the functionality loss of the endogenous TCRs could not be restored. Although in primary human lymphocytes it was shown that the second cysteine bridge improved the functionality of the transduced TCR [113]. When primary OT-I T cells were transduced with a P14 TCR with or without a second cysteine bridge, there was only a small difference seen in the FRET efficiencies for the P14 TCR and no difference for the mispaired TCR dimer of P14vα2 and OT-Ivβ5 chain. In conclusion, it can be that the there was no effect by the disulfide bond seen since only the combination of two TCRs were analyzed. The mentioned studies above were using polyclonal T cell populations. Therefore, analysis in wild-type cells was undertaken to determine the effect of the cysteine bridge in a polyclonal setting. Although a tendency of increasing FRET efficiencies between P14 TCR formats and for non-codon-optimized OT-I TCR formats with increasing optimization could be detected, these differences were not significant. The detection method by the FRET technology might not be sensitive enough. Differences might be better detectable with help of a sensitive *in vivo* model as used in the work of Bendle *et al.* [123].

5.2 SAFETY ANALYSIS OF TCR-TRANSDUCED T CELLS

The safety of gene therapy was questioned by trials where transduced HSCs were used as several patients in different trials treated with different γ-retroviral vectors and transgenes showed integration-related abnormal cell outgrowth (SCID, CGD, WAS). On the other side, trials treating ADA-SCID in 30 patients worldwide since 2000 showed no adverse event so far, although developing T cells have a growth advantage in these patients [187,188]. As the rsik of gene-modified stem cells was shown, for T cells there has been no evidence so far. In human gene therapy trials using gene-marked T cells malignancies were also not observed. The transfer of HSV-Tk transduced T cells for DLI to control GVHD was successful and safe [152,153,154,189]. Also the usage of the truncated NGF receptor (ΔLNGFR) for gene marking studies with T cells in mice, rats and dogs and DLIs in humans were safe [155]. Also, there have been clinical studies involving HIV-infected patients which received gene-modifed T cells. Cells were transduced with a chimeric CD4 receptor fused to the signaling domain CD3ζ [190,191,192] or an HIV entry-inhibitory peptide [193] were transferred. Patients were followed up to one year and cells persisted. In none of the patients adverse events due to the T cell product were observed.

The study of Newrzela *et al.* [156] showed that mature murine T cells do not transform even when transduced with known T cell oncogenes and transferred into lymphopenic RAG-1 mice. The chosen oncogenes LMO2 [194] and ΔTrkA [195] are shown to be responsible for immature T cell leukemias and the oncogene Tcl-1 even for mature T cell leukemias in mice [196] and humans [197]. In another study [198], T cells transduced with a γ-retroviral vector expressing a chimeric T-Body, which was directed against the tumor-associated Lewis-Y antigen, were transferred into non-myeloablative irradiated mice which did not express the antigen. The T-Body consists of an extracellular single-chain antibody and signaling regions of CD28 and CD3ζ. Tumor incidence and types of tumors were comparable to a group without T cell transfer. None of the lymphomas arising were of donor T cell origin. The transferred T cells persisted with 1.9- 16.7 % of total spleen cells in most of the mice as measured upon death after around two years or earlier after tumor burden. The polyclonality of the transferred T cell population was confirmed by staining the TCRvβ repertoire, although two mice had an unusual high percentage of certain TCRvβ chains. Concluding these studies the researchers did not find malignancies derived from γ-retrovirally-transduced T cells. But in humans normally T cell leukemias and lymphomas arise in old age. It is difficult to extrapolate the life time of mice to humans, but for example showed a study with γc-transduced HSC transfer into γc-deficient mice that lymphomas already developed after 6-12 months [199] which took 3 years in humans [135] . Mice can develop many types of tumors in two years which occur only at old age in humans.

In vitro TCR-transduced primary T cell clones were shown to keep a stable phenotype and redirected functionality after 6 months in culture [200]. But, there is one study showing the possible transformation of T cells *in vitro* using the proto-oncogene LMO2 [157]. In the transformed T cell clone, the retroviral vector had integrated near the *IL2RA* and *IL15RA* genes. The up-regulation of these genes together with the transgenic LMO2 expression led to the transformation process although this T cell clone could not grow *in vivo* and was still IL-2-dependent.

In the presented study no signs of malignancies due to the transfer of TCR-transduced T cells could be observed which goes in line with the studies mentioned above. Instead, the treatment with cyclophosphamide harbored a risk of toxicity.

5.2.1 Influence of preconditioning and of endogenous T cells on transferred T cells

Non-myeloablative treatment was used for a good T cell engraftment in recipient mice. The endogenous T cell pool was recovered after cyclophosphamide treatment of the mice in a short term view. The transfer of the high cell number probably influenced the T cell recovery due to competition for cytokines in the periphery. By day 200 after transfer, which corresponded to an age of around 10 or 12 months of the recipient mice, the T cells (which derived from 5-6 months old donors) increased in percentage in the CD8 compartment. In the OT-I+P14 I group, the transferred T cells made up 60 % in the one unstimulated mouse on day 416, 44 ± 26 % in the gp33 tumor cell-stimulated group (two mice) on day 501, 31 ± 9 % in the gp33 peptide-stimulated group (three mice) and 39 % in the ova peptide-stimulated mouse on day 416. Similarly, in the OT-I+P14 II experiment in unstimulated mice 28 ± 10 % and in tumor cell-stimulated mice 58 ± 18 % CD90.1-positive cells of CD8 T cells were found on day 365 after transfer. On day 450, transferred cells made up 28 ± 8 % of all CD8 T cells in the GFP-transduced T cell group. The increase of transferred T cells might be explained by the decreased T cell output of the thymus with age or also by late effects of cyclophosphamide treatment or the combination of both. The endogenous T cell repertoire declines with age and thymic involution, although the total number of T cells is maintained by homeostatic proliferation of peripheral memory T cells for some time [27,201]. In mice, the size of the thymus is already reduced by an age of 6 weeks. Therefore, the recipient mice used in this work have already a diminished T cell output from the thymus. But until the age of 3 - 4 months, the murine thymus is still able to reconstitute the peripheral T cell pool after its ablation by chemotherapy or irradiation. In humans, it was shown that patients older than 30 years have a reduced thymic capacity for T cell recovery [27].

The high cell number transferred into the mice might also have played a role. The endogenous T cell pool comprises 1-2 x 10^8 cells [201], transferred T cells made up 1/20 - 1/40 of the endogenous T cell pool upon transfer.

Already in 1984, it was shown by Greenberg and Cheever [202] that cyclophosphamide treatment was beneficial for T cell transfer in the treatment of leukemia in a mouse model. Here, a high number of 2 x 10^7 antigen-activated T cells were transferred into sick mice pretreated with 180 mg/kg cyclophosphamide. Leukemic cells were cleared in 26 of 32 mice. The follow-up observation of treated mice showed that transferred T cells persisted and made up 5 % of spleen cells on day 60 and 2 % on day 120. North *et al.* showed that tumor growth was delayed when mice were treated with 160 mg/kg cyclophosphamide, but only slightly when tumor-bearing mice were irradiated. In combination with T cell transfer the positive effect could be even increased. In clinical trials the benefit of preconditioning on T cell transfer was already confirmed [80,119].

The toxicity seen in the OT-I+P14 I and OT-I+GFP experiment was due to the high concentration of cyclophosphamide (200 mg/kg) used. The concentration was chosen based on a publication stating this amount in combination with OT-I T cell transfer and peptide stimulation with poly (I:C) adjuvant [177]. This treatment led to an expansion of 22 % OT-I T cells in the peripheral blood of C57BL/6 recipient mice on day 6. This approach seemed to be feasible for the experiments in this dissertation since a good stimulation and engraftment was required for the long-term observation of transferred cells in recipient mice. Salem and colleagues observed the mice only for a period of 21 days; therefore, they could not notice the toxicity occurring after day 50. In the second experiment, a lower dose of 100 mg/kg was chosen and 12 weeks old recipients were used. But also here, four mice probably died due to the cyclophosphamide. The lower dose of non-myeloablative treatment also led to an increase of transferred T cells in the CD8 T cell compartment of recipient mice.

5.2.2 Influence of stimulation on transferred T cells

After adoptive transfer into patients, T cells encounter tumor antigens which should trigger T cell response and proliferation. In patients with recurring disease, T cells would be triggered several times. During proliferation mutations could be accumulated. Transferred T cells develop into memory T cells after transfer which have a moderate turnover of 1-2 division per month [203] or less independent on antigen encounter [204] whereas T cells responding to antigen divide several times per day [205,206]. The proliferative capacity is exhausted by the seventh decade in humans, which is due to telomere lengths and therefore the capacity to respond to antigens is reduced [27,201,207]. How often a T cell really divides during life time depends on subtype and surrounding conditions.

In this work, T cells were repetitively stimulated to provide mutations the opportunity to establish during cell division. In OT-I+P14 I mice, stimulation with gp33 tumor cells enriched the transferred T cells more than peptide stimulation, but the one unstimulated mouse also enriched the transferred T cells to a high amount. Tumor cell stimulation was a better choice than peptide stimulation with CpG ODN 1826 and IFA which probably induced activation induced cell death. The group of OT-I+P14 II mice, stimulated with gp33 tumor cells, had a higher percentage of transferred T cells than the unstimulated group at the end of the experiment. The differences between the unstimulated mice from OT-I+P14 I and II might be due to the different concentrations of cyclophosphamide used. Also, unstimulated mice showed that the increase of transferred T cells was not only due to the stimulation but also due to the preconditioning.

The memory T cell pool for a certain antigen can increase in size overtime with secondary infection or heterologous boost stimulation [15,208]. This would go in line with the strong increase of cells in the tumor cell-stimulated group and to a lesser extend for the peptide-stimulated groups. In one study, it was shown that upon homologous boost stimulation (a recombinant virus expressing ova) T cells did not expand but upon heterologous boost (two different recombinant viruses expressing ova) [209] which was not the case using homologous Sendai virus reinfection [208]. In this presented work, homologous stimulation seemed to work since T cells proliferated upon second transfer and restimulation as shown by CFSE dilution. Nevertheless, the proliferative capacity is limited as older the T cells become. It was shown that T cell clones which arose two years after acute infection with Sendai virus in mice were mostly not as effective as young memory T cells against a second infection with Sendai virus [210]. In the mentioned study, a big cohort of 100 mice were observed for the occurrence of virus-specific T cell clones which was the case in most of the mice on day 780 as measured by virus-specific tetramer staining. These natural occurring T cell clones were not malignant. In the presented work 557 days after transfer of OT-I+P14 I or 365 days after transfer of OT-I+P14 II T cells did show proliferation when stimulated in secondary recipient. By others, it was also shown that nonspecifically activated and transduced T cells could respond to antigen 182 days after transfer [209] showing that at this time point the proliferative capacity is definitively not exhausted.

The stimulation with peptides and adjuvant showed a stronger activation after first stimulation and a more dominant effector memory T cell phenotype after following stimulations, whereas the tumor cell-stimulated group contained transferred T cells of a more pronounced central memory T cell phenotype and down-regulation of CD62L was not as strong on peaks of responses. This is definitively due to the types of stimulations. Whereas in a model of Sendai virus infection, the central memory T cells dominated recall responses [208] effector memory T cells were more important in

another model with parainfluenza virus [211]. In adoptive transfer studies into macaques the central memory T cells showed a better performance in terms of persistence and functional response [212]. In the presented work, the tumor cell-stimulated group had the highest percentage of CD62L-positive transferred cells and the highest percentage of transferred cells over time.

The vaccination with peptide in combination of CpG ODN and IFA was shown to be very effective in eliciting anti-tumor responses in mice [213] and triggering antigen-specific T cells in humans [214]. Long-term survival of transgenic T cells was seen five months after immunization [215]. Peptide and CpG ODN alone could also stimulate anti-viral response in mice [216]. Daily administration of 60 µg CpG ODN disturbed structure of lymphoid organs which led to a reduced primary humoral immune response and by day 20 liver necrosis and hemorrhagic ascites was observed [217]. Although the CpG ODN 1826 was not administered daily, it was given in total seven times over a period of more than one year. Indeed, mice which were killed at the end of the experiment had reduced liver size, spleen and lymph nodes. This might explain the lower level of transferred cells in the peptide-treated groups.

5.2.3 VECTOR INTEGRATION PATTERNS IN T CELLS

In studies with adoptive T cell transfer in mice, polyclonality of transduced T cells was confirmed by LM-PCR [156] or by TCR vβ repertoire staining [198]. In first case, at least oligoclonality to polyclonality was observed. Sequencing of integration sites revealed not more integrations near cell cycle genes and tumor-associated genes in ΔTrkA-transduced cells than in GFP-transduced T cells, but near genes involved in signaling and chromatin folding and unfolding. In the second study, transferred T cells were stained for TCRvβ chains which showed polyclonality. Only in two mice, unusual high percentage were observed for two TCR chains [198]. In humans, gene-modified T cells were analyzed for integration sites of the retroviral vector by LAM-PCR. HSV-Tk-transduced T cells of two patients showed integration clusters within chromatin regions with epigenetic marks of active promoters and regulatory elements in a cell-specific fashion. No preferential survival of T cells with integrations in cell-specific gene categories was seen and clonal dominance of T cells was absent [154]. A similar integration profile was seen in a study comparing transduced T cells from ADA-SCID patients which received either transduced T cells [143] or transduced HSCs [144]. The retroviral vector used in both studies showed a different integration behavior in the two target cells. The epigenetic state and the expression profile of the target cell influenced the insertions. In T cells, integrations were seen near genes involved in the immune system and T cell function and in T cell DNase hypersensitive sites. Long-term, there was no vector-driven bias seen in transduced T cell populations in patients [218].

In the presented experiment, LAM-PCR revealed polyclonality of the transferred T cells. Although stronger bands of integrations were observed for some time points, these disappeared again showing a dynamic behavior. Sequences of integrations sites were not analyzed yet, but will be in the future.

In the study using T-Body transduced T cells, the transgene copy number was determined at the end of the experiment. Copy numbers were 4.2 x 10^3 to 5.9 x 10^5 per million cells. Interestingly, the higher copy numbers correlated with increasing age of mice. This pointed to a better survival of transduced cells with a higher copy number of the transgene [198]. In the presented work here, an end point analysis of copy number was not done, but will be included in the future

In conclusion, in this work the transfer of TCR-transduced T cells in lymphodepleted mice showed long-term engraftment of transduced T cells which stayed polyclonal and functional over a period of one year and more.

6. OUTLOOK

For TCR gene therapy some obstacles still have to be solved. The transgenic TCR expression must be strong enough to confer anti-tumor responses. This is achieved by an efficient expression vector and also by the chosen TCR molecule. As seen in this work, the chosen TCR can mediate mispairing with the endogenous TCR chains and that even a second disulfide bond does not necessarily prevent mispairing, although it is probably reduced in a polyclonal T cell population [113,123]. Therefore, other strategies have to be explored to further decrease the mispairing potential. One strategy which could be further analyzed is the usage of chimeric TCRs with the intracellular domain of CD3ζ. FRET experiments showed that these TCR constructs only pair with its respective TCR chain and that the functionality of the endogenous TCR was not impaired while the transferred TCR gained function [116]. If such TCR constructs could confer a higher avidity remains to be analyzed. Another possibility would be the inversion of the constant region by mutating two residues which lead to a "hole-into-knob"-configuration of the interface of cα and cβ. These modified TCRs retain their avidity and TCR chains preferably pair with each other [108]. A similar approach is to minimally murinize the TCR constant regions [106,107]. Here, only few residues are mutated from human constant regions to murine ones. TCR construct show only slightly lower avidity than fully murinized TCRs and had a stronger association with the CD3 complex. Also, FRET efficiencies were higher for minimal murinized TCR than wt TCR [111]. The mispairing potential has to be analyzed not only for the TCR formats but also for the chosen TCR chains as it can be different from TCR to TCR. However, these strategies bear the risk to elicit immune responses as the transferred TCRs harbor mutations being foreign to the host. That indeed immune responses were seen in clinical trials was the case when murine TCRs specific for the human antigen p53 and gp100 were used. Antibodies directed against the variable regions of the murine TCRs were found in 23 % of the patients. The antibody detection did not correlate with persistence of transferred T cells and clinical outcome [219].

The ideal situation would be to have therapeutic T cells with only one TCR. This could be achieved by knocking down the endogenous TCR chains with small interference RNA vectors targeting the endogenous TCR chains [220,221]. Another possibility is the TCR transfer into HSCs and to differentiate these *in vitro* [222] or transfer them as a stem cell transplant [103,223,224]. The advantage would be that differentiated T cells only express the transgenic TCR. Therefore, mispairing problems would be avoided. But the potential risk of this technology would be insertional mutagenesis which was shown to occur in clinical trials with gene-modifed HSCs [135,136,138,142,150]. Another cell population which was tested for TCR gene transfer are γδ T cells. These cells were shown to be able to lyse tumor cells and leukemic cells and their TCR chains cannot form mixed dimers with TCRα and β chains [225]. TCRα and β transfer into these cells showed anti-

leukemic reactivity *in vitro* [226] and proliferative capacity, persistence and recall responsiveness *in vivo* [227]. Disadvantage is that these cells are not available in a high number, as they only make up 1-10 % of the peripheral T lymphocytes. Also, their functionality *in vivo* has to be further tested as it is still under debate. A reduction of possible mispairing combinations could be achieved when using T cell clones. This is an approach which was originally developed to confer a better survival of TCR-transduced T cells *in vivo* due to activation of the endogenous TCR specific for viral antigens of latent viruses [228,229]. Although one can be sure that the endogenous TCR is not self-reactive, even here it can be that TCR chains mispair with each other which can lead to neoreactivites [124].

The safety of TCR gene therapy not only depends on the proper pairing of TCR chains and recognition of only malignant tissue, it also depends on the safety of the gene transfer system. In this work, a γ-retroviral vector was used to transduce T cells which was shown to be safe so far. Nevertheless, γ-retroviral vectors show an integration pattern which is not as safe as of lentiviral vectors [230]. The safety can be even increased by using SIN vectors [231]. The ideal situation would be a targeted integration. Eventually, this might be achievable with zinc finger nucleases. These are engineered sequence-specific endonucleases which cleave at a chosen target site. During repair of the double-strand break gene insertion or targeted mutation can be done [232]. For TCR gene therapy the usage of zinc finger nucleases is under investigation. Another nonviral transfer technology is usage of DNA transposons. The Sleeping Beauty transposon system was shown to have a close-to-random insertion site pattern. DNA transposons function by a 'cut and paste' mechanism and were engineered for gene transfer, where the transgene is cut out of a donor plasmid and pasted into the cell DNA by the transposase enzyme which is provided on a separate plasmid [233]. The Sleeping Beauty transfer system was already employed for two TCRs which led to 16 % p53 pentamer and 33 % MART-1 tetramer staining in PBLs [234].

A last option to increase the safety of TCR gene therapy is the usage of either additional selection markers like HSV-Tk, CD20 or apoptosis-inducing fusion genes or cytotoxic tetramers. But these "suicide genes" or agents harbor great disadvantages. For HSV-Tk or apoptosis-inducing caspase 9 it was shown that the expression was down-regulated [235,236] or the HSV-Tk transgene was even lost [235]. For HSV-Tk it was also shown that its solely expression was not enough to provide tumor rejection [237]. Also, the susceptibility to the suicide effect was different between tumor cells with HSV-Tk [238]. Elimination of T cells expressing transgenic CD20 with the specific antibody Rituximab depended on the expression level [239]. Another disadvantage of some of these strategies is the immunogenicity (HSV-Tk, Cytosine deaminase) and cytotoxic side effects for cytotoxic tetramers [240]. An intrinsic safe guard for TCR gene therapy was developed by the application of a small tag (Myc tag) added to the N-terminus of the TCRvα chain. Transduced T cells could be eliminated with a

depleting anti-Myc tag antibody in two mouse models [123,241]. A drawback of this technology is the missing GMP-approved anti-Myc-antibody and that the additional Myc tag interferes with the function of some TCRs. Also, the tag would only be included in one of the TCR chain. Therefore, transduced T cells which down regulate the expression of this TCR chain would not be eliminated.

Many investigations are on the way for a safe future TCR gene therapy.

Abbreviations

ABC	Antibody-binding capacity
ADA-PEG	Polyethylene glycol-modified bovine ADA
ADA-SCID	Adenosine deaminase-deficient SCID
APC	Antigen-presenting cell
BAE	Background antibody equivalent
BM	Bone marrow
CEA	Carcinoembryonic antigen
CFSE	Carboxyfluorescein diacetate, succinimidyl ester
CDR	Complementary determining region
CGD	Chronic granulomatous disease
CMJ	Corticomedullary junction
CMV	Cytomegalovirus
CTL	Cytotoxic T lymphocytes
DC	Dendritic cells
dH_2O	Destilled water
DP	double-positive
dNTPs	Deoxynucleotides
Dox	Doxycycline
EBV	Epstein-Barr Virus
ELISA	Enzyme-linked immune-sorbent assay
FACS	Fluorescence activated cell sorting
FCS	Fetal calf serum
FRET	Fluorescence resonance energy transfer
GVHD	Graft-versus-host disease
Hepes	N-2-hydroxyethylpiperazine-N'-2-ethanesulfonic-acid
HIV	Human immunodeficiency virus
HPV	Human papilloma virus
HSC	Hematopoietic stem cells
HSV-Tk	Herpes simplex thymidine kinase
HTLV	Human T cell lymphotropic virus
H	Hour/ hours
IFA	Freund's adjuvant, incomplete
IFN	Interferon
Ig	Immunoglobulin
IL	Interleukine
IRES	Internal ribosomal entry site

ITAM	Immunoreceptor tyrosine-based activation motif
LAM	Linear amplification-mediated
LCL	EBV-transformed lymphoblastoid cell line
LN	Lymphnodes
LTR	Long terminal repeat
MHC	Major histocompatibility complexes
MFI	Mean fluorescence intensity
MLV	Murine leukemia virus
MOI	Multiplicity of infection
MPSV	Myeloproliferative sarcoma virus
MSCV	Murine stem cell virus
NADPH	Nicotinamide dinucleotide phosphate
Nt	Nucleotides
PBS	Phosphate-buffered salines
Pen/Strep	Penicillin/ streptomycin
Pgk	Phosphoglycerate kinase
PMT	Photomultiplier tube
PCR	Polymerase chain reaction
PMA	Phorbol-12-myristate-13-acetate
PRE	Posttranscriptional regulatory element
PTLD	Post-transplant lymphoproliferative disease
RAG	Recombination-activating gene
RN	RetroNectin
RT	Room temperature
SMAC	Supramolecular adhesion complex
SCID	Severe combined immunodeficiency disease
SCZ	Subcapsular zone
SIN	Self-inactivating
SP	Single-positive
SV	Simian virus
TAA	Tumor-associated antigen
T-ALL	T cell acute lymphoblastic leukemia
Tc	Tetracycline
TCR	T cell receptor
TEC	Thymic epithelial cortical cells
TEM	Thymic medullary epithelilal cells
TES	Thymic subcapsular cells
Tet	Tetracycline-regulated

TetR	Tet repressor protein
tetO	tet operator sequence
TILs	Tumor-infiltrating lymphocytes
TNF	Tumor necrosis factor
TRE	Tetracycline-responsive element
tTA	Tetracycline-controlled transactivator
rTetR	Reverse Tet repressor
UV	Ultraviolet light
γc	gamma chain
WAS/WASP	Wiskott-Aldrich syndrome/ protein
w/o	Without

References

[1] Nikolić-Zugić, J. and Carbone, F.R. (1991): Peptide presentation by class-I major histocompatibility complex molecules., Immunology Research 10 [1], pp. 54-65.

[2] Flutter, B. and Gao, B. (2004): MHC class I antigen presentation--recently trimmed and well presented., Cellular and Molecular Immunology 1 [1], pp. 22-30.

[3] Pieters, J. (1997): MHC class II restricted antigen presentation, Current Opinion in Immunology 9 [1], pp. 89-96.

[4] Robinson, J.H. and Delvig, A.A. (2002): Diversity in MHC class II antigen presentation, Immunology 105 [3], pp. 252-262.

[5] Irvine, D.J.; Purbhoo, M.A.; Krogsgaard, M. and Davis, M.M. (2002): Direct observation of ligand recognition by T cells, Nature 419 [6909], pp. 845-849.

[6] Purbhoo, M.A.; Irvine, D.J.; Huppa, J.B. and Davis, M.M. (2004): T cell killing does not require the formation of a stable mature immunological synapse, Nature Immunology 5 [5], pp. 524-530.

[7] Huppa, J.B.; Gleimer, M.; Sumen, C. and Davis, M.M. (2003): Continuous T cell receptor signaling required for synapse maintenance and full effector potential, Nature Immunology 4 [8], pp. 749-755.

[8] Kim, C. and Williams, M.A. (2010): Nature and nurture: T-cell receptor-dependent and T-cell receptor-independent differentiation cues in the selection of the memory T-cell pool, Immunology 131 [3], pp. 310-317.

[9] Alarcón, B.; Mestre, D. and Martínez-Martín, N. (2011): The immunological synapse: a cause or consequence of T-cell receptor triggering?, Immunology 133 [4], pp. 420-425.

[10] Potter, T.A.; Grebe, K.; Freiberg, B. and Kupfer, A. (2001): Formation of supramolecular activation clusters on fresh ex vivo CD8+ T cells after engagement of the T cell antigen receptor and CD8 by antigen-presenting cells, Proceedings of the National Academy of Sciences of the United States of America 98 [22], pp. 12624-12629.

[11] Jenkins, M.R. and Griffiths, G.M. (2010): The synapse and cytolytic machinery of cytotoxic T cells, Current Opinion in Immunology 22 [3], pp. 308-313.

[12] Harty, J.T. and Badovinac, V.P. (2002): Influence of effector molecules on the CD8+ T cell response to infection, Current Opinion in Immunology 14 [3], pp. 360-365.

[13] Klebanoff, C.A.; Finkelstein, S.E.; Surman, D.R.; Lichtman, M.K.; Gattinoni, L.; Theoret, M.R.; Grewal, N.; Spiess, P.J.; Antony, P.A.; Palmer, D.C.; Tagaya, Y.; Rosenberg, S.A.; Waldmann, T.A. and Restifo, N.P. (2004): IL-15 enhances the in vivo antitumor activity of tumor-reactive CD8+ T Cells, Proceedings of the National Academy of Sciences of the United States of America 101 [7], pp. 1969-1974.

[14] Stemberger, C.; Huster, K.M.; Koffler, M.; Anderl, F.; Schiemann, M.; Wagner, H. and Busch, D.H. (2007): A single naive CD8+ T cell precursor can develop into diverse effector and memory subsets, Immunity 27 [6], pp. 985-997.

[15] Huster, K.M.; Stemberger, C.; Gasteiger, G.; Kastenmüller, W.; Drexler, I. and Busch, D.H. (2009): Cutting Edge: Memory CD8 T cell compartment grows in size with immunological experience but nevertheless can lose function, The Journal of Immunology 183 [11], pp. 6898-6902.

[16] Labrecque, N.; Whitfield, L.S.; Obst, R.; Waltzinger, C.; Benoist, C. and Mathis, D. (2001): How much TCR does a T cell need?, Immunity 15 [1], pp. 71-82.

[17] Kuhns, M.S.; Davis, M.M. and Garcia, K.C. (2006): Deconstructing the form and function of the TCR/CD3 complex, Immunity 24 [2], pp. 133-139.

[18] Meuer, S.; Fitzgerald, K.; Hussey, R.; Hodgdon, J.; Schlossmann, S. and Reinherz, E. (1983): Clonotypic structures involved in antigen-specific human T cell function. Relationship to the T3 molecular complex., The Journal of Experimental Medicine 157 [2], pp. 705-19.

[19] McNicol, A.-M.; Bendle, G.; Holler, A.; Matjeka, T.; Dalton, E.; Rettig, L.; Zamoyska, R.; Uckert, W.; Xue, S.-A. and Stauss, H.J. (2007): CD8a/a homodimers fail to function as co-receptor for a CD8-dependent TCR, European Journal of Immunology 37 [6], pp. 1634-71.
[20] Janeway, C.A.; Travers, P.; Walport, M. and Shlomchik, M. (2005), 6. ed., Lawrence, E, Ed, Immunobiology, Garland Science Publishing, New York.
[21] Fugmann, S.D.; Lee, A.I.; Shockett, P.E.; Villey, I.J. and Schatz, D.G. (2000): The RAG proteins and V(D)J recombination: Complexes, ends, and transposition, Annual Review of Immunology 18 [1], pp. 495-527.
[22] Ebert, P.J.R.; Li, Q.-J.; Huppa, J.B. and Davis, M.M. (2010): Functional development of the T Cell receptor for antigen, Progress in Molecular Biology and Translational Science Volume 92, pp. 65-100.
[23] Kisielow, P. and Miazek, A. (1995): Positive selection of T cells: rescue from programmed cell death and differentiation require continual engagement of the T cell receptor., The Journal of Experimental Medicine 181 [6], pp. 1975-84.
[24] Liu, X. and Bosselut, R. (2004): Duration of TCR signaling controls CD4-CD8 lineage differentiation in vivo, Nature Immunology 5 [3], pp. 280-288.
[25] McCaughtry, T.M.; Baldwin, T.A.; Wilken, M.S. and Hogquist, K.A. (2008): Clonal deletion of thymocytes can occur in the cortex with no involvement of the medulla, The Journal of Experimental Medicine 205 [11], pp. 2575-2584.
[26] Ebert, P.J.R.; Ehrlich, L.I.R. and Davis, M.M. (2008): Low ligand requirement for deletion and lack of synapses in positive selection enforce the gauntlet of thymic T cell maturation, Immunity 29 [5], pp. 734-745.
[27] Taub, D.D. and Longo, D.L. (2005): Insights into thymic aging and regeneration, Immunological Reviews 205 [1], pp. 72-93.
[28] Ueno, T.; Saito, F.; Gray, D.H.D.; Kuse, S.; Hieshima, K.; Nakano, H.; Kakiuchi, T.; Lipp, M.; Boyd, R.L. and Takahama, Y. (2004): CCR7 signals are essential for cortex–medulla migration of developing thymocytes, The Journal of Experimental Medicine 200 [4], pp. 493-505.
[29] Misslitz, A.; Pabst, O.; Hintzen, G.; Ohl, L.; Kremmer, E.; Petrie, H.T. and Förster, R. (2004): Thymic T cell development and progenitor localization depend on CCR7, The Journal of Experimental Medicine 200 [4], pp. 481-491.
[30] Anderson, M.S.; Venanzi, E.S.; Klein, L.; Chen, Z.; Berzins, S.P.; Turley, S.J.; von Boehmer, H.; Bronson, R.; Dierich, A.; Benoist, C. and Mathis, D. (2002): Projection of an immunological self shadow within the thymus by the Aire protein, Science 298 [5597], pp. 1395-1401.
[31] Bonasio, R.; Scimone, M.L.; Schaerli, P.; Grabie, N.; Lichtman, A.H. and von Andrian, U.H. (2006): Clonal deletion of thymocytes by circulating dendritic cells homing to the thymus, Nature Immunology 7 [10], pp. 1092-1100.
[32] Surh, C.D. and Sprent, J. (1994): T-cell apoptosis detected in situ during positive and negative selection in the thymus, Nature 372 [6501], pp. 100-103.
[33] Scollay, R.G.; Butcher, E.C. and Weissman, I.L. (1980): Thymus cell migration: Quantitative aspects of cellular traffic from the thymus to the periphery in mice, European Journal of Immunology 10 [3], pp. 210-218.
[34] Goldrath, A.W. and Bevan, M.J. (1999): Selecting and maintaining a diverse T-cell repertoire, Nature 402 [6759], pp. 255-262.
[35] Ehrlich, P. (1909): Ueber den jetztigen Stand der Karzinomforschung, Nederlands Tijdschrift voor Geneeskunde, pp. 273-290.
[36] Klein, E. and Sjogren (1960): Humoral and cellular factors in homograft and isograft immunity, Cancer Research 20, p. 452.
[37] Old, L.J.; Boyse, E.A. and Clarke, D.A. (1962): Antigenic properties of chemically induced tumors, Annals of the New York Academy of Sciences 101, p. 80.
[38] Thomas, L. (1959): Reactions to homologous tissue antigens in relation to hypersensitivity, Lawrence, H S, Ed, Hoeber-Harper, New York.

[39] Burnet, F. (1970): The concept of immunological surveillance, Progress of Experimental Tumor Research 13, pp. 1-27.
[40] Hewitt, H.; Blake, E. and Walder, A. (1976): A critique of the evidence for active host defence against cancer, based on personal studies of 27 murine tumours of spontaneous origin, British Journal of Cancer 33 [3], pp. 241-259.
[41] Klein, G. and Klein, E. (1977): Immune surveillance against virus-induced tumors and nonrejectability of spontaneous tumors: contrasting consequences of host versus tumor evolution, Proceedings of the National Academy of Sciences 74 [5], pp. 2121-2125.
[42] Willimsky, G.; Czéh, M.; Loddenkemper, C.; Gellermann, J.; Schmidt, K.; Wust, P.; Stein, H. and Blankenstein, T. (2008): Immunogenicity of premalignant lesions is the primary cause of general cytotoxic T lymphocyte unresponsiveness, The Journal of Experimental Medicine 205 [7], pp. 1687-1700.
[43] Willimsky, G. and Blankenstein, T. (2005): Sporadic immunogenic tumours avoid destruction by inducing T-cell tolerance, Nature 437 [7055], pp. 141-146.
[44] Schreiber, R.D.; Old, L.J. and Smyth, M.J. (2011): Cancer Immunoediting: Integrating immunity's roles in cancer suppression and promotion, Science 331 [6024], pp. 1565-1570.
[45] Dunn, G.P.; Old, L.J. and Schreiber, R.D. (2004): The three Es of cancer immunoediting, Annual Review of Immunology 22 [1], pp. 329-360.
[46] Carbone, D.P.; Ciernik, I.F.; Kelley, M.J.; Smith, M.C.; Nadaf, S.; Kavanaugh, D.; Maher, V.E.; Stipanov, M.; Contois, D.; Johnson, B.E.; Pendleton, C.D.; Seifert, B.; Carter, C.; Read, E.J.; Greenblatt, J.; Top, L.E.; Kelsey, M.I.; Minna, J.D. and Berzofsky, J.A. (2005): Immunization with mutant p53- and K-ras–derived peptides in cancer patients: immune response and clinical outcome, Journal of Clinical Oncology 23 [22], pp. 5099-5107.
[47] Gjertsen, M.K. and Gaudernack, G. (1998): Mutated Ras peptides as vaccines in immunotherapy of cancer, Vox Sanguinis 74 [S2], pp. 489-495.
[48] Yugawa, T. and Kiyono, T. (2009): Molecular mechanisms of cervical carcinogenesis by high-risk human papillomaviruses: novel functions of E6 and E7 oncoproteins, Reviews in Medical Virology 19 [2], pp. 97-113.
[49] Young, L.S. and Murray, P.G. (2003): Epstein-Barr virus and oncogenesis: from latent genes to tumours, Oncogene 22 [33], pp. 5108-5121.
[50] Khanna, R.; Burrows, S. and Moss, D. (1995): Immune regulation in Epstein-Barr virus-associated diseases., Microbiology Reviews 59 [3], pp. 387-405.
[51] Mortreux, F.; Gabet, A.S. and Wattel, E. (2003): Molecular and cellular aspects of HTLV-1 associated leukemogenesis in vivo, Leukemia 17 [1], pp. 26-38.
[52] Parkhurst, M.R.; Fitzgerald, E.B.; Southwood, S.; Sette, A.; Rosenberg, S.A. and Kawakami, Y. (1998): Identification of a shared HLA-A*0201-restricted T-cell epitope from the melanoma antigen tyrosinase-related protein 2 (TRP2), Cancer Research 58 [21], pp. 4895-4901.
[53] Wang, R.-F.; Appella, E.; Kawakami, Y.; Kang, X. and Rosenberg, S.A. (1996): Identification of TRP-2 as a human tumor antigen recognized by cytotoxic T lymphocytes, The Journal of Experimental Medicine 184 [6], pp. 2207-2216.
[54] Kawakami, Y.; Eliyahu, S.; Sakaguchi, K.; Robbins, P.F.; Rivoltini, L.; Yannelli, J.R.; Appella, E. and Rosenberg, S.A. (1994): Identification of the immunodominant peptides of the MART-1 human melanoma antigen recognized by the majority of HLA-A2-restricted tumor infiltrating lymphocytes, The Journal of Experimental Medicine 180 [1], pp. 347-352.
[55] Kawakami, Y.; Eliyahu, S.; Jennings, C.; Sakaguchi, K.; Kang, X.; Southwood, S.; Robbins, P.F.; Sette, A.; Appella, E. and Rosenberg, S.A. (1995): Recognition of multiple epitopes in the human melanoma antigen gp100 by tumor-infiltrating T lymphocytes associated with in vivo tumor regression, The Journal of Immunology 154 [8], pp. 3961-3968.
[56] Bakker, A.B.; Schreurs, M.W.; de Boer, A.J.; Kawakami, Y.; Rosenberg, S.A.; Adema, G.J. and Figdor, C.G. (1994): Melanocyte lineage-specific antigen gp100 is recognized by melanoma-derived tumor-infiltrating lymphocytes, The Journal of Experimental Medicine 179 [3], pp. 1005-1009.

[57] Correale, P.; Nieroda, C.; Zaremba, S.; Zhu, M.; Schlom, J.; Tsang, K.Y. and Konstantin, W. (1997): In vitro generation of human cytotoxic T lymphocytes specific for peptides derived from prostate-specific antigen, Journal of the National Cancer Institute 89 [4], pp. 293-300.

[58] Corman, J.M.; Sercarz, E.E. and Nanda, N.K. (1998): Recognition of prostate-specific antigenic peptide determinants by human CD4 and CD8 T cells, Clinical & Experimental Immunology 114 [2], pp. 166-172.

[59] Jaramillo, A.; Majumder, K.; Manna, P.P.; Fleming, T.P.; Doherty, G.; Dipersio, J.F. and Mohanakumar, T. (2002): Identification of HLA-A3-restricted CD8+ T cell epitopes derived from mammaglobin-A, a tumor-associated antigen of human breast cancer, International Journal of Cancer 102 [5], pp. 499-506.

[60] Slamon, D.J.; Godolphin, W.; Jones, L.A.; Holt, J.A.; Wong, S.G.; Keith, D.E.; Levin, W.J.; Stuart, S.G.; Udove, J.; Ullrich, A. and et, a. (1989): Studies of the HER-2/neu proto-oncogene in human breast and ovarian cancer, Science 244 [4905], pp. 707-712.

[61] Aarnoudse, C.A.; Vallejo, J.J.G.; Saeland, E. and van Kooyk, Y. (2006): Recognition of tumor glycans by antigen-presenting cells, Current Opinion in Immunology 18 [1], pp. 105-111.

[62] De Smet, C.; Lurquin, C.; Lethe, B.; Martelange, V. and Boon, T. (1999): DNA methylation is the primary silencing mechanism for a set of germ line- and tumor-specific genes with a CpG-rich promoter, Molecular and Cellular Biology 19 [11], pp. 7327-7335.

[63] Sang, M.; Wang, L.; Ding, C.; Zhou, X.; Wang, B.; Wang, L.; Lian, Y. and Shan, B. (2011): Melanoma-associated antigen genes - An update, Cancer Letters 302 [2], pp. 85-90.

[64] Jäger, E.; Chen, Y.-T.; Drijfhout, J.W.; Karbach, J.; Ringhoffer, M.; Jäger, D.; Arand, M.; Wada, H.; Noguchi, Y.; Stockert, E.; Old, L.J. and Knuth, A. (1998): Simultaneous humoral and cellular immune response against cancer–testis antigen NY-ESO-1: definition of human histocompatibility leukocyte antigen (HLA)-A2–binding peptide epitopes, The Journal of Experimental Medicine 187 [2], pp. 265-270.

[65] Ayyoub, M.; Stevanovic, S.; Sahin, U.; Guillaume, P.; Servis, C.; Rimoldi, D.; Valmori, D.; Romero, P.; Cerottini, J.-C.; Rammensee, H.-G.; Pfreundschuh, M.; Speiser, D. and Lévy, F. (2002): Proteasome-assisted identification of a SSX-2-derived epitope recognized by tumor-reactive CTL infiltrating metastatic melanoma, The Journal of Immunology 168 [4], pp. 1717-1722.

[66] Bleakley, M. and Riddell, S.R. (2004): Molecules and mechanisms of the graft-versus-leukaemia effect, Nature Reviews Cancer 4 [5], pp. 371-380.

[67] Kolb, H.J.; Schattenberg, A.; Goldman, J.M.; Hertenstein, B.; Jacobsen, N.; Arcese, W.; Ljungman, P.; Ferrant, A.; Verdonck, L. and Niederwieser, D. (1995): Graft-versus-leukemia effect of donor lymphocyte transfusions in marrow grafted patients. European Group for Blood and Marrow Transplantation Working Party Chronic Leukemia, Blood 86 [5], pp. 2041-2050.

[68] Collins, R.H.; Shpilberg, O.; Drobyski, W.R.; Porter, D.L.; Giralt, S.; Champlin, R.; Goodman, S.A.; Wolff, S.N.; Hu, W.; Verfaillie, C.; List, A.; Dalton, W.; Ognoskie, N.; Chetrit, A.; Antin, J.H. and Nemunaitis, J. (1997): Donor leukocyte infusions in 140 patients with relapsed malignancy after allogeneic bone marrow transplantation, Journal of Clinical Oncology 15 [2], pp. 433-444.

[69] Riddell, S.R.; Watanabe, K.S.; Goodrich, J.M.; Li, C.R.; Agha, M.E. and Greenberg, P.D. (1992): Restoration of viral immunity in immunodeficient humans by the adoptive transfer of T cell clones, Science 257 [5067], pp. 238-241.

[70] Walter, E.A.; Greenberg, P.D.; Gilbert, M.J.; Finch, R.J.; Watanabe, K.S.; Thomas, E.D. and Riddell, S.R. (1995): Reconstitution of cellular immunity against cytomegalovirus in recipients of allogeneic bone marrow by transfer of T-cell clones from the donor, The New England Journal of Medicine 333 [16], pp. 1038-1044.

[71] Heslop, H.E.; Ng, C.Y.C.; Li, C.; Smith, C.A.; Loftin, S.K.; Krance, R.A.; Brenner, M.K. and Rooney, C.M. (1996): Long-term restoration of immunity against Epstein-Barr virus infection

by adoptive transfer of gene-modified virus-specific T lymphocytes, Nature medicine 2 [5], pp. 551-555.

[72] Rooney, C.M.; Ng, C.Y.C.; Loftin, S.; Smith, C.A.; Li, C.; Krance, R.A.; Brenner, M.K. and Heslop, H.E. (1995): Use of gene-modified virus-specific T lymphocytes to control Epstein-Barr-virus-related lymphoproliferation, The Lancet 345 [8941], pp. 9-13.

[73] Rooney, C.M.; Smith, C.A.; Ng, C.Y.C.; Loftin, S.K.; Sixbey, J.W.; Gan, Y.; Srivastava, D.-K.; Bowman, L.C.; Krance, R.A.; Brenner, M.K. and Heslop, H.E. (1998): Infusion of cytotoxic T cells for the prevention and treatment of Epstein-Barr virus-induced lymphoma in allogeneic transplant Recipients, Blood 92 [5], pp. 1549-1555.

[74] Bollard, C.M.; Aguilar, L.; Straathof, K.C.; Gahn, B.; Huls, M.H.; Rousseau, A.; Sixbey, J.; Gresik, M.V.; Carrum, G.; Hudson, M.; Dilloo, D.; Gee, A.; Brenner, M.K.; Rooney, C.M. and Heslop, H.E. (2004): Cytotoxic T lymphocyte therapy for Epstein-Barr virus+ Hodgkin's disease, The Journal of Experimental Medicine 200 [12], pp. 1623-1633.

[75] Straathof, K.C.M.; Bollard, C.M.; Popat, U.; Huls, M.H.; Lopez, T.; Morriss, M.C.; Gresik, M.V.; Gee, A.P.; Russell, H.V.; Brenner, M.K.; Rooney, C.M. and Heslop, H.E. (2005): Treatment of nasopharyngeal carcinoma with Epstein-Barr virus-specific T lymphocytes, Blood 105 [5], pp. 1898-1904.

[76] Louis, C.U.; Straathof, K.; Bollard, C.M.; Ennamuri, S.; Gerken, C.; Lopez, T.T.; Huls, M.H.; Sheehan, A.; Wu, M.-F.; Liu, H.; Gee, A.; Brenner, M.K.; Rooney, C.M.; Heslop, H.E. and Gottschalk, S. (2010): Adoptive transfer of EBV-specific T cells results in sustained clinical responses in patients with locoregional nasopharyngeal carcinoma, Journal of Immunotherapy 33 [9], pp. 983-990.

[77] Leen, A.M.; Christin, A.; Myers, G.D.; Liu, H.; Cruz, C.R.; Hanley, P.J.; Kennedy-Nasser, A.A.; Leung, K.S.; Gee, A.P.; Krance, R.A.; Brenner, M.K.; Heslop, H.E.; Rooney, C.M. and Bollard, C.M. (2009): Cytotoxic T lymphocyte therapy with donor T cells prevents and treats adenovirus and Epstein-Barr virus infections after haploidentical and matched unrelated stem cell transplantation, Blood 114 [19], pp. 4283-4292.

[78] Heslop, H.E.; Slobod, K.S.; Pule, M.A.; Hale, G.A.; Rousseau, A.; Smith, C.A.; Bollard, C.M.; Liu, H.; Wu, M.-F.; Rochester, R.J.; Amrolia, P.J.; Hurwitz, J.L.; Brenner, M.K. and Rooney, C.M. (2010): Long-term outcome of EBV-specific T-cell infusions to prevent or treat EBV-related lymphoproliferative disease in transplant recipients, Blood 115 [5], pp. 925-935.

[79] Dudley, M.E.; Wunderlich, J.R.; Shelton, T.E.; Even, J. and Rosenberg, S.A. (2003): Generation of tumor-infiltrating lymphocyte cultures for use in adoptive transfer therapy for melanoma patients, Journal of Immunotherapy 26 [4], pp. 332-342.

[80] Rosenberg, S.A. and Dudley, M.E. (2009): Adoptive cell therapy for the treatment of patients with metastatic melanoma, Current Opinion in Immunology 21 [2], pp. 233-240.

[81] Yee, C.; Thompson, J.A.; Roche, P.; Byrd, D.R.; Lee, P.P.; Piepkorn, M.; Kenyon, K.; Davis, M.M.; Riddell, S.R. and Greenberg, P.D. (2000): Melanocyte destruction after antigen-specific immunotherapy of melanoma, The Journal of Experimental Medicine 192 [11], pp. 1637-1644.

[82] Dudley, M.E.; Wunderlich, J.; Nishimura, M.I.; Yu, D.; Yang, J.C.; Topalian, S.L.; Schwartzentruber, D.J.; Hwu, P.; Marincola, F.M.; Sherry, R.; Leitman, S.F. and Rosenberg, S.A. (2001): Adoptive transfer of cloned melanoma-reactive T lymphocytes for the treatment of patients with metastatic melanoma, Journal of Immunotherapy 24 [4], pp. 363-373.

[83] Dembic, Z.; Haas, W.; Weiss, S.; McCubrey, J.; Kiefer, H.; von Boehmer, H. and Steinmetz, M. (1986): Transfer of specificity by murine [alpha] and [beta] T-cell receptor genes, Nature 320 [6059], pp. 232-238.

[84] Clay, T.M.; Custer, M.C.; Sachs, J.; Hwu, P.; Rosenberg, S.A. and Nishimura, M.I. (1999): Efficient transfer of a tumor antigen-reactive TCR to human peripheral blood lymphocytes confers anti-tumor reactivity, The Journal of Immunology 163 [1], pp. 507-513.

[85] Morgan, R.A.; Dudley, M.E.; Wunderlich, J.R.; Hughes, M.S.; Yang, J.C.; Sherry, R.M.; Royal, R.E.; Topalian, S.L.; Kammula, U.S.; Restifo, N.P.; Zheng, Z.; Nahvi, A.; de Vries, C.R.; Rogers-

Freezer, L.J.; Mavroukakis, S.A. and Rosenberg, S.A. (2006): Cancer regression in patients after transfer of genetically engineered lymphocytes, Science 314 [5796], pp. 126-129.

[86] Johnson, L.A.; Morgan, R.A.; Dudley, M.E.; Cassard, L.; Yang, J.C.; Hughes, M.S.; Kammula, U.S.; Royal, R.E.; Sherry, R.M.; Wunderlich, J.R.; Lee, C.-C.R.; Restifo, N.P.; Schwarz, S.L.; Cogdill, A.P.; Bishop, R.J.; Kim, H.; Brewer, C.C.; Rudy, S.F.; VanWaes, C.; Davis, J.L.; Mathur, A.; Ripley, R.T.; Nathan, D.A.; Laurencot, C.M. and Rosenberg, S.A. (2009): Gene therapy with human and mouse T-cell receptors mediates cancer regression and targets normal tissues expressing cognate antigen, Blood 114 [3], pp. 535-546.

[87] Robbins, P.F.; Morgan, R.A.; Feldman, S.A.; Yang, J.C.; Sherry, R.M.; Dudley, M.E.; Wunderlich, J.R.; Nahvi, A.V.; Helman, L.J.; Mackall, C.L.; Kammula, U.S.; Hughes, M.S.; Restifo, N.P.; Raffeld, M.; Lee, C.-C.R.; Levy, C.L.; Li, Y.F.; El-Gamil, M.; Schwarz, S.L.; Laurencot, C. and Rosenberg, S.A. (2011): Tumor regression in patients with metastatic synovial cell sarcoma and melanoma using genetically engineered lymphocytes reactive with NY-ESO-1, Journal of Clinical Oncology 29 [7], pp. 917-924.

[88] Parkhurst, M.R.; Yang, J.C.; Langan, R.C.; Dudley, M.E.; Nathan, D.-A.N.; Feldman, S.A.; Davis, J.L.; Morgan, R.A.; Merino, M.J.; Sherry, R.M.; Hughes, M.S.; Kammula, U.S.; Phan, G.Q.; Lim, R.M.; Wank, S.A.; Restifo, N.P.; Robbins, P.F.; Laurencot, C.M. and Rosenberg, S.A. (2011): T cells targeting carcinoembryonic antigen can mediate regression of metastatic colorectal cancer but induce severe transient colitis, Molecular Therapy 19 [3], pp. 620-626.

[89] Wang, Q.J.; Hanada, K.-i.; Feldman, S.A.; Zhao, Y.; Inozume, T. and Yang, J.C. (2011): Development of a genetically-modified novel T-cell receptor for adoptive cell transfer against renal cell carcinoma, Journal of Immunological Methods 366 [1-2], pp. 43-51.

[90] Kieback, E. and Uckert, W. (2010): Enhanced T cell receptor gene therapy for cancer, Expert Opinion on Biological Therapy 10 [5], pp. 749-762.

[91] Cooper, L.J.N.; Topp, M.S.; Pinzon, C.; Plavec, I.; Jensen, M.C.; Riddell, S.R. and Greenberg, P.D. (2004): Enhanced transgene expression in quiescent and activated human CD8+ T cells, Human Gene Therapy 15 [7], pp. 648-658.

[92] Engels, B.; Cam, H.; Schüler, T.; Indraccolo, S.; Gladow, M.; Baum, C.; Blankenstein, T. and Uckert, W. (2003): Retroviral vectors for high-level transgene expression in T lymphocytes, Human Gene Therapy 14 [12], pp. 1155-1168.

[93] Zufferey, R.; Donello, J.E.; Trono, D. and Hope, T.J. (1999): Woodchuck hepatitis virus posttranscriptional regulatory element enhances expression of transgenes delivered by retroviral vectors, The Journal of Virology 73 [4], pp. 2886-2892.

[94] Jones, S.; Peng, P.D.; Yang, S.; Hsu, C.; Cohen, C.J.; Zhao, Y.; Abad, J.; Zheng, Z.; Rosenberg, S.A. and Morgan, R.A. (2009): Lentiviral vector design for optimal T cell receptor gene expression in the transduction of peripheral blood lymphocytes and tumor-infiltrating lymphocytes, Human Gene Therapy 20 [6], pp. 630-640.

[95] Dossett, M.L.; Teague, R.M.; Schmitt, T.M.; Tan, X.; Cooper, L.J.N.; Pinzon, C. and Greenberg, P.D. (2009): Adoptive immunotherapy of disseminated leukemia with TCR-transduced, CD8+ T cells expressing a known endogenous TCR, Molecular Therapy 17 [4], pp. 742-749.

[96] Mizuguchi H, X.Z., Ishii-Watabe A, Uchida E, Hayakawa T (2000): IRES-dependent second gene expression is significantly lower than cap-dependent first gene expression in a bicistronic vector, Molecular Therapy 1 [4], pp. 376-82.

[97] Cohen, C.J.; Zheng, Z.; Bray, R.; Zhao, Y.; Sherman, L.A.; Rosenberg, S.A. and Morgan, R.A. (2005): Recognition of fresh human tumor by human peripheral blood lymphocytes transduced with a bicistronic retroviral vector encoding a murine anti-p53 TCR, The Journal of Immunology 175 [9], pp. 5799-5808.

[98] Engels, B.; Noessner, E.; Frankenberger, B.; Blankenstein, T.; Schendel, D.J. and Uckert, W. (2005): Redirecting human T lymphocytes toward renal cell carcinoma specificity by retroviral transfer of T cell receptor genes, Human Gene Therapy 16 [7], pp. 799-810.

[99] Leisegang, M.; Engels, B.; Meyerhuber, P.; Kieback, E.; Sommermeyer, D.; Xue, S.-A.; Reuß, S.; Stauss, H. and Uckert, W. (2008): Enhanced functionality of T cell receptor-redirected T cells is defined by the transgene cassette, Journal of Molecular Medicine 86 [5], pp. 573-583.

[100] Ryan, M.D.; King, A.M.Q. and Thomas, G.P. (1991): Cleavage of foot-and-mouth disease virus polyprotein is mediated by residues located within a 19 amino acid sequence, Journal of General Virology 72 [11], pp. 2727-2732.

[101] Palmenberg AC, P.G., Hall DJ, Ingraham RH, Seng TW, Pallai PV (1992): Proteolytic processing of the cardioviral P2 region: primary 2A/2B cleavage in clone-derived precursors, Virology 190 [2], pp. 754-762.

[102] Szymczak, A.L.; Workman, C.J.; Wang, Y.; Vignali, K.M.; Dilioglou, S.; Vanin, E.F. and Vignali, D.A.A. (2004): Correction of multi-gene deficiency in vivo using a single 'self-cleaving' 2A peptide-based retroviral vector, Nature Biotechnology 22 [5], pp. 589-594.

[103] Holst, J.; Vignali, K.M.; Burton, A.R. and Vignali, D.A.A. (2006): Rapid analysis of T-cell selection in vivo using T cell-receptor retrogenic mice, Nature Methods 3 [3], pp. 191-197.

[104] Gustafsson, C.; Govindarajan, S. and Minshull, J. (2004): Codon bias and heterologous protein expression, Trends in Biotechnology 22 [7], pp. 346-353.

[105] Scholten, K.B.J.; Kramer, D.; Kueter, E.W.M.; Graf, M.; Schoedl, T.; Meijer, C.J.L.M.; Schreurs, M.W.J. and Hooijberg, E. (2006): Codon modification of T cell receptors allows enhanced functional expression in transgenic human T cells, Clinical Immunology 119 [2], pp. 135-145.

[106] Sommermeyer, D.; Neudorfer, J.; Weinhold, M.; Leisegang, M.; Engels, B.; Noessner, E.; Heemskerk, M.H.M.; Charo, J.; Schendel, D.J.; Blankenstein, T.; Bernhard, H. and Uckert, W. (2006): Designer T cells by T cell receptor replacement, European Journal of Immunology 36 [11], pp. 3052-3059.

[107] Cohen, C.J.; Zhao, Y.; Zheng, Z.; Rosenberg, S.A. and Morgan, R.A. (2006): Enhanced antitumor activity of murine-human hybrid T-cell receptor (TCR) in human lymphocytes is associated with improved pairing and TCR/CD3 stability, Cancer Research 66 [17], pp. 8878-8886.

[108] Voss, R.-H.; Willemsen, R.A.; Kuball, J.; Grabowski, M.; Engel, R.; Intan, R.S.; Guillaume, P.; Romero, P.; Huber, C. and Theobald, M. (2008): Molecular design of the Cαβ interface favors specific pairing of introduced TCRαβ in human T cells, The Journal of Immunology 180 [1], pp. 391-401.

[109] Riddell, S.R.; Elliott, M.; Lewinsohn, D.A.; Gilbert, M.J.; Wilson, L.; Manley, S.A.; Lupton, S.D.; Overell, R.W.; Reynolds, T.C.; Corey, L. and Greenberg, P.D. (1996): T-cell mediated rejection of gene-modified HIV-specific cytotoxic T lymphocytes in HIV-infected patients, Nature medicine 2 [2], pp. 216-223.

[110] Bialer, G.; Horovitz-Fried, M.; Ya'acobi, S.; Morgan, R.A. and Cohen, C.J. (2010): Selected murine residues endow human TCR with enhanced tumor recognition, The Journal of Immunology 184 [11], pp. 6232-6241.

[111] Sommermeyer, D. and Uckert, W. (2010): Minimal amino acid exchange in human TCR constant regions fosters improved function of TCR gene-modified T cells, The Journal of Immunology 184 [11], pp. 6223-6231.

[112] Kuball, J.; Hauptrock, B.; Malina, V.; Antunes, E.; Voss, R.-H.; Wolfl, M.; Strong, R.; Theobald, M. and Greenberg, P.D. (2009): Increasing functional avidity of TCR-redirected T cells by removing defined N-glycosylation sites in the TCR constant domain, The Journal of Experimental Medicine 206 [2], pp. 463-475.

[113] Kuball, J.; Dossett, M.L.; Wolfl, M.; Ho, W.Y.; Voss, R.-H.; Fowler, C. and Greenberg, P.D. (2007): Facilitating matched pairing and expression of TCR chains introduced into human T cells, Blood 109 [6], pp. 2331-2338.

[114] Boulter, J.M.; Glick, M.; Todorov, P.T.; Baston, E.; Sami, M.; Rizkallah, P. and Jakobsen, B.K. (2003): Stable, soluble T-cell receptor molecules for crystallization and therapeutics, Protein Engineering 16 [9], pp. 707-711.

[115] Willemsen, R.A.; Weijtens, M.E.; Ronteltap, C.; Eshhar, Z.; Gratama, J.W.; Chames, P. and Bolhuis, R. (2000): Grafting primary human T lymphocytes with cancer-specific chimeric single chain and two chain TCR., Gene Therapy 7 [16], pp. 1369-77.

[116] Sebestyén, Z.; Schooten, E.; Sals, T.; Zaldivar, I.; San José, E.; Alarcón, B.; Bobisse, S.; Rosato, A.; Szöllosi, J.; Gratama, J.W.; Willemsen, R.A. and Debets, R. (2008): Human TCR that incorporate CD3ζ induce highly preferred pairing between TCRα and β chains following gene transfer, The Journal of Immunology 180 [11], pp. 7736-7746.

[117] Ahmadi, M.; King, J.W.; Xue, S.-A.; Voisine, C.; Holler, A.; Wright, G.P.; Waxman, J.; Morris, E. and Stauss, H.J. (2011): CD3 limits the efficacy of TCR gene therapy in vivo, Blood.

[118] Aggen, D.H.; Chervin, A.S.; Schmitt, T.M.; Engels, B.; Stone, J.D.; Richman, S.A.; Piepenbrink, K.H.; Baker, B.M.; Greenberg, P.D.; Schreiber, H. and Kranz, D.M. (2011): Single-chain V[alpha]V[beta] T-cell receptors function without mispairing with endogenous TCR chains, Gene Therapy.

[119] Dudley, M.E.; Wunderlich, J.R.; Robbins, P.F.; Yang, J.C.; Hwu, P.; Schwartzentruber, D.J.; Topalian, S.L.; Sherry, R.; Restifo, N.P.; Hubicki, A.M.; Robinson, M.R.; Raffeld, M.; Duray, P.; Seipp, C.A.; Rogers-Freezer, L.; Morton, K.E.; Mavroukakis, S.A.; White, D.E. and Rosenberg, S.A. (2002): Cancer regression and autoimmunity in patients after clonal repopulation with antitumor lymphocytes, Science 298 [5594], pp. 850-854.

[120] Gattinoni, L.; Finkelstein, S.E.; Klebanoff, C.A.; Antony, P.A.; Palmer, D.C.; Spiess, P.J.; Hwang, L.N.; Yu, Z.; Wrzesinski, C.; Heimann, D.M.; Surh, C.D.; Rosenberg, S.A. and Restifo, N.P. (2005): Removal of homeostatic cytokine sinks by lymphodepletion enhances the efficacy of adoptively transferred tumor-specific CD8+ T cells, The Journal of Experimental Medicine 202 [7], pp. 907-912.

[121] Yee, C.; Thompson, J.A.; Byrd, D.; Riddell, S.R.; Roche, P.; Celis, E. and Greenberg, P.D. (2002): Adoptive T cell therapy using antigen-specific CD8+ T cell clones for the treatment of patients with metastatic melanoma: In vivo persistence, migration, and antitumor effect of transferred T cells, Proceedings of the National Academy of Sciences of the United States of America 99 [25], pp. 16168-16173.

[122] Berger, C.; Berger, M.; Hackman, R.C.; Gough, M.; Elliott, C.; Jensen, M.C. and Riddell, S.R. (2009): Safety and immunologic effects of IL-15 administration in nonhuman primates, Blood 114 [12], pp. 2417-2426.

[123] Bendle, G.M.; Linnemann, C.; Hooijkaas, A.I.; Bies, L.; de Witte, M.A.; Jorritsma, A.; Kaiser, A.D.M.; Pouw, N.; Debets, R.; Kieback, E.; Uckert, W.; Song, J.-Y.; Haanen, J.B.A.G. and Schumacher, T.N.M. (2010): Lethal graft-versus-host disease in mouse models of T cell receptor gene therapy, Nature Medicine 16 [5], pp. 565-570.

[124] van Loenen, M.M.; de Boer, R.; Amir, A.L.; Hagedoorn, R.S.; Volbeda, G.L.; Willemze, R.; van Rood, J.J.; Falkenburg, J.H.F. and Heemskerk, M.H.M. (2010): Mixed T cell receptor dimers harbor potentially harmful neoreactivity, Proceedings of the National Academy of Sciences 107 [24], pp. 10972-10977.

[125] Leisegang, M.; Wilde, S.; Spranger, S.; Milosevic, S.; Frankenberger, B.; Uckert, W. and Schendel, D.J. (2010): MHC-restricted fratricide of human lymphocytes expressing survivin-specific transgenic T cell receptors, The Journal of Clinical Investigation 120 [11], pp. 3869-3877.

[126] Gladow, M.; Uckert, W. and Blankenstein, T. (2004): Dual T cell receptor T cells with two defined specificities mediate tumor suppression via both receptors, European Journal of Immunology 34 [7], pp. 1882-1891.

[127] Weinhold, M.; Sommermeyer, D.; Uckert, W. and Blankenstein, T. (2007): Dual T cell receptor expressing CD8+ T cells with tumor- and self-specificity can inhibit tumor growth without causing severe autoimmunity, The Journal of Immunology 179 [8], pp. 5534-5542.

[128] de Witte, M.A.; Coccoris, M.; Wolkers, M.C.; van den Boom, M.D.; Mesman, E.M.; Song, J.-Y.; van der Valk, M.; Haanen, J.B.A.G. and Schumacher, T.N.M. (2006): Targeting self-antigens through allogeneic TCR gene transfer, Blood 108 [3], pp. 870-877.

[129] Wu, X.; Li, Y.; Crise, B. and Burgess, S.M. (2003): Transcription start regions in the human genome are favored targets for MLV integration, Science 300 [5626], pp. 1749-1751.

[130] Laufs, S.; Nagy, K.Z.; Giordano, F.A.; Hotz-Wagenblatt, A.; Zeller, W.J. and Fruehauf, S. (2004): Insertion of retroviral vectors in NOD/SCID repopulating human peripheral blood progenitor cells occurs preferentially in the vicinity of transcription start regions and in introns, Molecular Therapy 10 [5], pp. 874-881.

[131] Schröder, A.R.W.; Shinn, P.; Chen, H.; Berry, C.; Ecker, J.R. and Bushman, F. (2002): HIV-1 integration in the human genome favors active genes and local hotspots, Cell 110 [4], pp. 521-529.

[132] Gaspar, H.B.; Parsley, K.L.; Howe, S.; King, D.; Gilmour, K.C.; Sinclair, J.; Brouns, G.; Schmidt, M.; Von Kalle, C.; Barington, T.; Jakobsen, M.A.; Christensen, H.O.; Al Ghonaium, A.; White, H.N.; Smith, J.L.; Levinsky, R.J.; Ali, R.R.; Kinnon, C. and Thrasher, A.J. (2004): Gene therapy of X-linked severe combined immunodeficiency by use of a pseudotyped gammaretroviral vector, The Lancet 364 [9452], pp. 2181-2187.

[133] Cavazzana-Calvo, M.; Hacein-Bey, S.; de Saint Basile, G.; Gross, F.; Yvon, E.; Nusbaum, P.; Selz, F.; Hue, C.; Certain, S.; Casanova, J.-L.; Bousso, P.; Deist, F.L. and Fischer, A. (2000): Gene therapy of human severe combined immunodeficiency (SCID)-X1 disease, Science 288 [5466], pp. 669-672.

[134] Hacein-Bey-Abina, S.; Le Deist, F.; Carlier, F.; Bouneaud, C.; Hue, C.; De Villartay, J.-P.; Thrasher, A.J.; Wulffraat, N.; Sorensen, R.; Dupuis-Girod, S.; Fischer, A.; Davies, E.G.; Kuis, W.; Leiva, L. and Cavazzana-Calvo, M. (2002): Sustained correction of X-linked severe combined immunodeficiency by ex vivo gene therapy, The New England Journal of Medicine 346 [16], pp. 1185-1193.

[135] Hacein-Bey-Abina, S.; Von Kalle, C.; Schmidt, M.; McCormack, M.P.; Wulffraat, N.; Leboulch, P.; Lim, A.; Osborne, C.S.; Pawliuk, R.; Morillon, E.; Sorensen, R.; Forster, A.; Fraser, P.; Cohen, J.I.; de Saint Basile, G.; Alexander, I.; Wintergerst, U.; Frebourg, T.; Aurias, A.; Stoppa-Lyonnet, D.; Romana, S.; Radford-Weiss, I.; Gross, F.; Valensi, F.; Delabesse, E.; Macintyre, E.; Sigaux, F.; Soulier, J.; Leiva, L.E.; Wissler, M.; Prinz, C.; Rabbitts, T.H.; Le Deist, F.; Fischer, A. and Cavazzana-Calvo, M. (2003): LMO2-associated clonal T cell proliferation in two patients after gene therapy for SCID-X1, Science 302 [5644], pp. 415-419.

[136] Hacein-Bey-Abina, S.; Garrigue, A.; Wang, G.P.; Soulier, J.; Lim, A.; Morillon, E.; Clappier, E.; Caccavelli, L.; Delabesse, E.; Beldjord, K.; Asnafi, V.; MacIntyre, E.; Dal Cortivo, L.; Radford, I.; Brousse, N.; Sigaux, F.; Moshous, D.; Hauer, J.; Borkhardt, A.; Belohradsky, B.H.; Wintergerst, U.; Velez, M.C.; Leiva, L.; Sorensen, R.; Wulffraat, N.; Blanche, S.; Bushman, F.D.; Fischer, A. and Cavazzana-Calvo, M. (2008): Insertional oncogenesis in 4 patients after retrovirus-mediated gene therapy of SCID-X1, The Journal of Clinical Investigation 118 [9], pp. 3132-3142.

[137] Gaspar, H.B.; Cooray, S.; Gilmour, K.C.; Parsley, K.L.; Adams, S.; Howe, S.J.; Al Ghonaium, A.; Bayford, J.; Brown, L.; Davies, E.G.; Kinnon, C. and Thrasher, A.J. (2011): Long-Term persistence of a polyclonal T cell repertoire after gene therapy for X-linked severe combined immunodeficiency, Science Translational Medicine 3 [97], p. 97ra79.

[138] Howe, S.J.; Mansour, M.R.; Schwarzwaelder, K.; Bartholomae, C.; Hubank, M.; Kempski, H.; Brugman, M.H.; Pike-Overzet, K.; Chatters, S.J.; de Ridder, D.; Gilmour, K.C.; Adams, S.; Thornhill, S.I.; Parsley, K.L.; Staal, F.J.T.; Gale, R.E.; Linch, D.C.; Bayford, J.; Brown, L.; Quaye, M.; Kinnon, C.; Ancliff, P.; Webb, D.K.; Schmidt, M.; von Kalle, C.; Gaspar, H.B. and Thrasher, A.J. (2008): Insertional mutagenesis combined with acquired somatic mutations causes leukemogenesis following gene therapy of SCID-X1 patients, The Journal of Clinical Investigation 118 [9], pp. 3143-3150.

[139] Grez, M.; Reichenbach, J.; Schwable, J.; Seger, R.; Dinauer, M.C. and Thrasher, A.J. (2010): Gene therapy of chronic granulomatous disease: the engraftment dilemma, Molecular Therapy.

[140] Ott, M.G.; Schmidt, M.; Schwarzwaelder, K.; Stein, S.; Siler, U.; Koehl, U.; Glimm, H.; Kuhlcke, K.; Schilz, A.; Kunkel, H.; Naundorf, S.; Brinkmann, A.; Deichmann, A.; Fischer, M.; Ball, C.; Pilz, I.; Dunbar, C.; Du, Y.; Jenkins, N.A.; Copeland, N.G.; Luthi, U.; Hassan, M.; Thrasher, A.J.; Hoelzer, D.; von Kalle, C.; Seger, R. and Grez, M. (2006): Correction of X-linked chronic granulomatous disease by gene therapy, augmented by insertional activation of MDS1-EVI1, PRDM16 or SETBP1, Nature medicine 12 [4], pp. 401-409.

[141] Bianchi, M.; Hakkim, A.; Brinkmann, V.; Siler, U.; Seger, R.A.; Zychlinsky, A. and Reichenbach, J. (2009): Restoration of NET formation by gene therapy in CGD controls aspergillosis, Blood 114 [13], pp. 2619-2622.

[142] Stein, S.; Ott, M.G.; Schultze-Strasser, S.; Jauch, A.; Burwinkel, B.; Kinner, A.; Schmidt, M.; Kramer, A.; Schwable, J.; Glimm, H.; Koehl, U.; Preiss, C.; Ball, C.; Martin, H.; Gohring, G.; Schwarzwaelder, K.; Hofmann, W.-K.; Karakaya, K.; Tchatchou, S.; Yang, R.; Reinecke, P.; Kuhlcke, K.; Schlegelberger, B.; Thrasher, A.J.; Hoelzer, D.; Seger, R.; von Kalle, C. and Grez, M. (2010): Genomic instability and myelodysplasia with monosomy 7 consequent to EVI1 activation after gene therapy for chronic granulomatous disease, Nature medicine 16 [2], pp. 198-204.

[143] Aiuti, A.; Vai, S.; Mortellaro, A.; Casorati, G.; Ficara, F.; Andolfi, G.; Ferrari, G.; Tabucchi, A.; Carlucci, F.; Ochs, H.D.; Notarangelo, L.D.; Roncarolo, M.G. and Bordignon, C. (2002): Immune reconstitution in ADA-SCID after PBL gene therapy and discontinuation of enzyme replacement, Nature Medicine 8 [5], pp. 423-425.

[144] Aiuti, A.; Slavin, S.; Aker, M.; Ficara, F.; Deola, S.; Mortellaro, A.; Morecki, S.; Andolfi, G.; Tabucchi, A.; Carlucci, F.; Marinello, E.; Cattaneo, F.; Vai, S.; Servida, P.; Miniero, R.; Roncarolo, M.G. and Bordignon, C. (2002): Correction of ADA-SCID by stem cell gene therapy combined with nonmyeloablative conditioning, Science 296 [5577], pp. 2410-2413.

[145] Gaspar, H.B.; Bjorkegren, E.; Parsley, K.; Gilmour, K.C.; King, D.; Sinclair, J.; Zhang, F.; Giannakopoulos, A.; Adams, S.; Fairbanks, L.D.; Gaspar, J.; Henderson, L.; Xu-Bayford, J.H.; Davies, E.G.; Veys, P.A.; Kinnon, C. and Thrasher, A.J. (2006): Successful reconstitution of immunity in ADA-SCID by stem cell gene therapy following cessation of PEG-ADA and use of mild preconditioning, Molecular Therapy 14 [4], pp. 505-513.

[146] Aiuti, A.; Cattaneo, F.; Galimberti, S.; Benninghoff, U.; Cassani, B.; Callegaro, L.; Scaramuzza, S.; Andolfi, G.; Mirolo, M.; Brigida, I.; Tabucchi, A.; Carlucci, F.; Eibl, M.; Aker, M.; Slavin, S.; Al-Mousa, H.; Al Ghonaium, A.; Ferster, A.; Duppenthaler, A.; Notarangelo, L.; Wintergerst, U.; Buckley, R.H.; Bregni, M.; Marktel, S.; Valsecchi, M.G.; Rossi, P.; Ciceri, F.; Miniero, R.; Bordignon, C. and Roncarolo, M.-G. (2009): Gene therapy for Iimmunodeficiency due to adenosine deaminase deficiency, New England Journal of Medicine 360 [5], pp. 447-458.

[147] Gaspar, H.B.; Cooray, S.; Gilmour, K.C.; Parsley, K.L.; Zhang, F.; Adams, S.; Bjorkegren, E.; Bayford, J.; Brown, L.; Davies, E.G.; Veys, P.; Fairbanks, L.; Bordon, V.; Petropolou, T.; Kinnon, C. and Thrasher, A.J. (2011): Hematopoietic stem cell gene therapy for adenosine deaminase–deficient severe combined immunodeficiency leads to long-term immunological recovery and metabolic correction, Science Translational Medicine 3 [97], p. 97ra80.

[148] Aiuti, A.; Cassani, B.; Andolfi, G.; Mirolo, M.; Biasco, L.; Recchia, A.; Urbinati, F.; Valacca, C.; Scaramuzza, S.; Aker, M.; Slavin, S.; Cazzola, M.; Sartori, D.; Ambrosi, A.; Di Serio, C.; Roncarolo, M.G.; Mavilio, F. and Bordignon, C. (2007): Multilineage hematopoietic reconstitution without clonal selection in ADA-SCID patients treated with stem cell gene therapy, The Journal of Clinical Investigation 117 [8], pp. 2233-2240.

[149] Boztug, K.; Schmidt, M.; Schwarzer, A.; Banerjee, P.P.; Díez, I.A.; Dewey, R.A.; Böhm, M.; Nowrouzi, A.; Ball, C.R.; Glimm, H.; Naundorf, S.; Kühlcke, K.; Blasczyk, R.; Kondratenko, I.; Maródi, L.; Orange, J.S.; von Kalle, C. and Klein, C. (2010): Stem-cell gene therapy for the Wiskott–Aldrich syndrome, New England Journal of Medicine 363 [20], pp. 1918-1927.

[150] Bünning, H. (2010): Stellungnahme der Deutschen Gesellschaft für Gentherapie (DG-GT e.V.) zu einer in einer Gentherapiestudie des Wiskott-Aldrich-Syndroms aufgetretenen Nebenwirkung.

[151] Cartier, N.; Hacein-Bey-Abina, S.; Bartholomae, C.C.; Veres, G.; Schmidt, M.; Kutschera, I.; Vidaud, M.; Abel, U.; Dal-Cortivo, L.; Caccavelli, L.; Mahlaoui, N.; Kiermer, V.; Mittelstaedt, D.; Bellesme, C.; Lahlou, N.; Lefrère, F.; Blanche, S.; Audit, M.; Payen, E.; Leboulch, P.; l'Homme, B.; Bougnères, P.; Von Kalle, C.; Fischer, A.; Cavazzana-Calvo, M. and Aubourg, P. (2009): Hematopoietic stem cell gene therapy with a lentiviral vector in X-linked adrenoleukodystrophy, Science 326 [5954], pp. 818-823.

[152] Bonini, C.; Ferrari, G.; Verzeletti, S.; Servida, P.; Zappone, E.; Ruggieri, L.; Ponzoni, M.; Rossini, S.; Mavilio, F.; Traversari, C. and Bordignon, C. (1997): HSV-TK gene transfer into donor lymphocytes for control of allogeneic graft-versus-leukemia, Science 276 [5319], pp. 1719-1724.

[153] Recchia, A.; Bonini, C.; Magnani, Z.; Urbinati, F.; Sartori, D.; Muraro, S.; Tagliafico, E.; Bondanza, A.; Stanghellini, M.T.L.; Bernardi, M.; Pescarollo, A.; Ciceri, F.; Bordignon, C. and Mavilio, F. (2006): Retroviral vector integration deregulates gene expression but has no consequence on the biology and function of transplanted T cells, Proceedings of the National Academy of Sciences of the United States of America 103 [5], pp. 1457-1462.

[154] Cattoglio, C.; Maruggi, G.; Bartholomae, C.; Malani, N.; Pellin, D.; Cocchiarella, F.; Magnani, Z.; Ciceri, F.; Ambrosi, A.; von Kalle, C.; Bushman, F.D.; Bonini, C.; Schmidt, M.; Mavilio, F. and Recchia, A. (2010): High-definition mapping of retroviral integration sites defines the fate of allogeneic T cells after donor lymphocyte infusion, PLoS ONE 5 [12], p. e15688.

[155] Bonini, C.; Grez, M.; Traversari, C.; Ciceri, F.; Marktel, S.; Ferrari, G.; Dinauer, M.; Sadat, M.; Aiuti, A.; Deola, S.; Radrizzani, M.; Hagenbeek, A.; Apperley, J.; Ebeling, S.; Martens, A.; Kolb, H.J.; Weber, M.; Lotti, F.; Grande, A.; Weissinger, E.; Bueren, J.A.; Lamana, M.; Falkenburg, J.H.F.; Heemskerk, M.H.M.; Austin, T.; Kornblau, S.; Marini, F.; Benati, C.; Magnani, Z.; Cazzaniga, S.; Toma, S.; Gallo-Stampino, C.; Introna, M.; Slavin, S.; Greenberg, P.D.; Bregni, M.; Mavilio, F. and Bordignon, C. (2003): Safety of retroviral gene marking with a truncated NGF receptor, Nature Medicine 9 [4], pp. 367-369.

[156] Newrzela, S.; Cornils, K.; Li, Z.; Baum, C.; Brugman, M.H.; Hartmann, M.; Meyer, J.; Hartmann, S.; Hansmann, M.-L.; Fehse, B. and von Laer, D. (2008): Resistance of mature T cells to oncogene transformation, Blood 112 [6], pp. 2278-2286.

[157] Newrzela, S.; Cornils, K.; Heinrich, T.; Schläger, J.; Yi, J.-H.; Lysenko, O.; Kimpel, J.; Fehse, B. and von Laer, D. (2011): Retroviral insertional mutagenesis can contribute to immortalization of mature T lymphocytes., Molecular Medicine.

[158] Gossen, M. and Bujard, H. (1992): Tight control of gene expression in mammalian cells by tetracycline-responsive promoters, Proceedings of the National Academy of Sciences of the United States of America 89 [12], pp. 5547-5551.

[159] Gossen, M.; Freundlieb, S.; Bender, G.; Müller, G.; Hillen, W. and Bujard, H. (1995): Transcriptional activation by tetracyclines in mammalian cells, Science 268 [5218], pp. 1766-1769.

[160] Yin, D.X.; Zhu, L. and Schimke, R.T. (1996): Tetracycline-controlled gene expression system achieves high-level and quantitative control of gene expression, Analytical Biochemistry 235 [2], pp. 195-201.

[161] Triezenberg, S.J.; Kingsbury, R.C. and McKnight, S.L. (1988): Functional dissection of VP16, the trans-activator of herpes simplex virus immediate early gene expression, Genes & Development 2 [6], pp. 718-729.

[162] Berens, C. and Hillen, W. (2003): Gene regulation by tetracyclines, European Journal of Biochemistry 270 [15], pp. 3109-3121.

[163] Corbel, S.Y. and Rossi, F.M.V. (2002): Latest developments and in vivo use of the Tet system: ex vivo and in vivo delivery of tetracycline-regulated genes, Current Opinion in Biotechnology 13 [5], pp. 448-452.

[164] Loew, R. (2009): The use of retroviral vectors for tet-regulated gene expression in cell populations Methods in Molecular Biology 506, pp. 221-242.

[165] Haack, K.; Cockrell, A.S.; Ma, H.; Israeli, D.; Ho, S.N.; McCown, T.J. and Kafri, T. (2004): Transactivator and structurally optimized inducible lentiviral vectors, Molecular Therapy 10 [3], pp. 585-596.
[166] Kafri, T.; van Praag, H.; Gage, F.H. and Verma, I.M. (2000): Lentiviral vectors: Regulated gene expression, Molecular Therapy 1 [6], pp. 516-521.
[167] Barde, I.; Zanta-Boussif, M.A.; Paisant, S.; Leboeuf, M.; Rameau, P.; Delenda, C. and Danos, O. (2006): Efficient control of gene expression in the hematopoietic system using a single Tet-on inducible lentiviral vector, Molecular Therapy 13 [2], pp. 382-390.
[168] Baron, U.; Freundlieb, S.; Gossen, M. and Bujard, H. (1995): Co-regulation of two gene activities by tetracycline via a bidirectional promoter, Nucleic Acids Research 23 [17], pp. 3605-3606.
[169] Hofmann, A.; Nolan, G.P. and Blau, H.M. (1996): Rapid retroviral delivery of tetracycline-inducible genes in a single autoregulatory cassette, Proceedings of the National Academy of Sciences of the United States of America 93 [11], pp. 5185-5190.
[170] Agha-Mohammadi, S.; O'Malley, M.; Etemad, A.; Wang, Z.; Xiao, X. and Lotze, M.T. (2004): Second-generation tetracycline-regulatable promoter: repositioned tet operator elements optimize transactivator synergy while shorter minimal promoter offers tight basal leakiness, The Journal of Gene Medicine 6 [7], pp. 817-828.
[171] Urlinger, S.; Baron, U.; Thellmann, M.; Hasan, M.T.; Bujard, H. and Hillen, W. (2000): Exploring the sequence space for tetracycline-dependent transcriptional activators: Novel mutations yield expanded range and sensitivity, Proceedings of the National Academy of Sciences of the United States of America 97 [14], pp. 7963-7968.
[172] Heinz, N.; Schambach, A.; Galla, M.; Maetzig, T.; Baum, C.; Loew, R. and Schiedlmeier, B. (2011): Retroviral and transposon-based Tet-regulated All-In-One vectors with reduced background expression and improved dynamic range, Human Gene Therapy 22 [2], pp. 166-76.
[173] Morita S; Kojima T and Kitamura, T. (2000): Plat-E: an efficient and stable system for transient packaging of retroviruses, Gene Therapy 7 [12], pp. 1063-1066.
[174] Spiotto MT and H., S. (2005): Rapid destruction of the tumor microenvironment by CTLs recognizing cancer-specific antigens cross-presented by stromal cells., Cancer Immunity 5, p. 8.
[175] Miller, A.D. and Rosman, G.J. (1989): Improved retroviral vectors for gene transfer and expression, Biotechniques 7 [9], pp. 980-990.
[176] Schmidt, M.; Schwarzwaelder, K.; Bartholomae, C.; Zaoui, K.; Ball, C.; Pilz, I.; Braun, S.; Glimm, H. and von Kalle, C. (2007): High-resolution insertion-site analysis by linear amplification-mediated PCR (LAM-PCR), Nature Methods 4 [12], pp. 1051-1057.
[177] Salem, M.L.; Kadima, A.N.; EL-Naggar, S.A.; Rubinstein, M.P.; Chen, Y.; Gillanders, W.E. and Cole, D.J. (2007): Defining the ability of cyclophosphamide preconditioning to enhance the antigen-specific CD8+ T-cell response to peptide vaccination: Creation of a beneficial host microenvironment involving type I IFNs and myeloid cells, Journal of Immunotherapy 30 [1], pp. 40-53.
[178] Krangel, M.S. (1987): Endocytosis and recycling of the T3-T cell receptor complex. The role of T3 phosphorylation., The Journal of Experimental Medicine 165 [4], pp. 1141-59.
[179] Minami, Y.; Samelson, L.E. and Klausner, R.D. (1987): Internalization and cycling of the T cell antigen receptor. Role of protein kinase C, The Journal of Biological Chemistry 262 [27], pp. 13342-13347.
[180] Liu, H.; Rhodes, M.; Wiest, D.L. and Vignali, D.A.A. (2000): On the dynamics of TCR:CD3 complex cell surface expression and downmodulation, Immunity 13 [5], pp. 665-675.
[181] Menné, C.; Sørensen, T.M.; Siersma, V.; von Essen, M.; Ødum, N. and Geisler, C. (2002): Endo- and exocytic rate constants for spontaneous and protein kinase C-activated T cell receptor cycling, European Journal of Immunology 32 [3], pp. 616-626.

[182] Cooper, L.J.N.; Kalos, M.; Lewinsohn, D.A.; Riddell, S.R. and Greenberg, P.D. (2000): Transfer of specificity for Human Immunodeficiency Virus type 1 into primary human T lymphocytes by introduction of T-cell receptor genes, The Journal of Virology 74 [17], pp. 8207-8212.

[183] Heemskerk, M.H.M.; Hagedoorn, R.S.; van der Hoorn, M.A.W.G.; van der Veken, L.T.; Hoogeboom, M.; Kester, M.G.D.; Willemze, R. and Falkenburg, J.H.F. (2007): Efficiency of T-cell receptor expression in dual-specific T cells is controlled by the intrinsic qualities of the TCR chains within the TCR-CD3 complex, Blood 109 [1], pp. 235-243.

[184] Dash, P.; McClaren, J.L.; Oguin, T.H.; Rothwell, W.; Todd, B.; Morris, M.Y.; Becksfort, J.; Reynolds, C.; Brown, S.A.; Doherty, P.C. and Thomas, P.G. (2011): Paired analysis of TCRα and TCRβ chains at the single-cell level in mice, The Journal of Clinical Investigation 121 [1], pp. 288-295.

[185] Morris, G.P. and Allen, P.M. (2009): Cutting Edge: Highly alloreactive dual TCR T cells play a dominant role in Graft-versus-Host disease, The Journal of Immunology 182 [11], pp. 6639-6643.

[186] Ji, Q.; Perchellet, A. and Goverman, J.M. (2010): Viral infection triggers central nervous system autoimmunity via activation of CD8+ T cells expressing dual TCRs, Nature Immunology 11 [7], pp. 628-634.

[187] Ferrua, F.; Brigida, I. and Aiuti, A. (2010): Update on gene therapy for adenosine deaminase-deficient severe combined immunodeficiency, Current Opinion in Allergy and Clinical Immunology 10 [6].

[188] Cassani, B.; Montini, E.; Maruggi, G.; Ambrosi, A.; Mirolo, M.; Selleri, S.; Biral, E.; Frugnoli, I.; Hernandez-Trujillo, V.; Di Serio, C.; Roncarolo, M.G.; Naldini, L.; Mavilio, F. and Aiuti, A. (2009): Integration of retroviral vectors induces minor changes in the transcriptional activity of T cells from ADA-SCID patients treated with gene therapy, Blood 114 [17], pp. 3546-3556.

[189] Borchers, S.; Provasi, E.; Benati, C.; Dammann, E.; Radrizzani, M.; Krons, A.; Kuehnau, W.; Schmidke, J.; von Neuhoff, N.; Stadler, M.; Ciceri, F.; Bonini, C.; Ganser, A.; Hertenstein, B. and Mischak-Weissinger, E.M. (2011): Genetically modified donor leukocyte transfusion and Graft–versus-Leukemia effect after allogeneic stem cell transplantation, Human Gene Therapy 22 [7], pp. 829-41.

[190] Deeks, S.G.; Wagner, B.; Anton, P.A.; Mitsuyasu, R.T.; Scadden, D.T.; Huang, C.; Macken, C.; Richman, D.D.; Christopherson, C.; June, C.H.; Lazar, R.; Broad, D.F.; Jalali, S. and Hege, K.M. (2002): A Phase II randomized study of HIV-specific T-cell gene therapy in subjects with undetectable plasma viremia on combination antiretroviral therapy, Molecular Therapy 5 [6], pp. 788-797.

[191] Walker, R.E.; Bechtel, C.M.; Natarajan, V.; Baseler, M.; Hege, K.M.; Metcalf, J.A.; Stevens, R.; Hazen, A.; Blaese, R.M.; Chen, C.C.; Leitman, S.F.; Palensky, J.; Wittes, J.; Davey, R.T., Jr; Falloon, J.; Polis, M.A.; Kovacs, J.A.; Broad, D.F.; Levine, B.L.; Roberts, M.R.; Masur, H. and Lane, H.C. (2000): Long-term in vivo survival of receptor-modified syngeneic T cells in patients with human immunodeficiency virus infection, Blood 96 [2], pp. 467-474.

[192] Mitsuyasu, R.T.; Anton, P.A.; Deeks, S.G.; Scadden, D.T.; Connick, E.; Downs, M.T.; Bakker, A.; Roberts, M.R.; June, C.H.; Jalali, S.; Lin, A.A.; Pennathur-Das, R. and Hege, K.M. (2000): Prolonged survival and tissue trafficking following adoptive transfer of CD4zeta gene-modified autologous CD4+ and CD8+ T cells in human immunodeficiency virus-infected subjects, Blood 96 [3], pp. 785-793.

[193] van Lunzen, J.; Glaunsinger, T.; Stahmer, I.; von Baehr, V.; Baum, C.; Schilz, A.; Kuehlcke, K.; Naundorf, S.; Martinius, H.; Hermann, F.; Giroglou, T.; Newrzela, S.; Muller, I.; Brauer, F.; Brandenburg, G.; Alexandrov, A. and von Laer, D. (2007): Transfer of autologous gene-modified T cells in HIV-infected patients with advanced immunodeficiency and drug-resistant virus, Molecular Therapy 15 [5], pp. 1024-1033.

[194] Grutz, G.G.; Bucher, K.; Lavenir, I.; Larson, T.; Larson, R. and Rabbitts, T.H. (1998): The oncogenic T cell LIM-protein Lmo2 forms part of a DNA-binding complex specifically in immature T cells, The EMBO Journal 17 [16], pp. 4594-4605.

[195] Meyer, J.; Rhein, M.; Schiedlmeier, B.; Kustikova, O.; Rudolph, C.; Kamino, K.; Neumann, T.; Yang, M.; Wahlers, A.; Fehse, B.; Reuther, G.W.; Schlegelberger, B.; Ganser, A.; Baum, C. and Li, Z. (2007): Remarkable leukemogenic potency and quality of a constitutively active neurotrophin receptor, [Delta]TrkA, Leukemia 21 [10], pp. 2171-2180.

[196] Virgilio, L.; Lazzeri, C.; Bichi, R.; Nibu, K.-i.; Narducci, M.G.; Russo, G.; Rothstein, J.L. and Croce, C.M. (1998): Deregulated expression of TCL1 causes T cell leukemia in mice, Proceedings of the National Academy of Sciences of the United States of America 95 [7], pp. 3885-3889.

[197] Ravandi, F.; Kantarjian, H.; Jones, D.; Dearden, C.; Keating, M. and O'Brien, S. (2005): Mature T-cell leukemias, Cancer 104 [9], pp. 1808-1818.

[198] Westwood, J.A.; Murray, W.K.; Trivett, M.; Shin, A.; Neeson, P.; MacGregor, D.P.; Haynes, N.M.; Trapani, J.A.; Mayura-Guru, P.; Fox, S.; Peinert, S.; Honemann, D.; Prince, H.M.; Ritchie, D.; Scott, A.M.; Smyth, F.E.; Smyth, M.J.; Darcy, P.K. and Kershaw, M.H. (2008): Absence of retroviral vector-mediated transformation of gene-modified T cells after long-term engraftment in mice, Gene Therapy 15 [14], pp. 1056-1066.

[199] Woods, N.-B.; Bottero, V.; Schmidt, M.; von Kalle, C. and Verma, I.M. (2006): Gene therapy: Therapeutic gene causing lymphoma, Nature 440 [7088], pp. 1123-1123.

[200] Hiasa, A.; Hirayama, M.; Nishikawa, H.; Kitano, S.; Nukaya, I.; Yu, S.S.; Mineno, J.; Kato, I. and Shiku, H. (2008): Long-term phenotypic, functional and genetic stability of cancer-specific T-cell receptor (TCR) [alpha][beta] genes transduced to CD8+ T cells, Gene Therapy 15 [9], pp. 695-699.

[201] Goronzy, J.J. and Weyand, C.M. (2005): T cell development and receptor diversity during aging, Current Opinion in Immunology 17 [5], pp. 468-475.

[202] Greenberg, P.D. and Cheever, M.A. (1984): Treatment of disseminated leukemia with cyclophosphamide and immune cells: tumor immunity reflects long-term persistence of tumor-specific donor T cells, The Journal Immunology 133 [6], pp. 3401-3407.

[203] Tough, D.F. and Sprent, J. (1994): Turnover of naive- and memory-phenotype T cells., The Journal of Experimental Medicine 179 [4], pp. 1127-35.

[204] Murali-Krishna, K.; Lau, L.L.; Sambhara, S.; Lemonnier, F.; Altman, J. and Ahmed, R. (1999): Persistence of memory CD8 T cells in MHC class I-deficient mice, Science 286 [5443], pp. 1377-1381.

[205] Murali-Krishna, K.; Altman, J.D.; Suresh, M.; Sourdive, D.J.D.; Zajac, A.J.; Miller, J.D.; Slansky, J. and Ahmed, R. (1998): Counting antigen-specific CD8 T cells: A reevaluation of bystander activation during viral infection, Immunity 8 [2], pp. 177-187.

[206] Butz, E.A. and Bevan, M.J. (1998): Massive expansion of antigen-specific CD8+ T cells during an acute virus infection, Immunity 8 [2], pp. 167-175.

[207] Zhou, J.; Shen, X.; Huang, J.; Hodes, R.J.; Rosenberg, S.A. and Robbins, P.F. (2005): Telomere length of transferred lymphocytes correlates with in vivo persistence and tumor regression in melanoma patients receiving cell transfer therapy, The Journal of Immunology 175 [10], pp. 7046-7052.

[208] Roberts, A.D.; Ely, K.H. and Woodland, D.L. (2005): Differential contributions of central and effector memory T cells to recall responses, The Journal of Experimental Medicine 202 [1], pp. 123-133.

[209] Coccoris, M.; Swart, E.; de Witte, M.A.; van Heijst, J.W.J.; Haanen, J.B.A.G.; Schepers, K. and Schumacher, T.N.M. (2008): Long-term functionality of TCR-transduced T cells in vivo, The Journal of Immunology 180 [10], pp. 6536-6543.

[210] Kohlmeier, J.E.; Connor, L.M.; Roberts, A.D.; Cookenham, T.; Martin, K. and Woodland, D.L. (2010): Nonmalignant clonal expansions of memory CD8+ T cells that arise with age vary in their capacity to mount recall responses to infection, The Journal of Immunology 185 [6], pp. 3456-3462.

[211] Roberts, A.D. and Woodland, D.L. (2004): Cutting Edge: Effector memory CD8+ T cells play a prominent role in recall responses to secondary viral infection in the lung, The Journal of Immunology 172 [11], pp. 6533-6537.

[212] Berger, C.; Jensen, M.C.; Lansdorp, P.M.; Gough, M.; Elliott, C. and Riddell, S.R. (2008): Adoptive transfer of effector CD8+ T cells derived from central memory cells establishes persistent T cell memory in primates, The Journal of Clinical Investigation 118 [1], pp. 294-305.

[213] Kochenderfer, J.N.; Chien, C.D.; Simpson, J.L. and Gress, R.E. (2007): Maximizing CD8+ T cell responses elicited by peptide vaccines containing CpG oligodeoxynucleotides, Clinical Immunology 124 [2], pp. 119-130.

[214] Speiser, D.E.; Liénard, D.; Rufer, N.; Rubio-Godoy, V.; Rimoldi, D.; Lejeune, F.; Krieg, A.M.; Cerottini, J.-C. and Romero, P. (2005): Rapid and strong human CD8+ T cell responses to vaccination with peptide, IFA, and CpG oligodeoxynucleotide 7909, The Journal of Clinical Investigation 115 [3], pp. 739-746.

[215] Beloeil, L.; Tomkowiak, M.; Angelov, G.; Walzer, T.; Dubois, P. and Marvel, J. (2003): In vivo impact of CpG1826 oligodeoxynucleotide on CD8 T cell primary responses and survival, The Journal of Immunology 171 [6], pp. 2995-3002.

[216] Vabulas, R.M.; Pircher, H.; Lipford, G.B.; Häcker, H. and Wagner, H. (2000): CpG-DNA activates in vivo T cell epitope presenting dendritic cells to trigger protective antiviral cytotoxic T cell responses, The Journal of Immunology 164 [5], pp. 2372-2378.

[217] Heikenwalder, M.; Polymenidou, M.; Junt, T.; Sigurdson, C.; Wagner, H.; Akira, S.; Zinkernagel, R. and Aguzzi, A. (2004): Lymphoid follicle destruction and immunosuppression after repeated CpG oligodeoxynucleotide administration, Nature medicine 10 [2], pp. 187-92.

[218] Biasco, L.; Ambrosi, A.; Pellin, D.; Bartholomae, C.; Brigida, I.; Roncarolo, M.G.; Di Serio, C.; von Kalle, C.; Schmidt, M. and Aiuti, A. (2011): Integration profile of retroviral vector in gene therapy treated patients is cell-specific according to gene expression and chromatin conformation of target cell, EMBO Molecular Medicine 3 [2], pp. 89-101.

[219] Davis, J.L.; Theoret, M.R.; Zheng, Z.; Lamers, C.H.J.; Rosenberg, S.A. and Morgan, R.A. (2010): Development of human anti-murine T-cell receptor antibodies in both responding and nonresponding patients enrolled in TCR gene therapy trials, Clinical Cancer Research 16 [23], pp. 5852-5861.

[220] Okamoto, S.; Mineno, J.; Ikeda, H.; Fujiwara, H.; Yasukawa, M.; Shiku, H. and Kato, I. (2009): Improved expression and reactivity of transduced tumor-specific TCRs in human lymphocytes by specific silencing of endogenous TCR, Cancer Research 69 [23], pp. 9003-9011.

[221] Ochi, T.; Fujiwara, H.; Okamoto, S.; An, J.; Nagai, K.; Shirakata, T.; Mineno, J.; Kuzushima, K.; Shiku, H. and Yasukawa, M. (2011): Novel adoptive T-cell immunotherapy using a WT1-specific TCR vector encoding silencers for endogenous TCRs shows marked anti-leukemia reactivity and safety, Blood 118 [6], pp. 1495-503.

[222] van Lent, A.U.; Nagasawa, M.; van Loenen, M.M.; Schotte, R.; Schumacher, T.N.M.; Heemskerk, M.H.M.; Spits, H. and Legrand, N. (2007): Functional human antigen-specific T cells produced in vitro using retroviral T cell receptor transfer into hematopoietic progenitors, The Journal of Immunology 179 [8], pp. 4959-4968.

[223] Holst, J.; Szymczak-Workman, A.L.; Vignali, K.M.; Burton, A.R.; Workman, C.J. and Vignali, D.A.A. (2006): Generation of T-cell receptor retrogenic mice, Nature Protocols 1 [1], pp. 406-417.

[224] Clay, T.M.; Custer, M.; Spiess, P. and Nishimura, M.I. (1999): Potential use of T cell receptor genes to modify hematopoietic stem cells for the gene therapy of cancer, Pathology and Oncology Research 5 [1], pp. 3-15.

[225] Gomes, A.Q.; Martins, D.S. and Silva-Santos, B. (2010): Targeting γδ T lymphocytes for cancer immunotherapy: from novel mechanistic insight to clinical application, Cancer Research 70 [24], pp. 10024-10027.

[226] van der Veken, L.T.; Hagedoorn, R.S.; van Loenen, M.M.; Willemze, R.; Falkenburg, J.H.F. and Heemskerk, M.H.M. (2006): αβ T-cell receptor engineered γδ T cells mediate effective antileukemic reactivity, Cancer Research 66 [6], pp. 3331-3337.

[227] van der Veken, L.T.; Coccoris, M.; Swart, E.; Falkenburg, J.H.F.; Schumacher, T.N. and Heemskerk, M.H.M. (2009): αβ T cell receptor transfer to γδ T cells generates functional effector cells without mixed TCR dimers in vivo, The Journal of Immunology 182 [1], pp. 164-170.

[228] Heemskerk, M.H.M.; Hoogeboom, M.; Hagedoorn, R.; Kester, M.G.D.; Willemze, R. and Falkenburg, J.H.F. (2004): Reprogramming of virus-specific T cells into leukemia-reactive T cells using T cell receptor gene transfer, The Journal of Experimental Medicine 199 [7], pp. 885-894.

[229] Griffioen, M.; van Egmond, H.M.E.; Barnby-Porritt, H.; van der Hoorn, M.A.W.G.; Hagedoorn, R.S.; Kester, M.G.D.; Schwabe, N.; Willemze, R.; Falkenburg, J.H.F. and Heemskerk, M.H.M. (2008): Genetic engineering of virus-specific T cells with T-cell receptors recognizing minor histocompatibility antigens for clinical application, Haematologica 93 [10], pp. 1535-1543.

[230] Montini, E.; Cesana, D.; Schmidt, M.; Sanvito, F.; Ponzoni, M.; Bartholomae, C.; Sergi, L.S.; Benedicenti, F.; Ambrosi, A.; Di Serio, C.; Doglioni, C.; von Kalle, C. and Naldini, L. (2006): Hematopoietic stem cell gene transfer in a tumor-prone mouse model uncovers low genotoxicity of lentiviral vector integration, Nature Biotechnology 24 [6], pp. 687-696.

[231] Huston, M.W.; van Til, N.P.; Visser, T.P.; Arshad, S.; Brugman, M.H.; Cattoglio, C.; Nowrouzi, A.; Li, Y.; Schambach, A.; Schmidt, M.; Baum, C.; von Kalle, C.; Mavilio, F.; Zhang, F.; Blundell, M.P.; Thrasher, A.J.; Verstegen, M.M.A. and Wagemaker, G. (2011): Correction of murine SCID-X1 by lentiviral gene therapy using a codon-optimized IL2RG gene and minimal pretransplant conditioning, Molecular Therapy.

[232] Urnov, F.D.; Rebar, E.J.; Holmes, M.C.; Zhang, H.S. and Gregory, P.D. (2010): Genome editing with engineered zinc finger nucleases, Nature Reviews Genetics 11 [9], pp. 636-646.

[233] Ivics, Z. and Izsvak, Z. (2010): The expanding universe of transposon technologies for gene and cell engineering, Mobile DNA 1 [1], p. 25.

[234] Peng, P.D.; Cohen, C.J.; Yang, S.; Hsu, C.; Jones, S.; Zhao, Y.; Zheng, Z.; Rosenberg, S.A. and Morgan, R.A. (2009): Efficient nonviral Sleeping Beauty transposon-based TCR gene transfer to peripheral blood lymphocytes confers antigen-specific antitumor reactivity, Gene Therapy 16 [8], pp. 1042-1049.

[235] Frank, O.; Rudolph, C.; Heberlein, C.; von Neuhoff, N.; Schröck, E.; Schambach, A.; Schlegelberger, B.; Fehse, B.; Ostertag, W.; Stocking, C. and Baum, C. (2004): Tumor cells escape suicide gene therapy by genetic and epigenetic instability, Blood 104 [12], pp. 3543-3549.

[236] Tey, S.-K.; Dotti, G.; Rooney, C.M.; Heslop, H.E. and Brenner, M.K. (2007): Inducible caspase 9 suicide gene to improve the safety of allodepleted T cells after haploidentical stem cell transplantation, Biology of Blood and Marrow Transplantation 13 [8], pp. 913-924.

[237] Uckert, W.; Kammertöns, T.; Haack, K.; Qin, Z.; Gebert, J.; Schendel, D.J. and Blankenstein, T. (1998): Double suicide gene (cytosine deaminase and herpes simplex virus thymidine kinase) but not single gene transfer allows reliable elimination of tumor cells in vivo, Human Gene Therapy 9 [6], pp. 855-865.

[238] Beck, C.; Cayeux, S.; Lupton, S.D.; Dörken, B. and Blankenstein, T. (1995): The thymidine kinase/Ganciclovir-mediated “suicide” effect is variable in different tumor cells, Human Gene Therapy 6 [12], pp. 1525-1530.

[239] van Meerten, T.; van Rijn, R.S.; Hol, S.; Hagenbeek, A. and Ebeling, S.B. (2006): Complement-induced cell death by rituximab depends on CD20 expression level and acts complementary to antibody-dependent cellular cytotoxicity, Clinical Cancer Research 12 [13], pp. 4027-4035.

[240] Hess, P.R.; Barnes, C.; Woolard, M.D.; Johnson, M.D.L.; Cullen, J.M.; Collins, E.J. and Frelinger, J.A. (2007): Selective deletion of antigen-specific CD8+ T cells by MHC class I tetramers coupled to the type I ribosome-inactivating protein saporin, Blood 109 [8], pp. 3300-3307.

[241] Kieback, E.; Charo, J.; Sommermeyer, D.; Blankenstein, T. and Uckert, W. (2008): A safeguard eliminates T cell receptor gene-modified autoreactive T cells after adoptive transfer, Proceedings of the National Academy of Sciences 105 [2], pp. 623-628.

Acknowledgements

During the work on my thesis many people helped me in different ways. A lot of thanks to my Ph.D. supervisor Prof. Dr. Wolfgang Uckert who gave me the possibility to work in his lab and to step into the field of TCR gene therapy. Beside the scientific topics he taught me how to give talks and prepare presentations.

I thank Prof. Dr. Blankenstein as well as his group for discussions and helping hands.

Molecular biology I was teached by Kordelia Hummel, cell culturing by Irmgard Küttner, Uta Fischer and Heidrun Peter. All of them as well as Martina Grabert, Janina Hauchwitz, Matthias Richter, Caro Schmitt, Klaus Zöllner gave me many helping hands over the time. I thank the other members or former members of the Uckert group Dr. Lilian Stärck, Dr. Matthias Leisegang, Mario Bunse, Dr. Daniel Sommermeyer, Dr. Elisa Kieback, Peter Meyerhuber, Inan Edes, Nicole Scheumann, Florian Helm for giving me a nice working atmosphere and providing advices.

My boss gave me the possibility to learn techniques by cooperation partners. Here, I would like to thank Dr. Ali Nowrouzi for teaching me the LAM-PCR and Dr. Manfred Schmidt and Prof. Dr. Christof von Kalle for inviting me to their group. Kordelia Hummel I thank for joining me for my second stay in the von Kalle lab. I also thank Dr. Zsolt Sebestyén teaching me the FRET technique and Dr. Reno Debets for discussions during my stay in his lab.

Finally, I'm thankful that I could already start my PostDoc in the lab of Prof. Dr. Pezzutto while still writing on my thesis. Dr. Daniel Sommermeyer and Dr. Oliver Schmetzer I thank for proofreading my thesis.

My family, friends and Christian I thank for encouraging me and being so thoughtful and understanding with my lacks of time and moods.

Publications

Leisegang M, Engels B, Meyerhuber P, Kieback K, Sommermeyer D, Xue S-A, Reuß S, Stauss H, Uckert W. “Enhanced functionality of T cell receptor-redirected T cells is defined by the transgene cassette” Journal of Molecular Medicine (2008) 86(5):573-83

Reuß S, Biese P, Cosset F-L, Takeuchi Y and Uckert W. “Suspension packaging cell lines for the simplified generation of T-cell receptor encoding retrovirus vector particles” Gene Therapy (2007) 14, 595–603

Statement

Hiermit erkläre ich gemäß der Promotionsordnung der Humboldt-Universität zu Berlin vom

01. September 2005, dass ich

- die vorliegende Arbeit eigenständig unter Anleitung und ohne Benutzung anderer als der angegebenen Hilfsmittel angefertigt habe.

- die Arbeit in gleicher oder ähnlicher Form nicht in anderen Promotionsverfahren vorgelegt

wurde.

- mir die geltende Promotionsordnung vom 01. September 2005 bekannt ist.

Berlin, den

Unterschrift